

**This dissertation has been
microfilmed exactly as received** 65-15,499

**DAWSON, John Alexander, 1935-
GEOMAGNETIC MICROPULSATIONS WITH EMPHASIS
PLACED ON THE PROPERTIES AND INTERPRETATION
OF PEARLS.**

**University of Alaska, Ph. D., 1965
Physics, general**

University Microfilms, Inc., Ann Arbor, Michigan

GEOMAGNETIC MICROPULSATIONS WITH EMPHASIS
PLACED ON THE PROPERTIES AND INTERPRETATION OF PEARLS

A
DISSERTATION

Presented to the Faculty of the
University of Alaska in Partial Fulfillment
of the Requirements
for the Degree of
Doctor of Philosophy

by
John Alexander Dawson, B.A., M.S.
College, Alaska
May 1965

GEOMAGNETIC MICROPULSATIONS WITH EMPHASIS
PLACED ON THE PROPERTIES AND INTERPRETATION OF PEARLS

APPROVED:

Charles R. Wilson

Russell E. Gorr

Malcolm K. Campbell

Masahisa Sugimura
Chairman

Chas. Sargen
Department Head

APPROVED:

Chas. Sargen
Dean of the College of Mathematics, Physical Science,
and Engineering

C. Lae
Vice President for Research and
Advanced Study

ABSTRACT

The thesis can be divided into three somewhat divergent parts, historical, experimental, and theoretical.

The first chapter is an attempt to survey the literature concerning all types of micropulsations. A classification scheme is presented which is in agreement with that adopted by the IAGA at Berkeley, California in 1963, though I have retained the older nomenclature. A summary of the known properties of the various types of micropulsations is presented along with a discussion of controversial points.

The next four chapters describe the experimental work performed in cooperation with the Boulder laboratories of NBS, and some observations resulting therefrom. In contrast to the first chapter this section is confined exclusively to pearls. Pearls were found to show little correlation with ionospheric and magnetic data. Exception should be made for two riometer absorption events which can possibly be matched against pearl events. As about 60 to 70 per cent of the pearls observed at College and Macquarie can be matched against each other, pearls are considered to occur simultaneously at conjugate points. At College pearls are shown to be polarized in a plane perpendicular to the magnetic field line.

The last chapter develops hydromagnetic wave theory as is pertinent to propagation through the upper magnetosphere. The various assumptions used are examined critically to justify their applicability to the upper magnetosphere. It is found that the magnetosphere below 10,000 km cannot be considered uniform for waves in the 1 cps range. Hence, harmonic solutions to the wave equation cannot be used and more elaborate techniques to treat this problem must be developed. It is suggested that pearls are Alfvén waves which propagate along field lines to auroral latitudes. These waves then couple to other modes for propagation to lower latitudes.

ACKNOWLEDGEMENTS

This work was supported through the Office of Naval Research, Washington, D. C., under contract number NONR 3010 (02). The author wishes to thank Dr. M. Sugiura, now at Goddard Space Flight Center, for initiating the project and for helpful criticism during the writing of the dissertation. I also wish to acknowledge my debt to Dr. W. Campbell and the Central Radio Propagation Laboratory of the National Bureau of Standards, for providing the equipment, aiding in the collection of data, and in the latter stages of the writing of the dissertation, providing office, library, and drafting facilities. I would like to extend thanks to Mr. D. Swift and Dr. C. Wilson for criticism and valuable discussions.

I am grateful to Mr. R. Heacock for use of his earth current records and to Mr. G. Lerfald for the loan of College riometer data. To Mr. D. Wilder for drafting many of the illustrations and to Mrs. A. Dupere for typing the manuscript, I also owe thanks.

TABLE OF CONTENTS

	Page
ABSTRACT	iii
ACKNOWLEDGEMENTS	iv
LIST OF ILLUSTRATIONS	vii
LIST OF TABLES	ix
CHAPTER I	
SURVEY OF LITERATURE ON MICROPULSATIONS	1
1.1 Introduction	1
1.2 Historical	1
1.3 Recent Work (Observational)	4
1.3.1 Regular Pulsations	5
1.3.2 Irregular Pulsations	13
1.4 A Short Note on Classification	18
1.5 Power Spectra	19
CHAPTER II	
EQUIPMENT AND OPERATION	21
2.1 Equipment	21
2.2 Operation	28
2.3 Errors	30
CHAPTER III	
SOME PROPERTIES OF PEARLS	33
3.1 Introduction	33
3.2 Diurnal Variation	33
3.3 Period	36
3.4 Correlation of Pearls with Ionospheric Data	43
3.4.1 Pearls vs. f_oF_2	43
3.4.2 Pearls vs. f_{min}	50
3.4.3 Pearls vs. f_oE	50
3.4.4 Riometer	50
3.4.5 Pearls vs. Magnetic Activity	55
3.4.6 Pearls vs. Blackouts	56
3.5 Areal Extent	57
CHAPTER IV	
CONJUGATE RELATIONS BETWEEN COLLEGE AND MACQUARIE	60
4.1 General	60
4.2 Coincidence with College	62
4.3 Comparison of Period at Conjugate Points	67
CHAPTER V	
THE POLARIZATION OF PEARLS	70
5.1 General	70
5.2 Method of Analysis	70
5.3 Discussion of Results	71

	Page
CHAPTER VI	
HYDROMAGNETIC WAVE PROPAGATION IN THE UPPER MAGNETOSPHERE	81
6.1 Introduction	81
6.2 Hydromagnetic Propagation in a Uniform Cold Plasma	82
6.3 The Effect of Ion-electron Collisions	94
6.4 Justification of Assumptions	96
6.5 Evidence that Pearls are Alfvén Waves	107
6.6 Generative Models	111
REFERENCES	115

LIST OF ILLUSTRATIONS

		Page
Fig. 2.1	Block diagram of the system.	22
Fig. 2.2	Loop input circuit for calibration unit.	24
Fig. 2.3	Frequency response of system.	27
Fig. 3.1	Typical pearl event, College, August 26, 1962.	34
Fig. 3.2	Diurnal variation for all pearls observed at College.	35
Fig. 3.3	Diurnal variation for the winter months.	37
Fig. 3.4	Diurnal variation for the summer months.	38
Fig. 3.5	Diurnal variation for the equinoctial months.	39
Fig. 3.6	Period distribution of the pearls studied.	40
Fig. 3.7	Scatter plot of period vs. local standard time.	42
Fig. 3.8	Scatter plot of period vs. amplitude.	44
Fig. 3.9	f_oF_2 vs. pearl amplitude for all pearls.	48
Fig. 3.10	f_oF_2 vs. pearl amplitude for strong events (exceeded 1 gamma at least once).	49
Fig. 3.11	f_{min} vs. pearl amplitude.	50
Fig. 3.12	Riometer comparison for the event of December 23, 1962.	54
Fig. 4.1	Diurnal variation of pearls at Macquarie Island.	60a
Fig. 4.2	An example of a pearl occurring simultaneously at Macquarie and College, January 1, 1962, 2050-2105 UT.	66
Fig. 4.3	Comparison of period at conjugate points for the event of February 11, 1962.	68
Fig. 4.4	Comparison of period at conjugate points for the event of February 21, 1962.	68

		Page
Fig. 5.1	Polarization diagrams for August 16, 1962; 0330 UT.	72
Fig. 5.2	Polarization diagrams for August 26, 1962; 2032 UT.	73
Fig. 5.3	Polarization diagrams for August 16, 1962; 0304 UT.	74
Fig. 5.4	Polarization diagrams (horizontal only) for August 16, 1962; 0256:14-54.	75
Fig. 5.5	Polarization diagrams (horizontal only) for August 16, 1962; 0258:02-26.	76
Fig. 5.6	Polarization diagrams (horizontal only) for August 16, 1962; 0338:00-24.	77
Fig. 6.1	Conditions under which a uniform plasma may be assumed. Plasma is considered uniform when density changes by less than 10 per cent within one wavelength. Propagation is radial in the equatorial plane.	98
Fig. 6.2	Same, but propagation is along a field line.	100

LIST OF TABLES

		Page
Table 3.1	List of pearl events used in study	45
Table 3.2	Monthly daytime averages of f_{\min} and f_oF_2 for days with pearls and for days without pearls	58
Table 4.1	List of pearls recorded at Macquarie Island	61
Table 4.2	A comparison of pearls at College and Macquarie	63
Table 5.1	Summary of polarization diagrams	80
Table 6.1	Comparison of density gradients and wavelengths for four model magnetospheres	101
Table 6.2	Ion-electron collision frequencies based on the low temperature model	104
Table 6.3	Some magnetospheric parameters	106

CHAPTER I

SURVEY OF LITERATURE ON MICROPULSATIONS

1.1 Introduction

The subject of geomagnetic micropulsations, because of its recent rapid expansion, is suffering from a lack of adequate nomenclature and classification schemes. That which was developed historically and officially adopted at the Toronto meeting of the IUGG in 1957 (IAGA, 1960) does not adequately treat the shorter period pulsations, which are of current interest. Benioff's (1960) system, based mostly on frequency, is used by several workers but suffers from mixing several morphologically distinct types of pulsations together, simply because they share a frequency band. Many workers have invented their own schemes to suit particular purposes which they have in mind. Thus, at the present time, it would be valuable to survey the literature pertaining to micropulsations, particularly for pulsations with periods less than 10 seconds.

1.2 Historical

Historically, pulsations have been classified into three groups, pt, pc, and pg. As defined by the IUGG, pt is a "phenomenon consisting of several series of oscillations, each series lasting generally 10 to 20 minutes, the whole phenomenon lasting for periods of not more than about one hour." Pc's are "pulsations having a considerable element of continuity, having periods between 10 and 40 seconds (and exceptionally to 50 seconds) lasting a number of hours." Pg refers to pulsations mostly confined to the auroral zone and of much larger amplitude and longer period than the others.

Before the turn of the century, Eschenhagen (1897) reported waves of about 30 second period. Because of equipment limitations, he mistakenly called these elementary waves, believing them to constitute the fastest oscillations of the geomagnetic field. They were shown to occur primarily during the day, and from comparisons between Potsdam and Wilhelmshaven, they were observed simultaneously over several hundred kilometers. During the next decade, several researchers extended this early work. (Ebert, 1907; van Bemmelen, 1908). Waves of longer period were found primarily at night. The amplitude of pulsations in the horizontal component greatly exceeded that of the vertical component. Measurements from Potsdam to Batavia (Djakarta) showed the diurnal occurrence pattern to be dependent on local time, thus establishing the sun as the causative agent. Annual variation was most pronounced for the shorter periods, which tended toward maximums in October and February. Eschenhagen's notion of elementary waves was demolished when Ebert showed the existence of 40 cps waves with an induction coil.

It was recognized that pulsations often fell into one of two broad classes. Podder (1926) characterized the two divisions as follows: Type I - "Very regular periodical vibrations of the magnet continuing over many hours or even days; the periods are well defined and vary in the limits of from 5 to 14 seconds approximately"; Type II - "Comparatively irregular vibrations having, however, a pronounced periodical character with considerably longer periods of a mean value of 34 seconds." Later Type I would be designated pc and Type II, pt. In retrospect, it appears that Eschenhagen's "Elementarwellen" were pc's, but limitations in equipment response allowed him to see primarily only those with the longer periods. This might explain why his waves had longer periods than those of later researchers.

In 1931 Rolf reported the existence of large pulsations at Abisko in northern Sweden. With amplitudes sometimes exceeding 30 gammas, these were called giant pulsations or pg. The mean period observed was 96 seconds with a mean deviation of 22 seconds. Comparison with other Scandinavian stations showed that while both Abisko (geomagnetic latitude 66.1) and Tromso (67.2) observed pg's strongly, Sodankyla (63.7) recorded only moderate amplitudes and Lovo (58.2) nothing at all. Thus pg's were confined to auroral latitudes, i.e. those roughly greater than 65 degrees. At this time, no stations were in existence that would indicate the presence of pg's in the polar cap. Based on Abisko data from 1921-1930, the annual variation had a maximum at the autumnal equinox, while the daily maximum occurred from 0300-0500 LT. Using more data from Tromso, Harang (1936) substantiated Rolf's results, with the exception of adding an occurrence maximum at the vernal equinox. Sucksdorff (1939) added the results of a study of 150 pg's recorded at Sodankyla from 1914 to 1938. He divided the pulsations into two groups: Type A "the most regular and beautiful; the greatest pulsations belong to this group, and they often more or less resemble a shuttle;" Type B "have almost the same amplitude during a considerable time or change irregularly." Type A has a maximum at 0300 LT, while Type B's maximum is at 1000. Sucksdorff has deduced a rather complicated set of rules for the occurrence of annual and diurnal maximums as related to the position in the sunspot cycle. One suspects that the data are insufficient statistically to draw these elaborate conclusions. Certainly the equinoctial months contain the most pg's, and the summer has more than the winter.

For the most part, the early work was confined to the longer period pulsations. But often there was reference to faster oscillations, e.g. Van Bemmelen's "spasms" and Harang's "vibrations". Of particular interest here is a paper by Sucksdorff (1936), in which pulsations of 2-3 seconds period and with the general appearance of a "shuttle", are described. "It is seldom that such an oscillation occurs singly; usually there is a number of oscillations, interrupted by short intervals, for one hour, for several hours, sometimes even for more than 24 hours continuously, when the curve often resembles a pearl necklace consisting of oval pearls of different sizes." These are the same pulsations which were later to be designated as PP by Troitskaya, as Type A by Benioff, and as pearls by general usage. It is interesting to note that Sucksdorff reported pearls to be an essentially daytime phenomenon with a maximum about 1400 LT. Much later pearls were considered to be nocturnal (Benioff, 1960; Teplay and Wentworth, 1962) on the basis of studies made at middle latitudes. Heacock and Hessler (1962) restated the fact that in auroral latitudes pearls occur primarily during the day. To return to Sucksdorff's work, he concluded that September was the most favorable month, that no 27 day recurrence pattern was evident, and that though the pulsations were local in detail, general characteristics might be spread over several hundred kilometers.

1.3 Recent Work (Observational)

In general, pulsations can be placed into two groupings, regular and irregular. A regular event is characterized by a narrow frequency spectrum, and though statistical patterns of occurrence are evident,

there is usually little correlation with other geophysical phenomena. The irregular group, on the other hand, has broad frequency spectrums and is often associated with auroras, ionospheric activity, etc.

1.3.1 Regular Pulsations

Probably the best way to subdivide these pulsations is by period, which is the method used historically, i.e. pc and pg, and which is used by many current workers. Most of the regular pulsations could be classified into three groups.

- 1) PP-pearl pulsations, with periods from 0.5 to 5 sec
- 2) Pc-continuous pulsations, " " 10 50 "
- 3) Pg-giant pulsations, " " 50 200 "

PP (pearl pulsations): Characterized by a smooth sinusoidal signal with pronounced amplitude modulation, these pulsations are among the most esthetically pleasing of all micropulsations. Attempts to relate them to other geophysical phenomena have at best met with limited success. Troitskaya (1961) indicated a tendency for them to precede magnetic storms and to coincide with increases in cosmic ray intensity. Heacock (1963) showed several examples of pearls having rather sudden onsets accompanied by increased cosmic noise absorption. However, it should be emphasized that, in general, no correlation between pearls and ionospheric data has been shown. Some authors have stated that pearls occur during magnetically quiet periods, but evidence will be presented later which indicates pearls to be independent of general magnetic activity. Possibly, the relative ease of detecting pearls at quiet times led to the

former conclusion. It has been suggested that pearls are less common at sunspot maximum (Troitskaya, 1961).

Though much of the early work, and also the work discussed in this report, are based on amplitude-time or wave-form records, increasing use is being made of frequency-time analysis. This type of display shows that pearls often have a fine-structure consisting of a series of rising frequencies. It is the overlapping of these frequencies which produce the beating observed on wave-form records. In contrast, other classes of micropulsations in the same frequency range fail to show this characteristic fine-structure. Thus, besides displaying the structure of pearls, frequency-time records provide a convenient means of objectively recognizing pearls.

The determination of the daily variation of pearls has produced a certain measure of confusion. Troitskaya (1961) states, "A statistical analysis of PP has shown that these pulsations arise in middle latitudes mainly in the evening, night, and early morning. In polar latitudes a diurnal distribution of pearls is less definite." Yet, researchers making measurements in auroral latitudes invariably come up with definite conclusions. As stated previously auroral zone pearls are essentially a daytime phenomenon, reaching a maximum in mid-afternoon. However, in contradiction to this, Yanagihara (1963) states, "The diurnal variation of the occurrence frequency (in the auroral zone) is very similar to that found in lower latitudes by Benioff." Benioff's (1960) Type A oscillations, which correspond to PP, start just before sunset, rise to a secondary peak about 2000, drop to a minimum from 2100 to 2400, then rise to the primary peak just before dawn, finally falling to zero for

the daylight hours. Now, Yanagihara does have his PP's, based on one week's data, occurring from 0200 to 0800 and again from 1600 to 2000, and this does roughly coincide with Benioff's two peaks. But, Yanagihara has two other classes of pulsations, CPsp and CPlp (continuous pulsation, short and long period, respectively), which, if they had been considered PP's, would have given them a decidedly daytime distribution. I suspect that differences in the subjective classification of micropulsations, by the individuals involved, has caused some of the reported discrepancies. From the illustrations shown in Yanagihara's paper, I would have called the CPlp example a PP, though I would not have so labeled the CPsp example. But allowing for this, one would expect PP pulsations in the auroral zone to exhibit a longer period toward afternoon, i.e., if they are manifestations of field line resonances. As will be shown later, at College there is a slight tendency in this direction, but the difference in average period is only 0.5 sec between morning and afternoon.

The consensus now, based on the more objective frequency-time analysis, is that pearls occur during the night, primarily after midnight, at low and middle latitudes, but that the time of maximum shifts toward the afternoon for high latitude stations. In an effort to explain this shift, Wentworth (1964) has suggested that differential attenuation in the ionosphere may be responsible. He calculated attenuation factors based on f_oF_2 data for Uppsala, Sweden; College, Alaska; and southern California, and adjusted the corresponding pearl data to bring them into approximate agreement. This effect could also be explained by postulating that different field lines are excited as the day progresses (Campbell and Stiltner, 1965).

Another point of contention is that of possible simultaneous properties exhibited at conjugate points. It is generally agreed that when pearls occur in one hemisphere, it is likely that there are pearls at the conjugate. However, the details at the two places are often quite different. But, occasionally the details agree, and at these times beats have been observed out of phase (Jacobs and Watanabe, 1963; Yanagihara, 1963). This result was also verified for low latitude stations (Tepley, 1964). Tepley also noted that at Canton Island, near the equator, pearls sometimes showed a double-structure, as if the station were receiving signals from both hemispheres. This apparent reflection of energy between hemispheres is used as evidence that either particles or Alfvén waves are bouncing back and forth along field lines.

Polarization of the waves is apparently elliptical in the plane perpendicular to the magnetic field lines. More will be said later about this, but suffice it for the present to remark that this is often considered evidence of Alfvén waves.

Pc (Continuous pulsations): The period of these regular pulsations can range from 10 to 50 sec. Several workers (Holmberg, 1953; Kato and Watanabe, 1957a) report two frequency groups, one with periods from 20 to 30 sec., the other around 55 sec. Holmberg's records were taken at Eskdalemuir, Scotland, which is just south of the auroral zone at 58° geomagnetic latitude. Though there is some confusion due to classification, Kato and Saito (1962) show similar results for Fredericksburg, Virginia data. This paper calls all regular pulsations with periods from 10 to 900 sec., pc, and divides these into three groups: Type I, 10-50 sec.; Type II, 50-150 sec.; Type III, 150-900 sec. Types I and II show similar

diurnal and latitudinal distributions, but Type III differs in these respects. At any rate, the occurrence maximum in Type II is about 75 sec., somewhat longer than Holmberg's second maximum. Both show the period increasing as the afternoon progresses. Santirocco and Parker (1963), using data from Bermuda, have found that the period decreases sharply between 0600 and 0900 LT, reaches a minimum at 1000 and then increases slowly during the rest of the day. Using data from 17 stations with worldwide distribution, Jacobs and Sinno (1960b) verified the existence of two frequency groups and showed, that while the period of the shorter group did not depend on latitude, the longer group tended toward shorter periods at higher latitudes. This checks with the aforementioned results. It would appear that Kato and Saito are quite right in classifying pc's into Types I and II.

Though there is some contention about the time of the diurnal maximum, it is well agreed that pc's are an essentially daytime phenomenon. The time of maximum is probably close to local noon. Hutton (1962) reports that the shorter period pc's have three maxima near the equator. These are at 6, 12, and 19 hours local time. The longer period pc's still had one maximum, noon. These results have been observed at Legon, Ghana; Bangui, Central African Republic; Paramaribo, Surinam; Hollandia, New Guinea; Guam; and Koror, Caroline Islands. (Discussion after Hutton's paper; Kato and Saito, 1962.)

In common with most magnetic pulsations, pc's are most common at the equinoxes, and least common during the winter (Holmberg, 1953), though the data is not yet fully conclusive on this point. Kato and Watanabe (1957b) agreed that the amplitudes were greatest at the equinoxes, but

felt that greater numbers were observed near the summer solstice. Also, there are indications the number of pc's increases with the sunspot cycle (Benioff, 1960; Kato and Watanabe, 1957b). A 27 day recurrence tendency has been observed along with a positive correlation with the Kp index.

A pc event is often worldwide in its distribution with strong amplitude enhancement in the auroral zone. Typically, an auroral zone amplitude will be about 10 gamma, while at lower latitudes, it will only be a few tenths of a gamma (Kato and Saito, 1962). It should be noted that most of the published results on the geographical distribution of amplitudes deal with individual events and not statistically with large numbers of events.

It has already been stated that pc's show a strong local time dependence. A study of longitudinal effects on the events should reveal whether there is also a universal time dependence. Work on this topic has been undertaken by Troitskaya (1955), Jacobs and Sinno (1960a), and Kato and Saito (1962). The middle group showed that the universal factor modulated the local factor by about 50%, with the maximum occurring at 2100 GMT in the northern hemisphere. The southern hemisphere has its maximum 12 hours later. Troitskaya earlier held that there was only a universal time dependence and that it occurred at 0400 GMT, some seven hours later than Jacob and Sinno's results. A discussion of this discrepancy appears in E. R. Hope's introduction to his translation of Troitskaya's paper. With possible reference to this topic, Shand, Wright, and Duffus (1959) report the simultaneous occurrence of pc's between Victoria, B.C. and Ralston, Alberta, in spite of there being almost 1 hour difference in longitude. This argues for a universal time dependence.

With regard to polarization the situation is again confused. Kato (1962) believes pc's to oscillate in the poloidal mode at low and middle latitudes, but in the toroidal mode at auroral latitudes. In the poloidal mode the magnetic perturbation lies in the magnetic meridian, while the other mode has the perturbation vector confined to an L shell. Thus an oscillation in the poloidal mode has no D-component. Kato shows examples from Onagawa, Japan ($\phi=28.4^\circ$). To contrast with this, Green, List, and Zengel (1962) show examples of both short and long period pc's with elliptical polarization in the horizontal plane. These records were taken at Dallas, Texas ($\phi\sim40^\circ$).

Pc's show coherence over large areas, both in relative amplitudes and phases. In fact, it was the close similarity between Victoria and Ralston that led Shand, Wright, and Duffus to conclude that pc's have no local time dependence. The above paper reports on coherence studies between a base station at Victoria and secondary stations at Albert Head, William Head, Bear Creek, Summerland, all in B. C., Ralston, Alta., and Borrego, California, respectively 0.6, 5, 31, 191, 593, and 1106 miles away. Many types of activity were recognizable at all stations. Besides pc's, this includes onsets and terminations of general magnetic activity. Of course, the near stations showed agreements in most details. But while individual excursions on the distant stations were often dissimilar, the envelopes usually showed agreement. The Z-component consistently produced the least similarity and was influenced the most by local topography. Uniform terrain, such as at Ralston produced the least Z-component in pulsations, whereas stations along the coast showed the strongest Z trace.

Pg (Giant Pulsations): As most of the observational features were noted early by such workers as Rolf, Harang, and Sucksdorff and have already been discussed, there is not too much material to add in this section. The most important properties of pg's are confinement to the auroral zone, period of around a minute, large amplitude, and infrequent occurrence.

There is some question as to the geographical extent of an individual pg event. Though there is no doubt as to its confinement to the auroral zone, its longitudinal extent is undetermined, mostly due to the lack of suitably placed stations.

Kato and Watanabe (1955 and 1956) report the existence of harmonically related periods. By plotting number of occurrences against frequency, it is seen that peaks occurred at the required intervals. Type A (Sucksdorff's classification) is claimed to have a fundamental period of 615 sec., with peaks observed at the 5th through 13th harmonics. These observations are used as evidence for some sort of resonance phenomenon.

Other Pulsations: Though pulsations with periods longer than a few minutes are beyond the scope of this chapter, perhaps a few words would be in order. Sugiura (1961) reports the existence of regular pulsations with periods from 4 to 8 minutes at College and Kotzebue, Alaska and Macquarie Island, which is south of New Zealand. Since the pulsations are elliptically polarized and show simultaneity at magnetically conjugate points, they are considered to be manifestations of hydromagnetic waves propagating in the Alfvén mode.

There is also an entire class of pulsations, covering the whole frequency spectrum, associated with magnetic storms. A good discussion of the types of pulsations to be seen during different phases of magnetic storms can be found in Troitskaya et al (1962). Wilson and Sugiura (1961) report the observed polarization properties of sudden commencements, while Ohl (1962) discusses pulsations during sudden commencements.

1.3.2 Irregular Pulsations

As a group, pulsations with irregular waveforms contrast greatly with pulsations already discussed. They occur mostly at night and during magnetically disturbed times. Often they are associated with ionospheric disturbances, auroras, and other disturbances of the upper atmosphere. The following classifications will include most of the irregular micro-pulsations:

- 1) pt - pulsation trains
- 2) aurorally associated
- 3) storm oscillations

The pt's are almost intermediate between regular and irregular pulsations. The waveform is more regular than the others and they sometimes occur during magnetically quiet periods. But still they share more characteristics with the irregular than with the regular group.

Pt - pulsation train: With a period from 40 to 120 sec., these pulsations appear as a series of damped oscillations, each series lasting from 10 to 20 minutes. Definitely confined to the night hemisphere, a maximum is observed around local midnight. As with magnetic disturbances more events are observed near the equinoxes. But curiously enough, the occurrence of pt is inversely related to the sunspot cycle (Yanagihara, 1959).

Though pt's certainly occur during magnetically quiet periods, Yanagihara reports that up to $K_p=6$, the probability of occurrence is proportional to the planetary magnetic index. In addition, pt's are often associated with magnetic bays, starting with the commencement of the bay and continuing until the bay reaches its maximum phase. Duncan (1961) reports that pt's often precede bays by about 15 minutes. Jacobs and Sinno (1960b) studied those pt's accompanying bays and divided them into pt^+ and pt^- , according to whether it was a positive or negative bay. They found pt^- to be essentially confined to the auroral zone, while pt^+ had its peak in the subauroral zone with secondary peaks in the polar and equatorial regions. Since the corresponding bays display similar properties, pt's are considered to be closely linked with them. Some workers have noted a similarity between pt and sudden commencements. To quote Duncan (1961): "The sudden commencements observed by the induction magnetometers were always oscillatory, and we have found no clear dividing line between the two phenomena; the oscillations usually termed Pt seem to be weak sudden commencements."

Secondary oscillations, called spt by Yanagihara, are often observed superimposed upon pt's. They either start simultaneously with the pt or their amplitude is enhanced at this time. Their period of 5 to 10 sec. is apparently independent of the period of the parent pt wave. Yanagihara has also observed that there is less chance of pt carrying spt at sunspot minimum.

Pt's show much greater areal extent than do the regular pulsations. Often they are almost world-wide in extent (Kato et al., 1956). Apparently, pt's occur on a GMT basis, but their amplitude, and occurrence are

modulated on a local time basis, thus giving pt's at a given station a local time dependence.

Kato et al. report that approximately 70 per cent of pt's show linear polarization, and that before local midnight the polarization lies in the NE-SW quadrants, while after midnight it rotates to the other two quadrants. For those cases showing elliptical polarization, about two-thirds of them showed clockwise rotation before midnight and counterclockwise after. Though these time dependent changes in direction are observed, the perturbation vector is nearly confined to the meridian plane, indicating an essentially poloidal oscillation (Kato and Akasofu, 1956). In a pure poloidal oscillation, all simultaneous observers would see the wave in the same phase. The fact that there is some local time dependence in the phase, indicates some degree of coupling to the toroidal mode.

Auroral Micropulsations: Much work has been done in correlating auroral, magnetic, and ionospheric activity (Troitskaya et al., 1962; Campbell and Rees, 1961; Campbell and Leinbach, 1961; Brown and Campbell, 1962). During aurora, micropulsation records usually are quite noisy and irregular in appearance. But two basically different types of pulsations must be distinguished. A fast oscillation with period of about a second occurs during the early stages of aurora, and a slower oscillation with period about 8 sec. follows the auroral breakup.

The rapid oscillations are often associated with rayed forms prior to the auroral breakup. Passage of an arc through the zenith will correspond to an enhancement of rapid pulsations. During the breakup the amplitude of these pulsations can become quite large, on the order of 10 gamma. But after breakup the aurora changes into diffuse forms, whose

luminosity will pulsate with periods from 6 to 10 sec. The magnetic pulsations then acquire a longer period and are in phase with the luminosity changes.

At the time micropulsation activity increases there is often an increase in cosmic noise absorption as recorded by riometers. Sometimes micropulsations decrease with an increase in absorption, but these are polar cap events as opposed to auroral absorption.

Because of the close correlation with aurora, the areal coherence of this type of micropulsation is probably limited to a few tens of kilometers.

Storm Micropulsations: Pulsations are generally associated with those magnetic storms which contain negative bays. Starting with the sudden commencement they will last until the bay reaches its maximum development. Campbell and Matsushita (1962) reported on 31 micropulsation storms recorded at College, Alaska. Of these, 20 were associated with full-fledged magnetic storms of the negative bay type, 3 occurred at sudden impulses (si), and the remaining 11 occurred during negative bay-shaped disturbances. The shorter period pulsations tended to occur closer to the storm onset and their amplitude increases with the K-index. Longer period oscillations of around 30 seconds tend to be independent of the K-index. During daytime storms, micropulsations sometimes showed a secondary peak about 65 minutes after the commencement (Campbell, 1959). Also associated with negative bays are auroral X-rays from electron bremsstrahlung and increased ionospheric absorption.

The frequency characteristics of storm oscillations are quite wideband, ranging from a period of a fraction of a second to a few hours.

Most workers probably limit the range from 1 second to 5 minutes. The bulk of storm pulsation energy is between 5 and 40 seconds. Sometimes regular pulsation trains which last for several minutes are observed among the other irregular pulsations. Berthold et al. (1960) reported a storm in which a 7 sec. pulsation lasted for 2.5 minutes. A check of observatory records showed these pulsations to be worldwide in extent.

Disregarding some local time modulation and latitude amplitude effects, storm micropulsations are worldwide in occurrence, with simultaneous phase everywhere (Grenet et al., 1954). However, small differences in phase over large distances have been observed with accurately timed records. For example, Berthold, using simultaneous vertical component records from Arizona and New Jersey, found that, during the storm of August 28, 1958, the Arizona pulsations lagged by 1 to 3 seconds, thus indicating propagation from east to west. The longer periods had the greater delay. Variations, with periods on the order of 15 minutes, were often reversed in sign between the two stations.

The distinction between auroral and storm micropulsations is not precise and there are some similarities between them. Both are wideband in their frequency characteristics and are associated with negative bays. Auroras are often observed in conjunction with magnetic storms and negative bays are associated with both. Thus pulsations occurring during an aurora while a magnetic storm is in progress could be classified in either group. At any rate the aurora will certainly enhance the storm micropulsations. Perhaps some of the eleven micropulsation storms which Campbell and Matsushita observed during negative bay-shaped disturbances

are auroral pulsations by my criteria. One could say that pulsations with great areal extent were storm type, while those of limited extent were auroral.

1.4 A Short Note on Classification

Recently, the IAGA passed a resolution establishing a uniform classification scheme for micropulsations. (Resolution #13 at Berkeley, 1963) Pulsations are divided into regular and irregular categories, which are further subdivided by frequency. The following compares the new scheme with that which I have used.

<u>New</u>	<u>Period Range</u>	<u>Old</u>
Regular		
pc 1	0.2 to 5 sec	PP
pc 2	5 to 10 sec	} Pc
pc 3	10 to 45 sec	
pc 4	45 to 150 sec	} Pg
pc 5	150 to 600 sec	
Irregular		
pi 1	1 to 40 sec	auroral and storm pulsations
pi 2	40 to 150 sec	Pt

Note that here the pi 1 subclass lumps all irregular pulsations from 1 to 40 sec., whereas I have tried to separate them according to apparent origin. On the other hand, I have lumped pc 4 and pc 5 together and called them Pg. The pc 2 subclass is a rather odd one. There is no morphologically distinct group in this frequency range. A few Pc's appear here and sometimes PP's intrude from the high frequency end. In general the power spectrum shows a minimum in this range.

A concise summary of notation used by various workers through the years has been given by Matsushita (1963).

1.5 Power Spectra

There is very little in the literature concerning the energy distribution throughout the entire micropulsation spectrum. A few workers (Lokken, 1961; Smith et al., 1961; Heirtzler, 1963; Oguti, 1963; Kato and Saito, 1964; Saito, 1962; Santirocco and Parker, 1963; Davidson, 1964) have produced power spectra for specific stations, over limited durations, and usually for waves with periods longer than 10 sec.

Starting with the long periods, there is usually a peak between 200 and 400 sec., corresponding to Pg. Near the auroral zone this peak is strongly emphasized. As one proceeds to lower latitudes the peak becomes smaller and moves to shorter periods.

The Pc's show two peaks, one around 65 sec. and the other between 20 and 30 sec. The former is prominent in middle latitudes, but is less pronounced at higher latitudes. Smith et al. (1961) found the short-period pc peak at 18 sec. for Austin, Texas.

Between 5 and 10 sec. is a minimum, somewhat of a no man's land, in which no morphologically distinct pulsation occurs.

The peak for PP occurs between 1 and 2 sec., with higher latitudes tending toward longer periods. This interval also contains many of the irregular pulsations produced during magnetic storms and auroral events. This means, of course, that auroral zone stations contain a higher fraction of pulsation energy in this interval than do other stations.

At still shorter periods the energy decreases until the first of the Schumann resonances is reached at 8 cps. Also in this region, energy from spheric slow tails is beginning to appear. Now we are out of the region of true magnetic micropulsations and into the region of sferics and whistlers, which are linked to worldwide thunderstorm activity.

Davidson (1964) has produced rather complete power spectra for the period range of 4.5 to 1000 sec. for micropulsations recorded in southern New Jersey. Disregarding the spectral peaks, the spectral power density B^2/f is proportional to $T^{1.3}$ for periods shorter than 13 sec., while for longer periods it is proportional to $T^{2.6}$, where T is the period. Since the spectral continuum does not show significant diurnal variation, Davidson believes that it is produced by horizontally propagating micropulsations. This would tend to cancel variations due to local time.

CHAPTER II

EQUIPMENT AND OPERATION

2.1 Equipment

Between December 1961 and April 1963 geomagnetic pulsations were recorded at College with equipment supplied by Dr. Wallace Campbell of the Central Radio Propagation Laboratory, National Bureau of Standards, Boulder, Colorado. The sensing element was a 16,000 turn loop, 1.97 meters in diameter, placed with its plane vertical and axis aligned along the magnetic meridian. After September 1962 an 8000 turn loop was used. Figure 2.1 shows a simplified block diagram of the layout. The loop output went to a preamplifier which provided sufficient gain to send the signal 1000 feet back to the main building. Here it was further amplified, filtered into three frequency channels, and sent to paper recorders.

The loop, which was a tightly wound air coil affair, was designed and built at NBS. Its output potential for a sinusoidal signal, $B = B_0 \exp i2\pi t/T$, is $V_0 = \frac{\pi^2 N D^2 B_0}{2T} = 3.06 \times 10^5 \frac{B_0}{T}$, where N is the number of turns, D the diameter in meters, T the period in seconds, and B_0 is in weber/m². (10^9 gamma = 1 weber/m²). Thus, a one gamma signal with a period of two seconds will produce a loop output of 153 microvolts.

From the loop the signal went into a solid state DC amplifier, an Electro Instruments Model A-14, which provided a gain of approximately 200, sufficient to give a good signal to noise ratio in the coaxial cable running back to the recorders. The power supply for the preamplifier was placed back at the building to eliminate possible hum pickup by the loop. Because the transistorized preamplifier was not designed to operate below 0° C, it was placed in an insulated box equipped with a heater. Once, during the period of operation, the outside temperature dipped to -52°C.

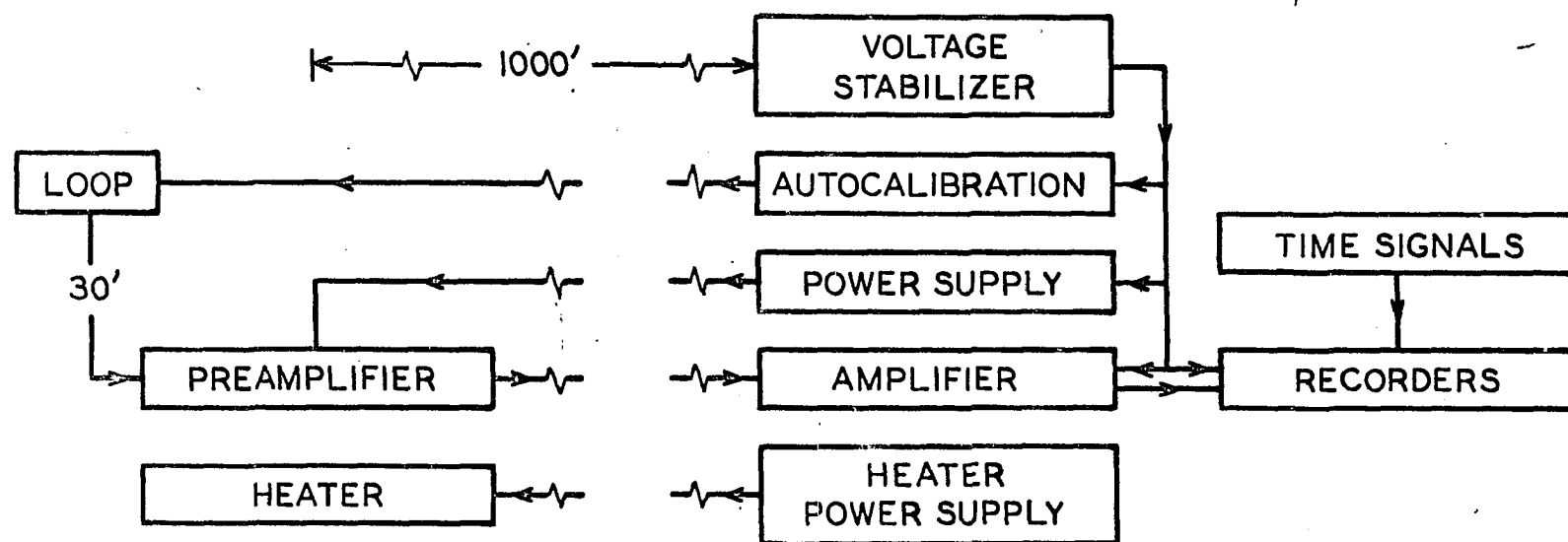


Figure 2-1
Block diagram of the system

Besides providing final gain, the amplifier built by NBS, filtered the signal into three frequency ranges, centered in turn on 0.01, 0.1, and 2 cps. These were recorded on two Texas Instruments dual channel Recti-Riters. The fourth available channel was used to record the total unfiltered loop output. Time marks were put on the records with a side pen triggered by pulses received from the Minitrack station, which is operated for NASA by the Geophysical Institute. These pulses had an accuracy within a few microseconds, which far exceeded the requirements of a paper recorder running at six inches per minute at the fastest. A relay operating once an hour eliminated the minute mark on the hour. In addition to minute marks, seconds were added with another side pen, used when operating at three inches per minute or faster. For my purposes the high frequency channel was the only one of interest. The others were recorded for NBS's purposes.

To provide a means to calibrate the recorded signal and to maintain a running check on the system's reliability, an auto-calibration unit was added. A sinusoidally varying potential of 1.3 v supplied from a mercury cell was applied to the coil and then fed back through the system. A resistor network ahead of the loop attenuated the calibrate signal by 10^4 (see Fig. 2.2). This signal was cycled between two frequencies, 0.5 and 0.067 cps. A timing unit turned on the device for a few minutes every day at a preset time. The system was calibrated for frequency response by replacing the auto-calibrate unit with a low frequency generator with a known potential output, and tuning through a range of frequencies, recording the results on the Recti-Riters. Essentially this gives the response of the preamplifier, amplifier, and recorder as a system, which is in reality an ac voltmeter of high impedance. It is now necessary

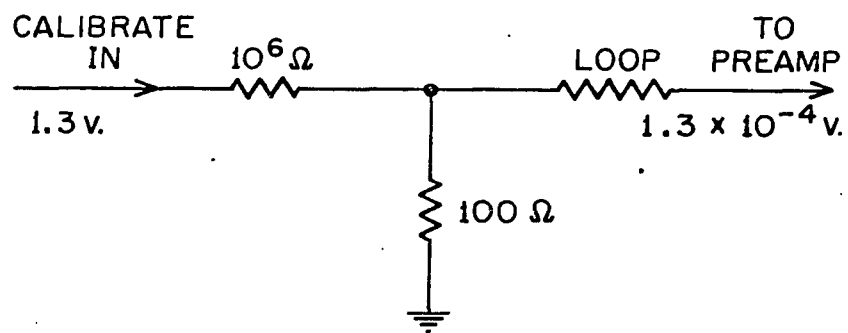


Figure 2-2

Loop input circuit for calibration unit

to consider the loop response as a function of the magnetic input. One would expect the output to be proportional to the frequency, other parameters being constant, provided one is well away from possible resonances of the loop, so that the loop can be considered as a resistance in series with a potential generator. As the lowest resonance occurred at about 130 cps, this was the case as long as the working frequencies were below 10 cps. Thus the response of the entire system to a constant magnetic signal could be obtained by plotting the recorded amplitude multiplied by the frequency against the frequency. Now all that is left is to tie the relative amplitudes to an absolute calibration. This is done by noting that the auto-calibration signal produces 1.3×10^{-4} volt peak-to-peak at the loop output, which is equivalent to a peak-to-peak magnetic signal of $\frac{B}{T} = \frac{1.3 \times 10^{-4}}{3.06 \times 10^5} = 4.25 \times 10^{-10}$ weber/m²-sec =

0.425 gamma/sec. Since this paper is primarily concerned with micro-pulsations around 0.5 cps, only the calibration of the high frequency channel will be described. For the calibrate signal, $T = 2$ sec., hence the size of the signal on the chart is 0.85 gamma at a period of 2 seconds. As the auto-calibration appears daily on the records, it is convenient to state the frequency response in terms of this signal. The results for the high frequency channel are as follows:

<u>Period</u>	<u>Frequency</u>	<u>Daily Calibration Signal is Equivalent to</u>
1 sec	1 cps	0.25 gamma
1.5	0.667	0.54
2	0.5	0.85
3	0.333	1.76
4	0.25	2.32
5	0.2	2.90

Thus it takes a magnetic pulsation 11.6 times as large at five seconds as it does at one second to produce the same size recorded signal (see Fig. 2.3).

All equipment had its line potential supplied by a Sorenson Voltage Stabilizer.

During this operation the coil was placed in a hole four feet deep. Earth packed around the base provided support with good damping characteristics, while the hole shielded the coil from wind. A wooden A-frame covered with canvas protected the top two feet of the coil from air movements. All trees within forty feet of the coil were removed, in order to reduce the chance of wind induced vibrations from reaching the coil through the ground. Fortunately, since the Fairbanks climate is noted for its lack of wind, this isn't much of a problem.

The equipment was located at the Ballaine Lake Field Site approximately a mile north of the Geophysical Institute. The coil and preamplifier were placed in a small clearing about a thousand feet west of the building which housed the rest of the equipment. The coil site was generally quiet enough, but unfortunately it proved to be swampy. Often the very act of making a clearing will produce a swamp where none existed before. Originally the ground is in permafrost. By removing the plant cover the ground receives more solar radiation forcing the frost level down. Now a pocket exists which will trap ground water and keep the soil saturated. At least this is the author's theory of why the ground was much damper during the second summer of operation. This meant that the hole filled with water during spring breakup and rainy spells. In spite of careful waterproofing, the coil would eventually leak and turns would be shorted out. This was by far the largest single source of loss of

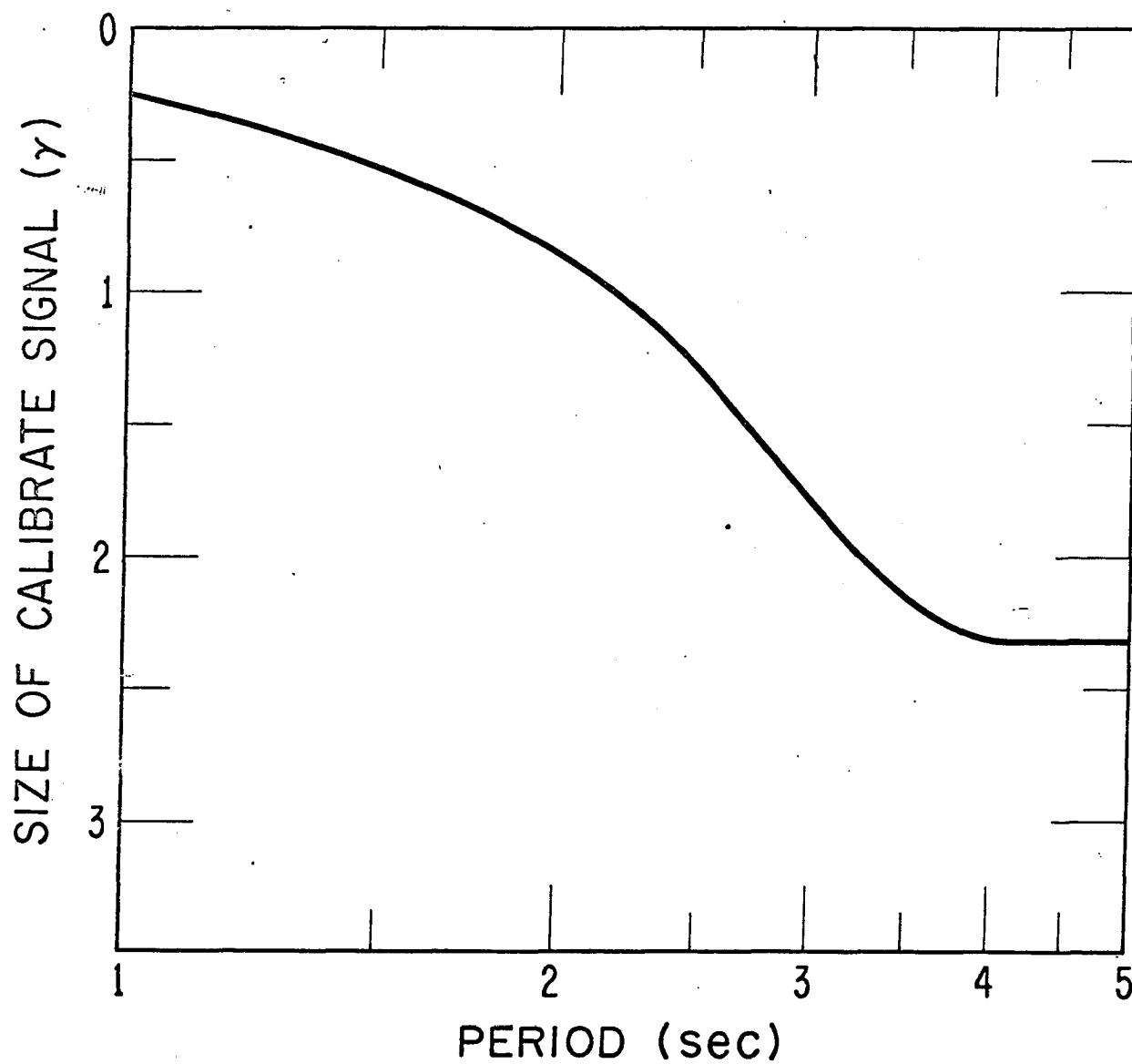


Figure 2-3

Frequency response of system

records. This problem will probably be common to any level site in interior Alaska, all of which will be poorly drained. One solution would be to choose a site on a hillside. Another would be to house the coil completely above ground in a wooden enclosure.

2.2 Operation

Normally the paper ran through the recorder at 3/4 in/min, which was the slowest speed possible that would still resolve the individual excursions during a pearl event. This also permitted once a day servicing, as a standard 100 foot roll would last a little over 26 hours at this speed. A quick summary of operation follows:

<u>Inclusive Dates</u>	<u>Chart Speed</u>	<u>Remarks</u>
12/10/61-1/3/62	3/4 in/min	
1/3/62-2/10/62	1 ft/hr	
2/10/62-2/25/62	3 in/min	also fast run at Macquarie
2/25/62-3/2/62	3/4 in/min	
3/2/62-3/6/62	3 in/min	balloon flights Macquarie and Alaska
3/6/62-3/23/62	6 in/hr	
3/23/62-4/26/62	6 in/hr and 6 in/min	photometer on 2nd channel
6/15/62-8/6/62	3/4 in/min	
8/23/62-8/28/62	3 in/min	3 components, also at Ft. Yukon
10/18/62-4/23/63	3/4 in/min	

Probably the single most valuable part of the entire program was the five days of three-component operation in conjunction with a similar program at Fort Yukon, 225 km to the north of College, during August 1962.

Three coils were oriented so as to record dH/dt , dD/dt , and dZ/dt , where H , D , and Z are the standard magnetic components. Each coil had a system associated with it similar to that described in the preceding section under equipment. Paper was fed through the recorders at three inches per minute, which provided excellent resolution, though it necessitated a chart change every six hours. This meant that every day we accumulated twelve 100 foot rolls between all the components.

Besides the five days of three-component operation in conjunction with Fort Yukon, several other special programs were run. For fifteen days commencing on February 10, 1962, fast run (3 in/min) data was taken simultaneously with similar data recorded at Macquarie Island. Also at Macquarie during this same period, R. R. Brown and company of the University of California were flying balloons recording X-rays produced by electron bremsstrahlung. Balloons were also flown from College during February and March 1962. (Anderson et al., 1962; Anger et al., 1963 Brown et al., 1963). It was intended that these two stations would provide a measure of conjugate activity. Actually Macquarie is more nearly conjugate to Kotzebue than to College. The geomagnetic latitude is about the same, but Kotzebue is about 725 km west of College. Four days of fast run were also made at the beginning of March to accompany some of the balloon runs.

During the period between March 23 and April 26, 1962, a dual channel recorder was used to compare auroral luminosity with magnetic pulsations. The micropulsations, filtered to pass only the high frequencies, were fed to one channel, while the other recorded the output of a zenith photometer set up by the optics division under Albert Belon. Covering a field of $1^\circ \times 4^\circ$, the photometer looked through a blue filter at the first negative band system of N_2^+ . During an aurora the paper was run at six inches per

minute, a speed which uses up a roll in just three hours. For the rest of the time the pace was a more leisurely six inches per hour. These speeds were chosen to take advantage of the fast-slow switch on the Recti-Riter, which changes speeds by a factor of sixty. To choose other speeds would necessitate changing gears. An automatic timer turned the photometer on at dusk and off at dawn. Spring breakup finally put a stop to the entire program. However, it made little difference to this particular aspect, with so little night left because of the advancing season.

2.3 Errors

There are several sources of non-random, but unknown errors, which enter into the calibration. To begin, the auto-calibration unit sends out a triangular wave, not a sinusoidal one. This would make no difference if the amplifiers and recorders had a flat frequency response, but in actuality some of the higher harmonics are weighted more than the fundamental. A triangular wave with peak-to-peak amplitude A can be written in a Fourier series as follows:

$$y = \frac{A}{2} \sum_{n=1}^{\infty} \frac{(-1)^{n+1} 8}{(2n-1)^2 \pi^2} \sin \frac{2(2n-1)\pi x}{T}$$

Only the odd harmonics are present and all the coefficients add absolutely to form the peak of the triangular wave. By giving each coefficient its appropriate weighting the following results are obtained for the 0.5 cps calibration signal.

<u>Harmonic</u>	<u>Coefficient</u>	<u>Weighting</u>	<u>Product</u>
1st	0.811	1.000	0.811
3rd	0.090	2.407	0.217
5th	0.032	1.956	0.063
7th	0.017	0.919	0.015
9th	0.010	0.526	0.005
11th	<u>0.007</u>	0.363	<u>0.002</u>
Sum	0.967		1.113

It can be seen that the first eleven harmonics, which account for 96.7% of the original wave, give an over-reading of 11.3%, due primarily to the large weighting given the third and fifth harmonics. Thus, apparently, all amplitudes should be increased by this factor. Unfortunately, it is not quite so simple. The system will introduce phase shifts, which depend on frequency, and hence the harmonics cannot be merely added. The absolute sum represents the maximum possible error from this source.

Ideally, it would be desirable to know the amplitudes of incoming magnetic signals without the effect of induced earth currents included. These would reduce the observed vertical component and increase the horizontal components. Though the extent of these corrections is difficult to estimate from theoretical considerations, it is believed not to exceed 20% at College and is most likely smaller. Evidence to support this is that a sizable vertical signal is observed at this station and the important properties of the signal often do not differ drastically between neighboring stations, even though the geology, and hence the ground conductivity, do change appreciably. Earth currents, on the other hand, do depend greatly on the local geology (Wescott and Hessler, 1962).

These non-random errors will not change any results in chapter three and its only effect in chapter five will be to change the tilt of polarization in the H - Z diagrams. Even here, assuming a 20% error in each component, producing a 40% error in the tangent of the inclination, the inclination only changes by 5 degrees. In the horizontal components the tendency of these two errors would be to cancel each other.

As for the random errors, most of these occur in the measurements of the charts and hence represent an absolute error, rather than a percentage error. An estimate of the inaccuracy in reading would be 2% of the calibration signal. For example, at $T = 2$ sec., the calibration equals 0.85 gamma and the error is ± 0.02 gamma. For other frequencies this error can be calculated from Fig. 2.3.

CHAPTER III

SOME PROPERTIES OF PEARLS

3.1 Introduction

Pearl pulsations or PP are one of the more esthetically pleasing and interesting of the various types of geomagnetic micropulsations. Their distinguishing characteristics are a smooth sinusoidal carrier signal of about 2 sec period and a somewhat irregular amplitude modulation. The envelope has a tendency to repeat its general shape over an interval of several minutes. Sometimes the carrier period will increase over the course of an event, but more often the period remains constant, ignoring minor fluctuations, for the entire event, which can last several hours.

These properties are illustrated in Fig. 3.1, which shows a small section of a typical pearl event, recorded at College, Alaska, on August 26, 1962. The top trace, which is the output of the high channel is the one of interest here. Chart speed in this case was 3 in/min. Both minutes and seconds are indicated along the bottom, with the minutes labeled in local standard time, i.e. 150 WMT. At this period, each small division represents 0.07 gamma.

A list of all the pearl events used in this study is given in Table 3.1.

3.2 Diurnal Variation

The question of the diurnal variation of the occurrence of pearls has already been examined to some extent in chapter one. Figure 3.2 shows the diurnal variation for all the pearl events observed at College. A day was considered to have a pearl at a specific hour if a pearl was observed within 30 minutes of that hour. The second curve, which shows f_oF_2 , can

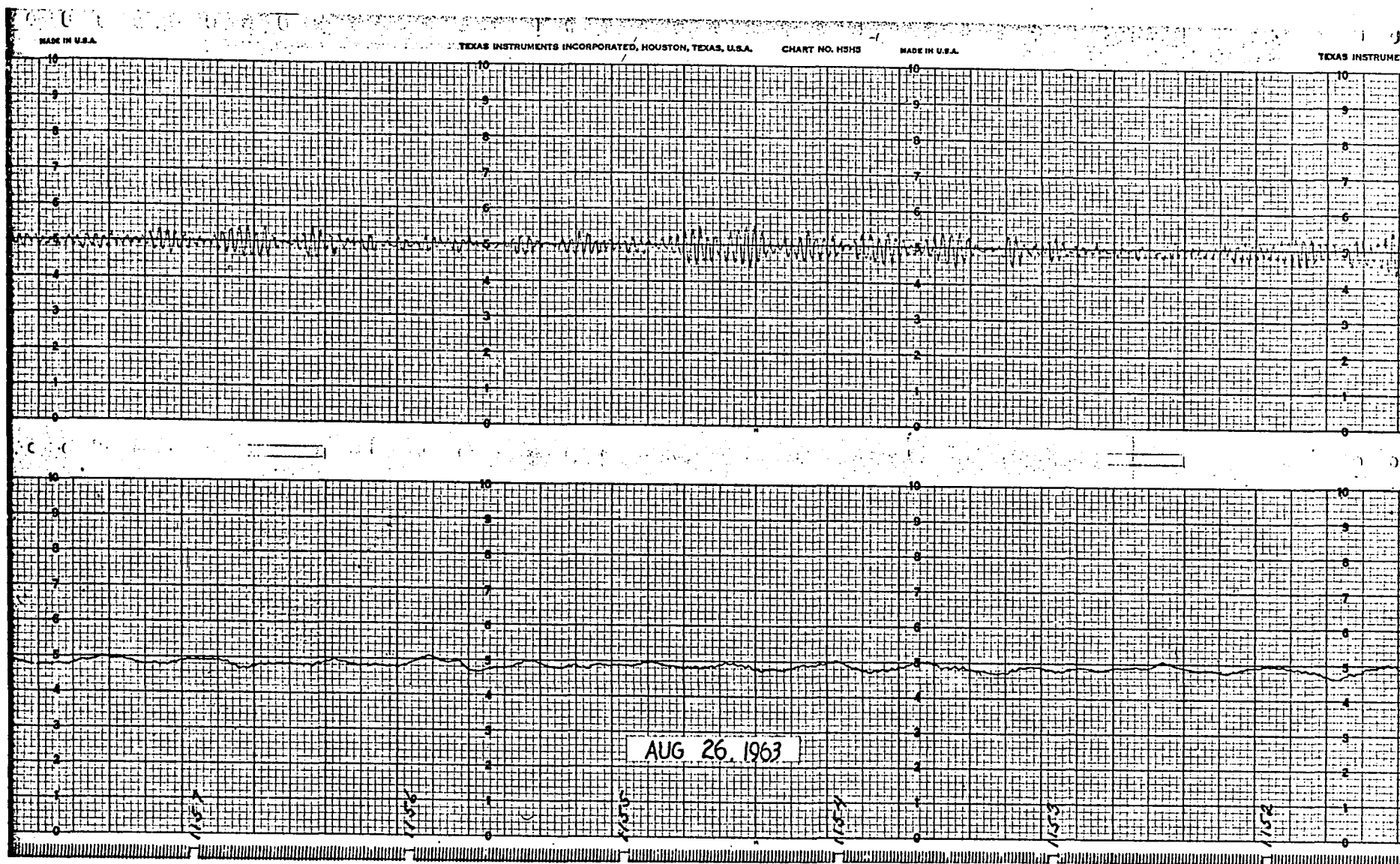


Figure 3-1

A typical pearl event at College

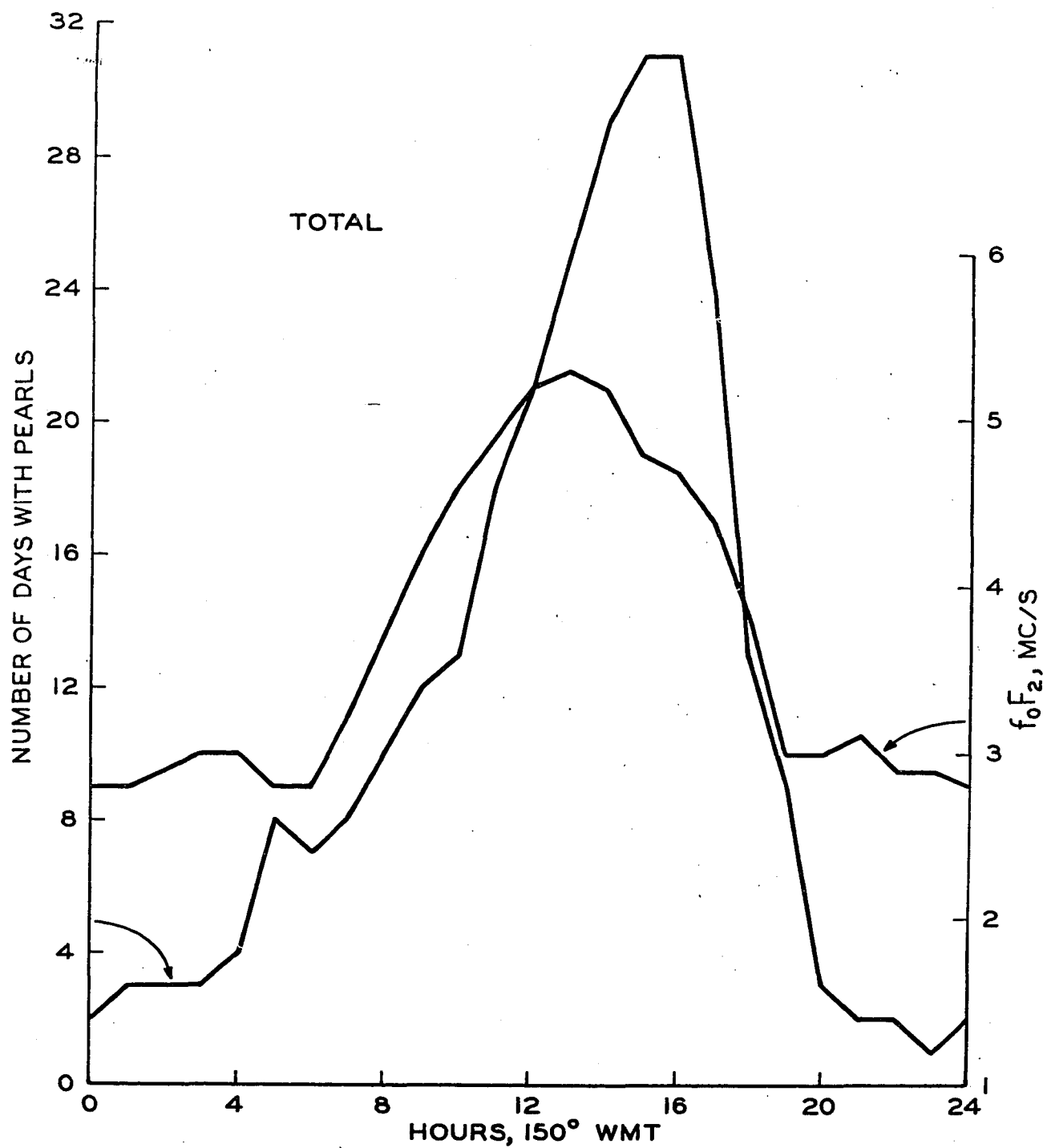


Figure 3-2

Diurnal variation for all pearls observed at College

be neglected for the present. As can be seen the curve makes a sharp — climb at about 0800, reaches a peak at 1500, and then makes a rapid decline terminating at 2000. Eighty per cent of the pearl events at College occur between 0800 and 2000. These results are similar to those obtained by R. R. Heacock at College independently with earth current equipment. Fig. 3.3 shows the variation for just the winter months. The general features are the same, but there is an interesting early morning peak at about 0530. However, this may not be significant. The similar curve for the summer months (Fig. 3.4) shows a very broad peak extending from 1100 to 1800. Since the number of events recorded during the summer was small, due mostly to equipment troubles rather than a lack of pearls, this result may not be important. Finally, the curve for the equinoctial months (Fig. 3.5) has a morning peak at 0800 in addition to the main peak at 1600. Though some of the details may be insignificant, it appears that pearls are essentially a daytime phenomenon in the auroral zone, and their main peak is in the late afternoon.

3.3 Period

The period of the pearls used in this study ranged from 1.1 sec. to 4.0 sec. (see Fig. 3.6). Most of the pearls were concentrated between 1.7 and 2.6 sec. with 2.2 sec. being the most probable value. This probably does not represent the true period distribution of pearls, as the selection has been influenced by equipment response and subjective judgment. For one thing, as the period lengthens, it becomes harder to recognize pearls of small amplitude. Some pulsations, with periods between 5 and 10 sec. and which show periodic amplitude modulation, were

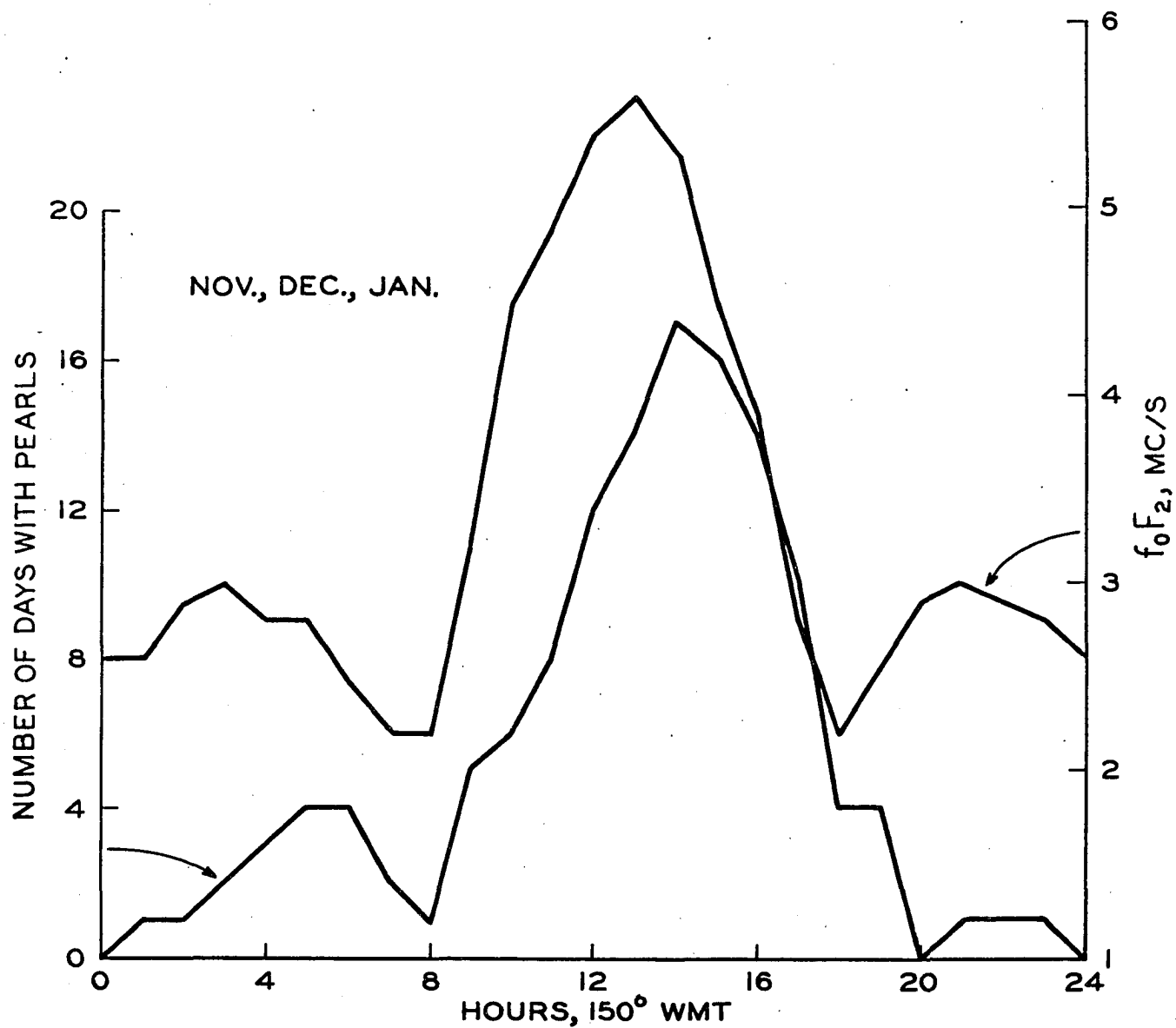


Figure 3-3
Diurnal variation for the winter months

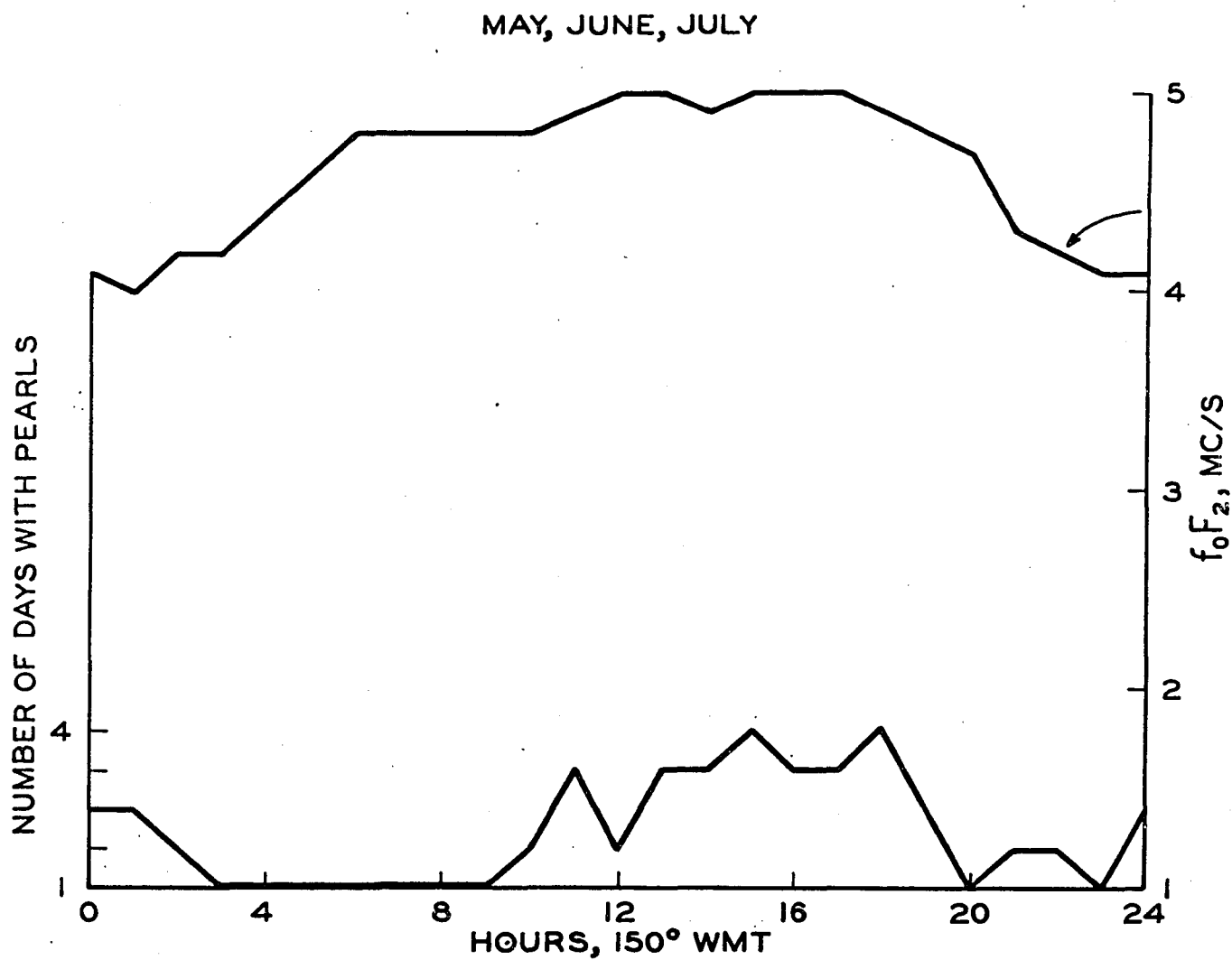


Figure 3-4
Diurnal variation for the summer months

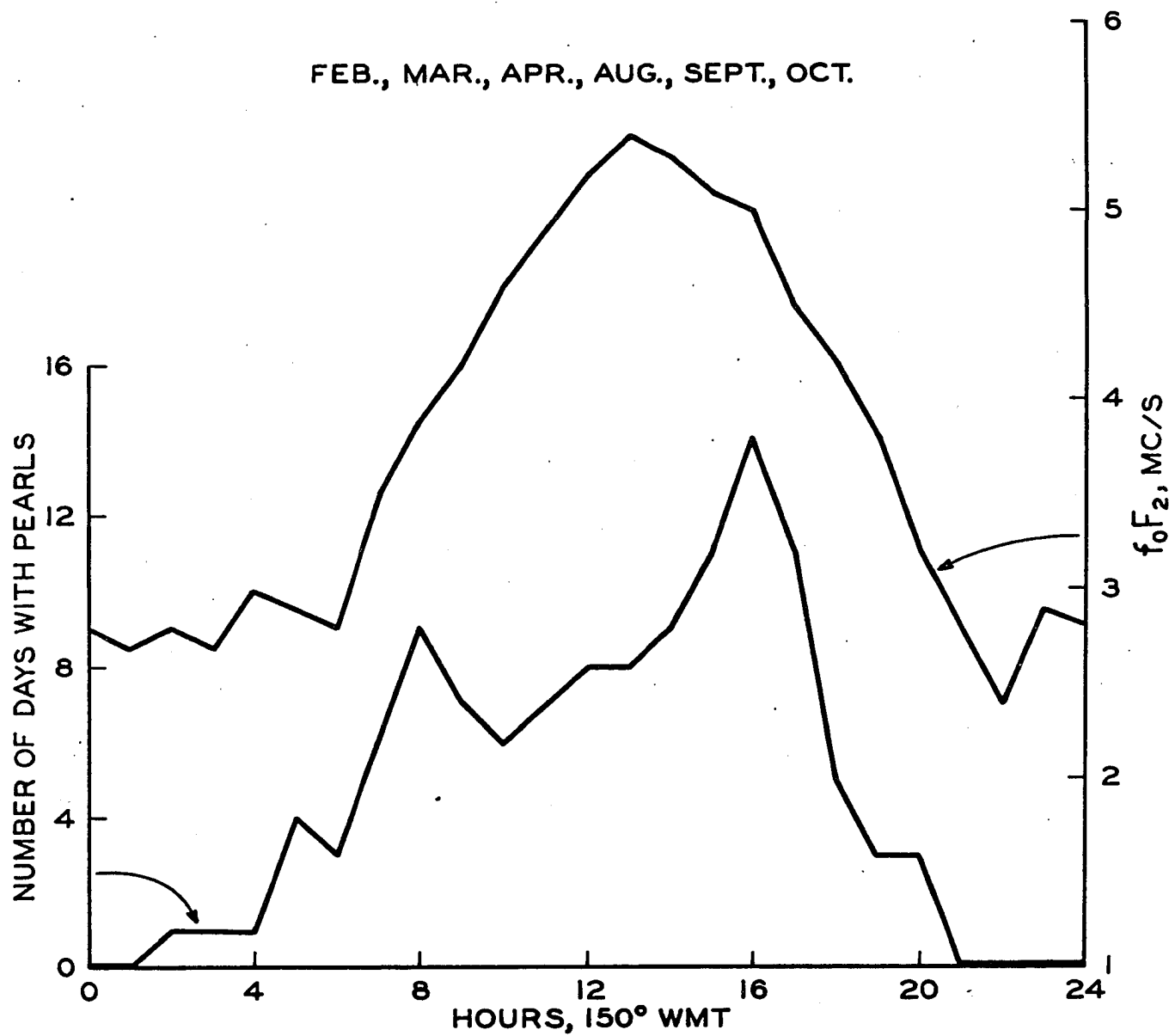


Figure 3-5
Diurnal variation for the equinoctial months

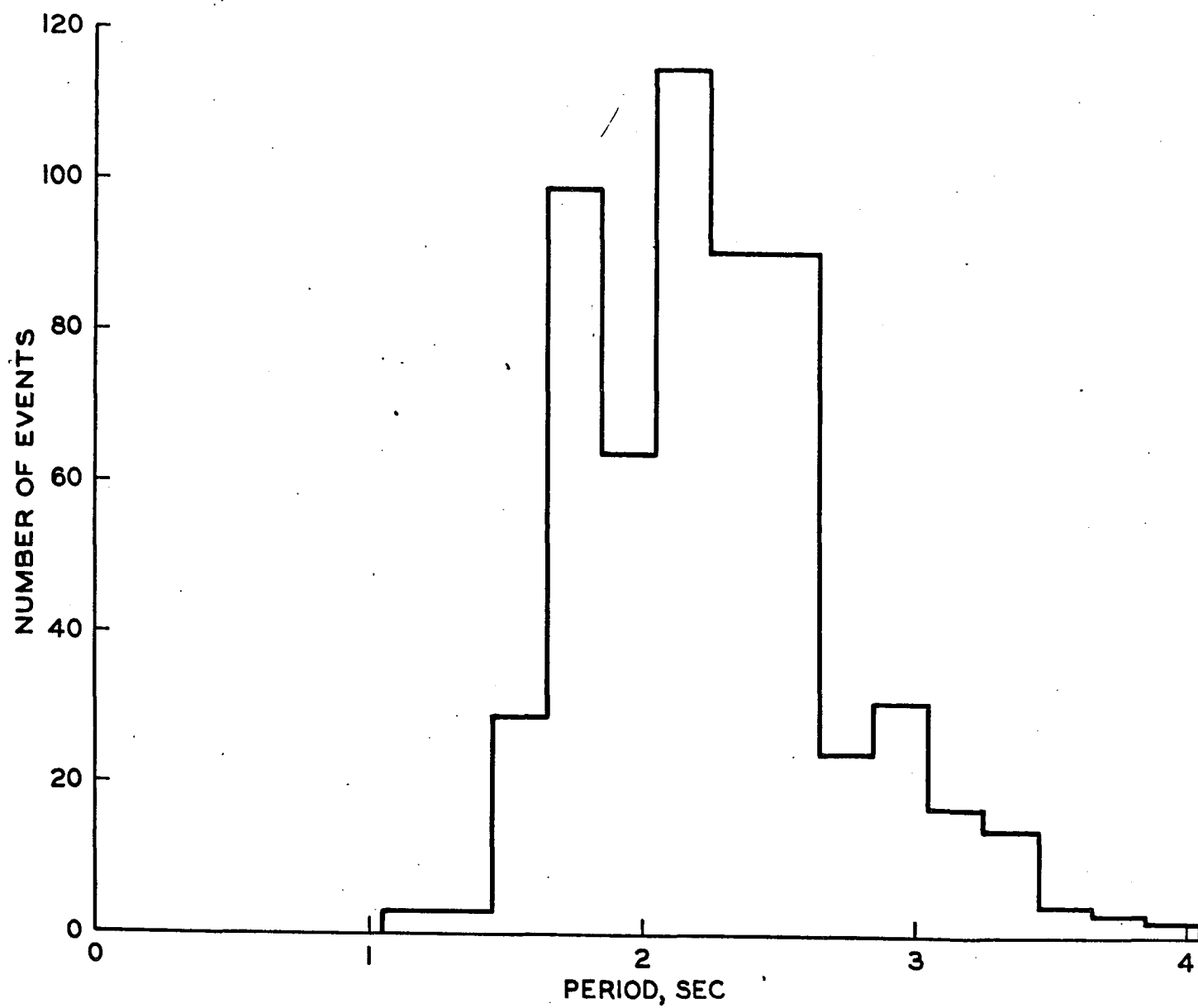


Figure 3-6
Period distribution of the pearls studied

observed. Since their period was drastically longer than most pearls, these were not counted. Of course, this was a subjective decision.

Does the period tend to vary as a function of local time? To check this a scatter plot (Fig. 3.7) was made. The points have a wide scatter, but there appears to be a slight increase in period between early morning and late afternoon, from 2.1 to 2.6 sec. This might be a result of the increase in period which some events show during their lifetime. The large excursions of the average from the horizontal during the night hours are meaningless because of the few data points in this region.

In these scatter plots each point represents a 15 minute interval during a pearl event. The arrows (in Fig. 3.8 to 3.11) mean the actual point is to the right of the point shown, either because the record went off scale or because the point is off the end of the plot. Here I thought it worth more to show more detail at the smaller amplitudes and to lose a few points off the end. These remarks apply to all the scatter plots used in the thesis.

With the exception of Fig. 3.7, a least-mean-squares straight line was computed and drawn on each of the scatter plots. Essentially, a random scatter of points, i.e. one variable does not depend on the other, means the line should be horizontal, which is the case in all the scatter plots. Because of its cyclic abscissa, Fig. 3.7 had to be treated differently. The requirement of having the same ordinate at 0 and 24 hours would guarantee a horizontal line regardless of point distribution. To circumvent this problem an average for each hourly interval was computed and the points connected by straight lines.

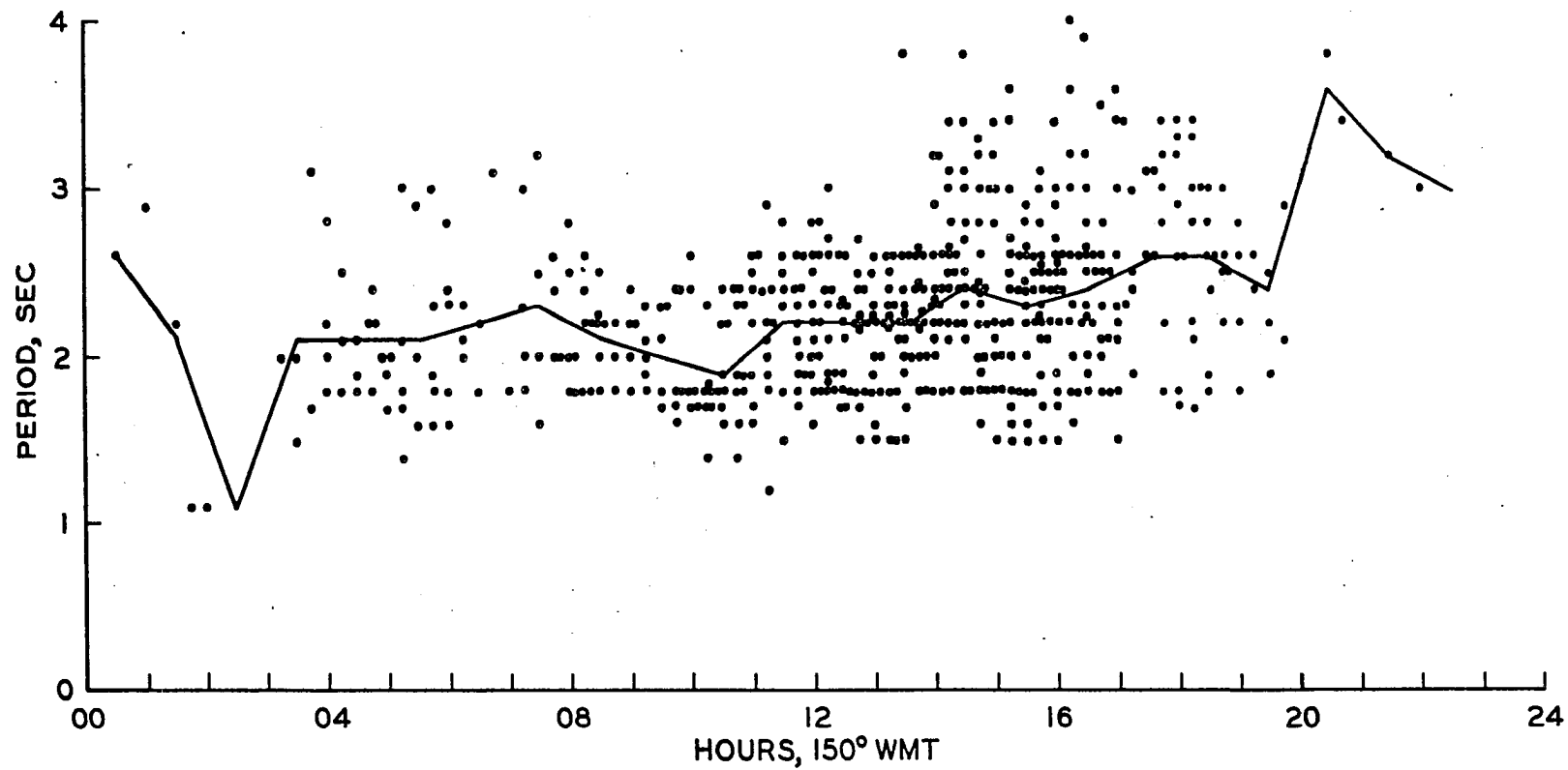


Figure 3-7
Scatter plot of period vs. local standard time

To check a possible dependence between amplitude and period, another scatter plot was made (Fig. 3.8). Again the results are random, meaning no relationship.

3.4 Correlation of Pearls with Ionospheric Data

Though pearls occur during the day at College, they have been mostly observed at night at lower latitudes. Tepley and Wentworth (1962) have postulated that the nighttime observance in California was due to lower ionospheric absorption at night. One might then explain the daytime incidence at College by saying that increased absorption, due to aurora, blocked nighttime pearls. But this would not explain why pearls are not observed on nights free of aurora. At any rate, it was considered worthwhile to see if a correlation between ionospheric parameters and pearls could be found.

College f-plots were used to compare ionospheric activity with PP micropulsations. Table 3.1 provides a list of all pearl events used in this comparison study. For each event, f_oF_2 , f-min, f_oE , fbE_s , and the magnetic K-index were tabulated beginning two hours before the event started and ending two hours after the termination of the event. During the event, peak amplitude and period of the micropulsations were tabulated at 15 minute intervals.

3.4.1 Pearls vs. f_oF_2

Figure 3.2 shows the diurnal distribution for all the pearls tabulated. Also plotted is the median value of f_oF_2 for the same months for which pearls were recorded. Figs. 3.3, 3.4, and 3.5 show similar

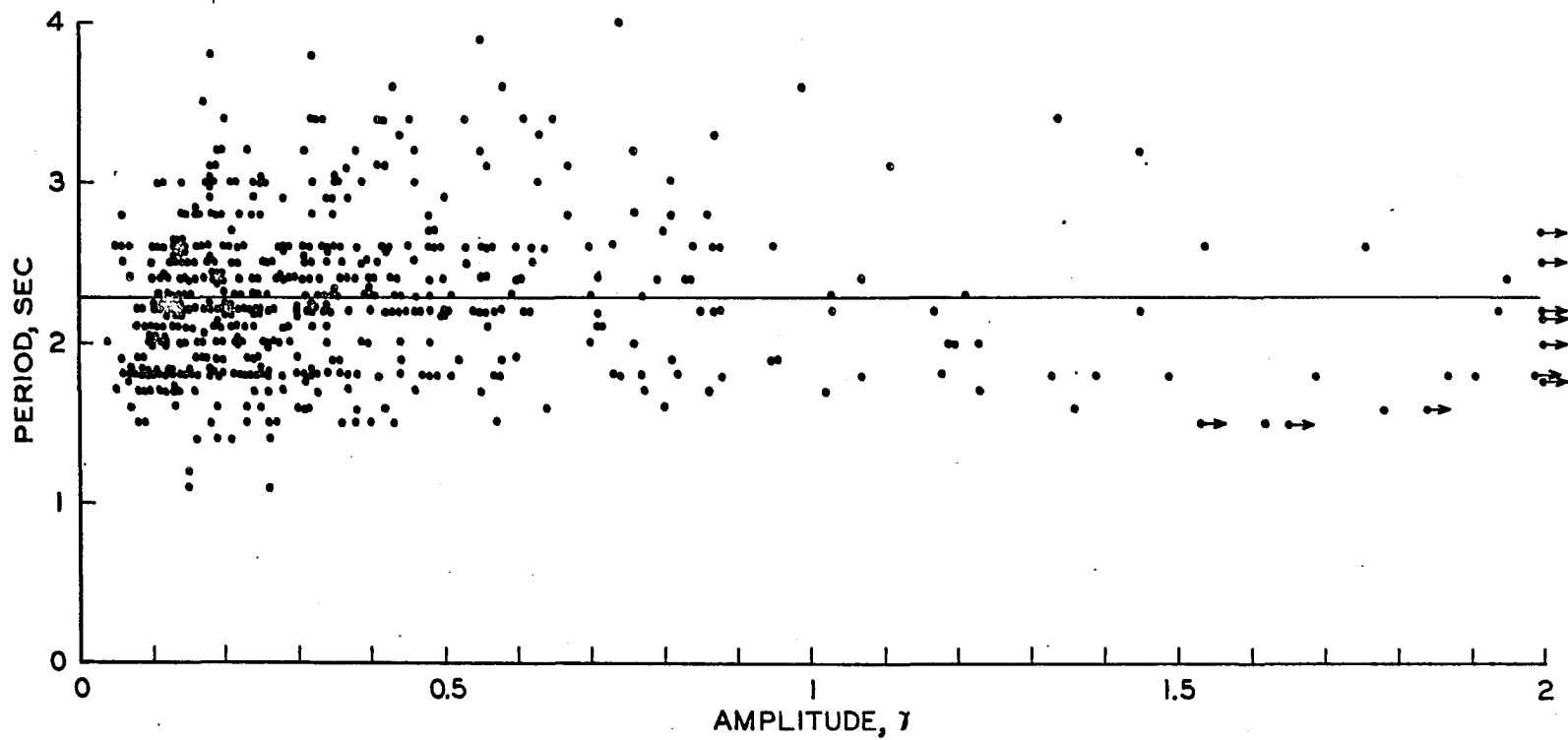


Figure 3-8
Scatter plot of period vs. amplitude

TABLE 3.1
List of Pearl Events Used in Study

Date	Time (150 WMT)	
Dec. 12, 1961	1042-1906	
18	0138-0203	
26	1451-1633	
31	1837-1844	
	2038-2110	
Jan. 1, 1962	1024-1127	
	1233-1415	
Feb. 11	0500-1308	Not used in comparison with ionospheric data
13	0220-0305	
16	1513-1633	
19	0742-0750	
20	1150-1308	
Mar. 4	1036-1318	
	1524-1659	
June 18	1304-1344	
19	0956-1056	
24	1555-1728	
26	1438-1522	
	1819-1904	
July 2	2121-2207	
20	1820-1913	
25	1056-1808	
26	1656-1748	
29	1507-1607	
29/30	2341-0055	
30	1325-1520	
31	1104-1121	
Aug. 1	1544-1807	
26	0952-1210	
Nov. 2	1412-1433	
10	0956-1702	
14	1046-1056	
27	1533-1554	
29	1303-1713	
Dec. 3	0935-1845	
6	1144-1511	
7	1306-1712	
10	1407-1541	
14	1512-1829	
16	0549-0835	
	1530-1831	
22	0319-0403	
	1633-1700	
	2216-2249	
23	0445-0519	
	0901-1433	
24	0453-0653	
	1144-1319	
25	0853-0913	
	1518-1549	

TABLE 3.1 (con't.)

Date	Time (150 WMT)
Jan. 2, 1963	1521-1602
3	0900-1500
12	1139-1343
18	1355-1424
21	0312-0604
22	0350-0553
	1333-1700
26	1330-1420
27	0851-1610
29	1158-1311
Feb. 3	1237-1610
5	0712-0746
6	0538-1651
9	0711-1154
16	1443-1500
18	1428-1540
19	1927-1954
Mar. 1	0439-0519
7	0750-0908
	1431-1930
11	1541-1619
16	1359-1611
19	1345-1352
20	0703-0832
22	0800-0834
31	1604-1952
Apr. 1	0542-0657
3	1145-1317
4	1531-1648
10	1314-1421
11	0813-1537
13	1636-1713
14	1406-1644
18	1718-1823
19	0400-0455
21	1611-1644
22	1347-1510
	1751-1830

curves for the winter (November, December, January), summer (May, June, July), and equinoctial (February, March, April, August, September, October) months, respectively. The pairs of curves show a great similarity, especially in the total and winter curves. Of course, this is only an agreement in statistics, and could be the result of both phenomena having the same ultimate cause, the sun.

Next, it was considered worthwhile to look at the relationship between individual events and f_oF_2 . Figure 3.9 shows a scatter plot of f_oF_2 vs. pearl amplitude. Each point represents a quarter hour during a pearl event. During blackout conditions no point was plotted. Pearl amplitude means the largest peak-to-peak amplitude within one minute of the f_oF_2 scaling. As can be seen, the results show essentially random scatter, which indicates that no causal relationship exists. It was thought that perhaps only the larger events would correlate with f_oF_2 . Thus, Fig. 3.10 shows a scatter plot for only those events whose amplitude exceeded 1 gamma at least once. Again the points are randomly scattered. Since f_oF_2 indicates the electron density at F_2 heights, i.e. about 300 km, it appears that changes there have little effect on pearls as recorded on the ground.

The average value of f_oF_2 for the two hours preceding pearl events was 4.6 mc/sec. During the events f_oF_2 averaged 4.6 mc/sec and for the two hours after termination the average came to 4.0 mc/sec. On several days pearl events occurred with less than four hours between them. On these occasions the average during the between pearl period was 3.9 mc/sec. The change from 4.6 to 4.0 mc/sec during an event is probably related to the fact that the average diurnal variation for f_oF_2 peaks two hours before the maximum for pearl activity and hence the two hours following an event will on the average have a lower f_oF_2 than the two hours preceding an event.

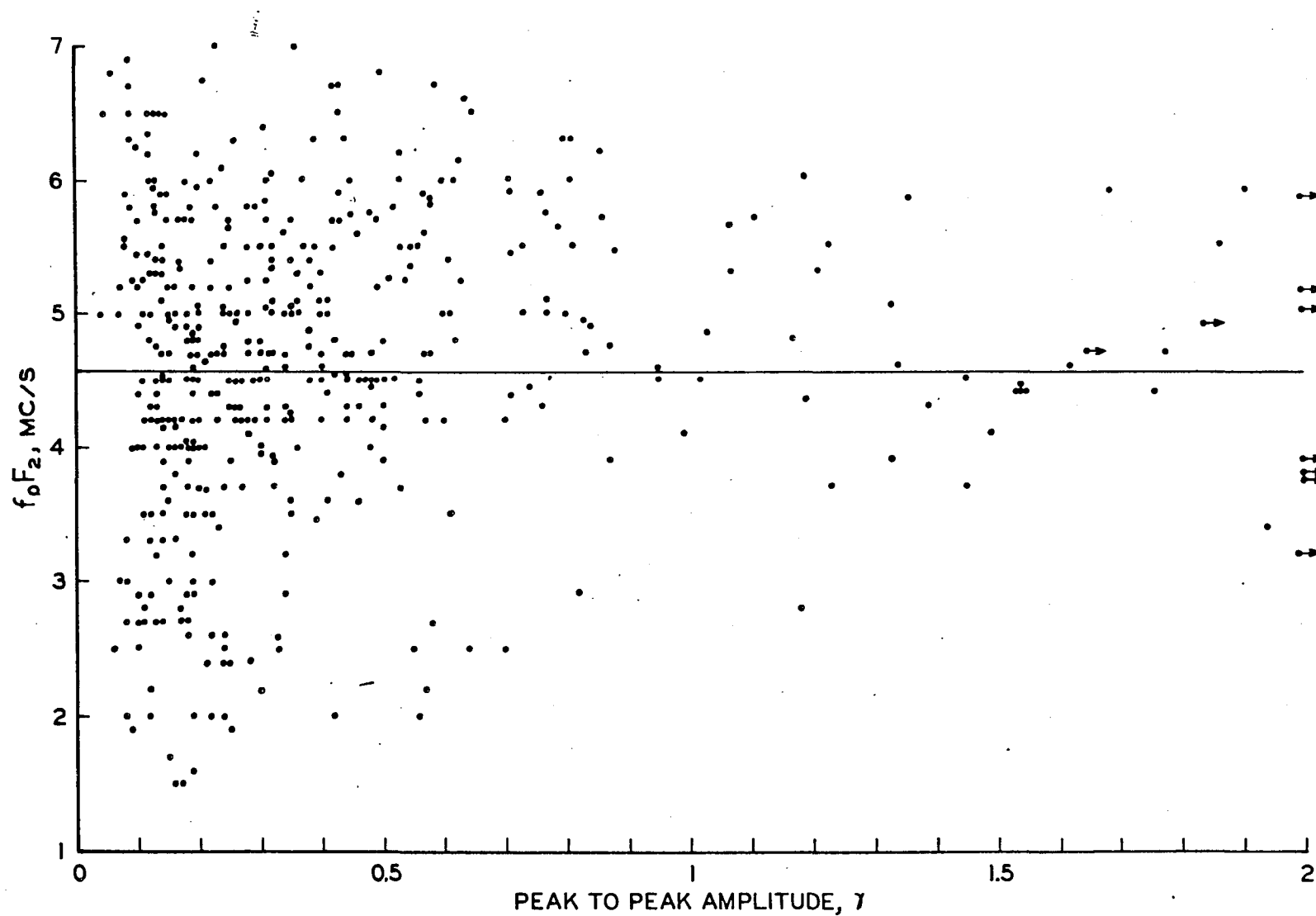


Figure 3-9

$f_0 F_2$ vs. pearl amplitude for all pearls

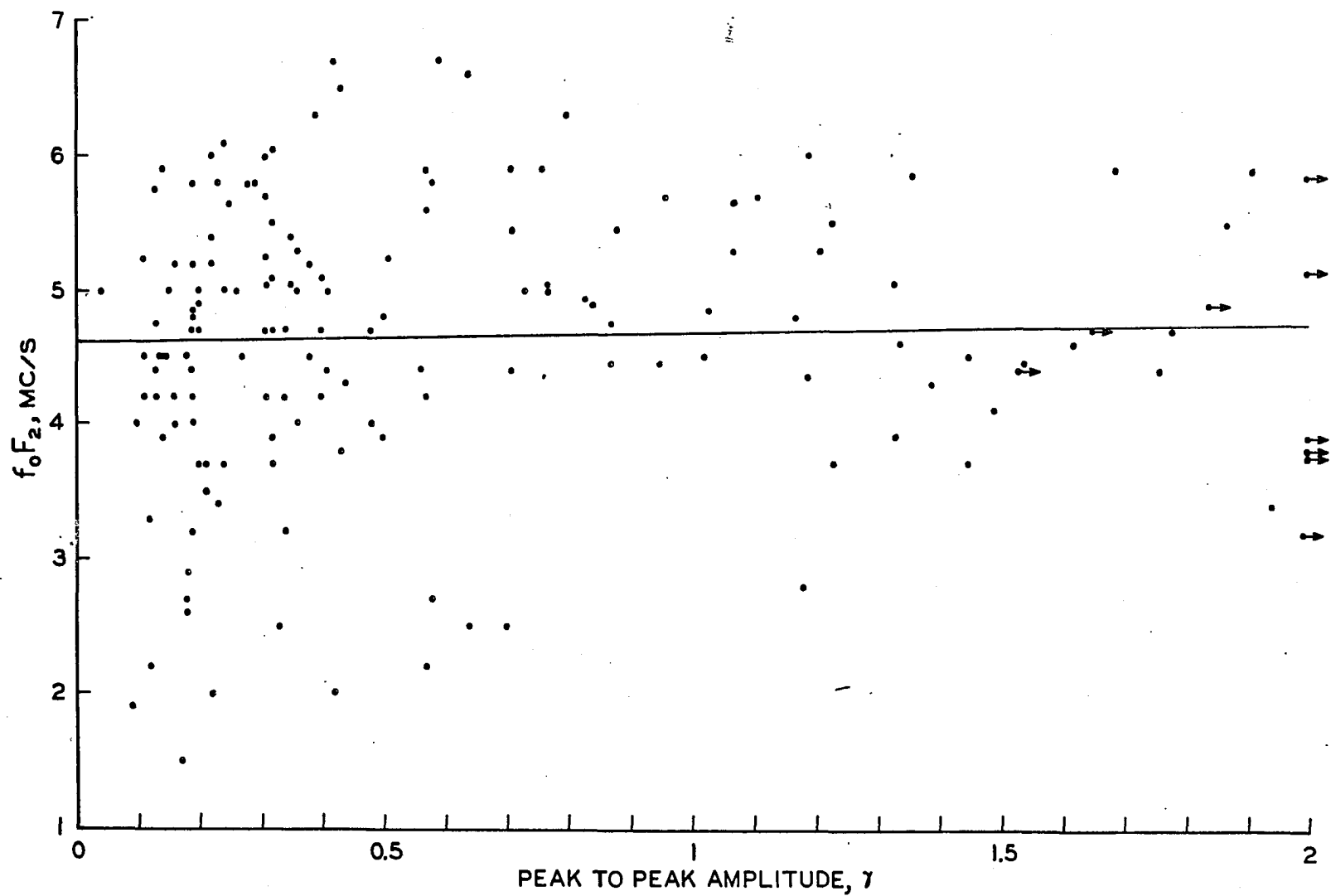


Figure 3-10

$f_o F_2$ vs. pearl amplitude for strong events (exceeded one gamma at least once)

3.4.2 Pearls vs. f-min

Figure 3.11 shows a scatter plot for f-min vs. pearl amplitude. This was made in a similar fashion to that for f_oF_2 . Again the points are random, indicating no causal relationship. Since f-min indicates loosely the electron density in the D-region, i.e. about 80 km, the propagation of pearls is probably little affected by electron density changes here.

During the two hours preceding pearls, f-min averaged 1.9 mc/sec, during the events 1.9 mc/sec, and for the two hours after events 1.8 mc/sec. For those periods between adjacent pearl events the average was 1.8 mc/sec. There appears to be no significant change here.

3.4.3 Pearls vs. foE

Unfortunately, E-layer data at College is rather limited and often unreliable. Normally foE can only be tabulated during the summer and then blanketing Es often makes the value ambiguous. To make matters worse most of the recorded pearl events occurred during the winter. No consistent changes in FoE were observed between the periods prior to pearls, during pearls, and after pearls. But because of the foregoing, no valid conclusions can be drawn from this.

3.4.4 Riometer

The riometer provides information on ionospheric electron densities by monitoring the signal strength of incoming cosmic radio noise. Greater electron densities mean greater attenuation of these signals as received on the ground. Its primary advantage over ionospheric vertical soundings is that it tells more about electron densities at heights under 100 km,

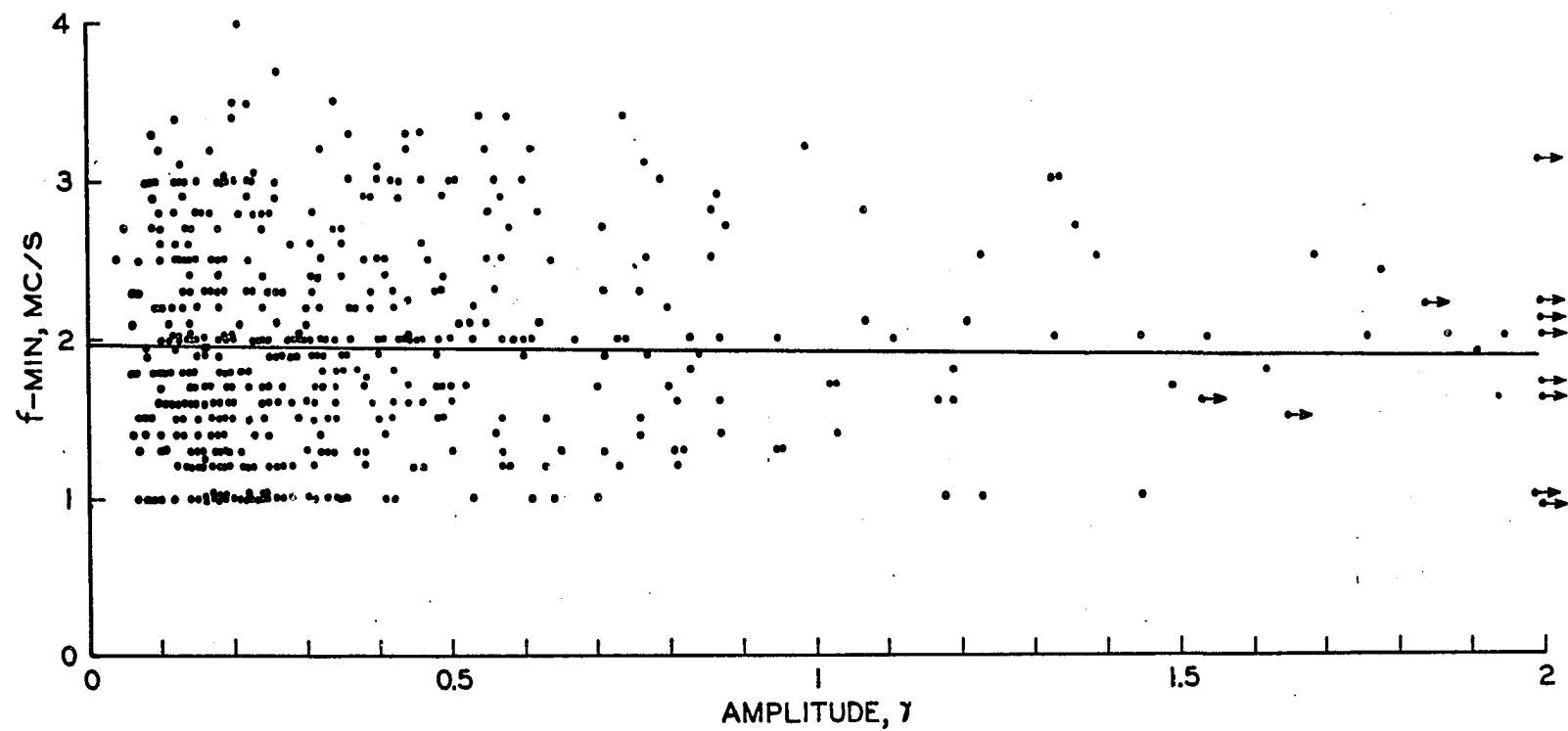


Figure 3-11
 f_{min} vs. pearl amplitude

and it provides data during radio blackouts. These instruments operate on a variety of frequencies, generally between 5 and 50 mc/sec, with the lower frequencies offering greater sensitivity. General information on radio wave absorption can be found in Basler (1963).

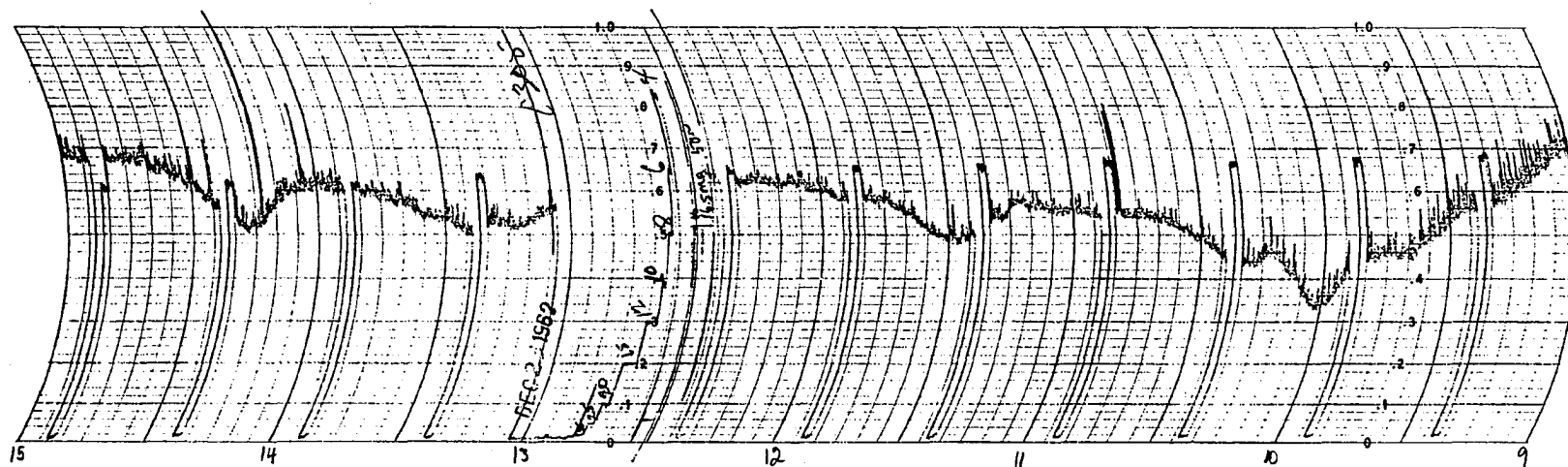
Even though hydromagnetic theory predicts greatest attenuation of Alfvén waves at about 140 km (Francis and Karplus, 1960) and riometers give information about significantly lower heights, it was considered worthwhile to examine the data. Micropulsations and riometer absorption could also be related via a common causative mechanism, the injection of particles from the solar wind. Other workers have reported occasional correlation between pearls and riometer data (Heacock, 1963), though in general, the correlation does not exist. To some extent, this duplicates the study of correlation with f-min, although f-min is controlled mostly at 80 km, while the 10 mc/sec riometer data is controlled by the electron density profile between 60 and 70 km. The 10 mc/sec records were chosen as a compromise between sufficient sensitivity and the desirability of remaining on scale during storms.

Visual comparison of College records was made for forty pearl events during 1961 and 1962. Only three showed any resemblance in activity and these will be discussed shortly. As for the others, they occurred during both quiet and active periods on the riometer. When the riometer was moderately disturbed, pearls often occurred during periods of decreasing absorption. But as a typical absorption event starts suddenly and decays slowly, this is to be expected from purely chance occurrences. Fourteen of the events occurred during quiet periods, fifteen at times with moderate riometer activity, and the remaining eleven during times of strong absorption.

Perhaps the most interesting event studied, in regard to the riometer data, is that of December 23, 1962. Lasting roughly from 0900 to 1500 (150 WMT), the event contains three peaks of activity which coincide on the micropulsation and riometer records (Fig. 3.12). A sharp peak at 1000 agrees within five minutes, while a broader peak occurs on both records at about 1130. The third peak at 1415 coincides almost exactly. Both records are quiet during the rest of the day, excepting some small amplitude micropulsation activity around 0500. The Thule riometer record is quiet during the entire time, ruling out the possibility of polar cap absorption. The College magnetograms are also very quiet at this time.

On December 26, 1961, there was a small short pearl event lasting from 1515 to 1630 with its maximum amplitude of 0.6 gamma reached at 1545. The 10 mc/sec riometer shows an increase in absorption of about 5 db at 1530. By 1600 the record has returned to normal. The rest of the day is quiet on both records. The College magnetogram is very quiet until 1457, when there is a small sudden commencement. The College magnetic observatory reported this as a ssc*, which means a sudden commencement with a small initial reverse impulse, with an amplitude of 37 gammas in the positive H-component. Sixteen magnetic observatories reported this event as a sudden impulse (si), fourteen as a storm sudden commencement (ssc*), and two as a positive bay (bp) (Lincoln, 1962). A period of slight to moderate magnetic activity follows for the next several hours, which may or may not be related to the micropulsation activity. Unfortunately, Thule riometer data for this event was unavailable.

The event of July 20, 1962 provides the third example of agreement with riometer data. Lasting from 1830 to 1900 this pearl only reached an



Micropulsation record compared with 10 mc/sec riometer record for the pearl event of Dec. 23, 1962 at College

amplitude of less than 0.2 gamma. The College riometer shows a sharp increase in absorption at 1840, with a peak at 1850, and recovery by 1905. However, it should be admitted that other similar riometer events occur on this date without micropulsation accompaniment. This makes one skeptical of the relationship between the two phenomena, but it was included as a possibility. Thule riometer records are very quiet at this time. College magnetograms show slight activity, mainly long period (about 30 min) waves.

It is obvious that only a few pearl events show any correlation with riometer absorption, and some of these are probably spurious. The remaining events are daytime, with little magnetic activity and no polar cap absorption. These absorption events appear to be of the type discussed by Z. A. Ansari (1963) in chapter six of his doctoral thesis, although Ansari's events occurred between 0800 and 1100, while mine are a few hours later.

The lack of Thule absorption notwithstanding, Ansari speculates that these may be proton events with a magnetic latitude cutoff. Another possible explanation is electrons with energies sufficient to penetrate to 60 to 70 km. Thus their contribution to the conductive regions of the ionosphere, and hence magnetic effects, would be small.

3.4.5 Pearls vs. Magnetic Activity

There are several magnetic indices tabulated which provide a measure of general magnetic activity. K-indices are computed for each three hour period by each station. K_p is the average of the results from 12 stations internationally selected and provides a planetary index for each three hour period. C_p gives a planetary index for each day. K and K_p are

logarithmic scales. In addition, A_p provides an absolute measure of worldwide magnetic activity on a daily basis. K_p is defined in J. Geophys. Res., 54, p. 296-8, 1949 and A_p in 59, p. 423-4, 1954.

The average College K-index for all the pearls studied is 1.4. The average of all K-indices for the same months used in the studies is 2.0, indicating that pearls tend to occur during periods quieter magnetically than average. But this could also be caused by the fact that pearls are essentially a daytime phenomenon and the day has less magnetic activity than the night. To check this the K-indices from 0800 to 2000 (150 WMT) for all days over the same period were averaged. This time the average was 1.4, the same as for the three hour periods containing pearls, indicating pearls to be independent of geomagnetic activity.

It might be more meaningful to use K_p , instead of the local K-index, as a measure of general activity. This would eliminate diurnal effects and the effect of local ionospheric currents. The average K_p -index during pearl events was 1.8, while the overall average was 2.0. The small difference here is probably insignificant. It should also be noted that there is a subjective bias toward quieter times, as it is easier to recognize pearls when other disturbances are at a minimum. Strong pearls have been observed during major magnetic storms, indicating they do occur at disturbed times.

3.4.6 Pearls vs. Blackouts

In order to determine the possible effects of ionospheric blackouts, pearl amplitudes were averaged for blackout and non-blackout conditions. During blackouts the average amplitude computed from 54 tabulations was

0.32 gamma. For non-blackout conditions, 524 entries gave 0.41 gamma. The overall average was 0.40 gamma. A difference of 0.09 gamma between the two conditions is probably insignificant inasmuch as the standard deviation was 0.40 gamma.

The foregoing results indicate that there are no significant changes in ionospheric values in the period preceding, during, and following a pearl event. It would be of interest to compare the average daytime f_oF_2 and f_{min} for days that had pearls and days that did not. If there were significant differences it might indicate that on some days the ionosphere is more propitious to the transmission of pearls.

Table 3.2 gives these averages by the month. Only values of f_{min} and f_oF_2 between the hours of 0800 and 1900 (150 WMT) inclusive were considered, as these are the hours most likely to have pearls. Averaging in the more disturbed nighttime values would only complicate the situation. In computing the total average, the monthly averages were weighted according to the number of days in each category. Again the results indicate a negative correlation.

It should be emphasized that a negative proposition is difficult to prove. The most that can be said, is that the data do not support any relation between pearls and the ionosphere.

3.5 Areal Extent

Because of the lack of simultaneous data and the distance between stations it is difficult to make positive statements on the question of the extent of a pearl event.

Data from Australia's Macquarie Island shows many of the same pearls observed at College. The reason for believing them to be the same pearls

TABLE 3.2

Monthly Daytime Averages of f_{\min} and f_oF_2
for Days with Pearls and for Days without Pearls

	f_{\min} (mc/sec)		f_oF_2 (mc/sec)	
	<u>No pearls</u>	<u>Pearls</u>	<u>No pearls</u>	<u>Pearls</u>
Dec. 1961	1.8	1.8	4.4	4.7
Jan. 1962	1.4	1.9	4.2	4.8
Feb.	2.1	2.4	4.9	5.0
Mar.	2.2	2.1	5.3	5.3
Jun.	2.1	1.8	5.0	5.3
Jul.	1.9	2.1	4.7	4.3
Aug.	2.1	2.0	4.4	4.2
Oct.	2.6	none recorded	4.6	
Nov.	2.5	2.5	4.5	4.6
Dec.	2.0	2.0	3.8	4.2
Jan. 1963	2.0	2.2	3.8	4.1
Feb.	1.9	2.3	4.4	4.4
Mar.	1.8	2.0	4.4	4.8
Apr.	2.0	2.1	4.0	4.2
Total Average	2.0	2.1	4.4	4.4

and discussion of the conjugacy between College and Macquarie are given in the next chapter. If it is believed that pearls are likely to occur simultaneously at conjugate points, then since Macquarie's conjugate point is about 1000 km west of College, pearls must, at least occasionally, have this extent.

Campbell examined simultaneous data from Fort Yukon and College, and often found differences as far as pearls were concerned (private communication). Since Fort Yukon is only 227 km north of College, this indicates that pearls can be fairly well confined along a meridian.

However, R. R. Heacock informs me that he has been able to match College pearls with ones observed by Lee Tepley in southern California. Both investigators have been using frequency vs. time analysis (sonagram) and have demonstrated striking similarities in some events. It is not known how often such comparisons can be made nor are the relative polarizations known. Since the two stations are drastically different in both latitude and longitude, the existence of such similarities implies great areal extent to a pearl event.

This question of extent is still unsettled and the data and interpretations at present conflicting. The resolution of this point would be a great aid in developing causative models for the creation of pearls.

CHAPTER IV

CONJUGATE RELATIONS BETWEEN COLLEGE AND MACQUARIE

4.1 General

During December 1961, January, and February 1962, Dr. Campbell operated a micropulsation station, identical to the one at College, at Macquarie Island, an Australian station located between Australia and Antarctica. With geomagnetic coordinates of 61.1°S , 243.1°E , it is nearly conjugate to Kotzebue, Alaska. College, with coordinates of 64.7°N , 256.5°E , is about 725 km east of the conjugate point. Wescott and Mather (1964) have worked on the problem of linking conjugate points and deciding the areal extent over which conjugate phenomena can be expected. A full discussion appears in their final report.

Data taken at 5/8 in/min was available for the inclusive dates, December 19, 1961 to February 28, 1962. This chart speed on Australia's 50 cps power is equivalent to 3/4 in/min at 60 cps. The data from February 10 to 24 were only available as Ozalid copies. Since these copies were not as legible as the originals, the data is not quite as reliable as the rest. Primarily, this would affect recognizing pearls of small amplitude.

Pearls seem to occur frequently at Macquarie, as they were recorded on half of the days (36 out of 72) for which records were available. These events with their terminal times are listed in Table 4.1. One obvious feature of the list is the preponderance of morning events. A plot of the diurnal distribution (Fig. 4.1) shows a peak at 0800 and a smaller peak at 1400 LT. Though Macquarie nominally uses 150 EMT to coincide with the east coast of Australia, 165 EMT is used here as the local time for

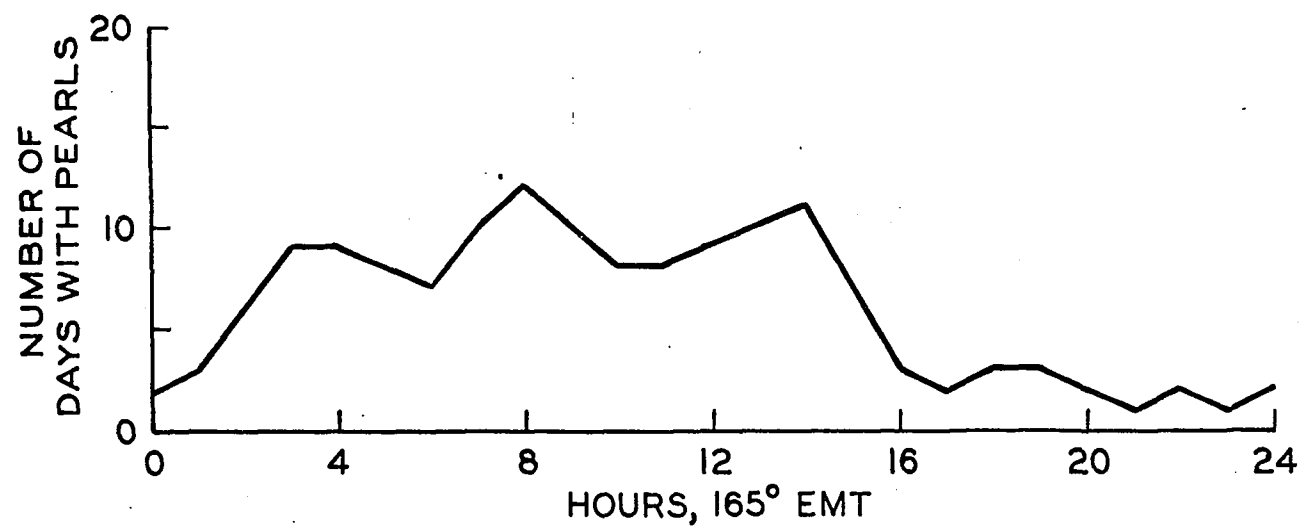


Figure 4-1

Diurnal variation of pearls at Macquarie Island

TABLE 4.1

List of Pearls Recorded at Macquarie Island

<u>Date</u>	<u>Time (165 EMT)</u>
Dec. 24, 1961	0325-0511
26	1941-2010
27	1201-1258
	1408-1615
Jan. 1, 1962	1746-1809
2	0435-1320
5	0804-0910
6	0503-1020
7	0743-0940
8	0516-0802
9	0203-0258
11	1416-1437
14	0037-0133
	0255-0422
	0632-0648
16	0313-0342
17	0334-0351
18	0641-1449
19	0355-1520
	1800-1959
26	0700-0739
	2132-2140
28	0153-0521
30	1900-1916
Feb. 2	0536-0815
	1355-1406
3	0953-1105
4	2041-2323
5	1327-1416
6	0621-0924
10	0801-1400
11	0833-1453
12	0019-0456
	1208-1450
14	1127-1428
	1702-1832
15	1537-1643
16	0222-0327
17	1410-1422
19	0308-0401
20	1124-1309
	1453-1608
21	0234-0929
26/27	2353-0231

the station. It should be remembered that this distribution may not be representative of the entire year, but only of the summer and fall equinoctial months. Here 63 per cent of the pearls occurred in the forenoon as opposed to only 29 per cent for the summer and equinoctial months at College.

4.2 Coincidence with College

A quick check with the list of College pearls reveals that only 15 out of 44 Macquarie pearls can be matched with College. However, for five of the events I had no data, and it is possible that a pearl occurring at College was just too weak to be observed.

Here R. R. Heacock helped by loaning me his College earth current records. This not only filled in some of the gaps but provided a more sensitive monitoring of College micropulsations.

To digress a moment; earth current installations are cheaper, easier to set up, and often show greater sensitivity than induction magnetometers. The advantage of the latter is that they allow quantitative measurements and three component recording. Earth currents are affected by the local geology with respect to both directions and magnitude. Finally, measurement of the vertical component with earth current equipment is difficult.

Using earth current records in conjunction with the magnetic records, pearls, or suspected pearls, were found at College during 27 out of 44 Macquarie events. Table 4.2 lists all pearls and their terminal times for both stations during the period Macquarie was in operation. On many of them the times of beginning and or end agree within a few minutes. Others do not agree as well. The question marks after some of the College events indicate the amplitude was so small as to make their identification as

TABLE 4.2

A Comparison of Pearls at College and Macquarie

Period covered is December 19, 1961 to February 10, 1962 and February 24 to February 28, 1962. All times in UT.

E from earth current records taken by R. R. Heacock
 M from magnetic induction records (NBS's coil)
 EM earth current data missing
 MM magnetic data missing
 ? identification as PP not positive

<u>Date</u>	<u>College</u>	<u>Macquarie</u>
Dec. 22, 1961	1151-1223 ? E	
23	1629-1810 E	1625-1811
24	0426-0438 ? E	
26	0837-0906 E	0841-0910
27	0051-0233 M, EM	0101-0158
	EM, MM	0308-0515
Jan. 1, 1962	0305-0716 E, M	0646-0709
1/2	1500-0152 E, M	1735-0220
4	2001-2250 E, M	2104-2210
5	1400-2334 ? E, M	1803-2320
6	EM, MM	2043-2240
7	1809-2054 E, M	1816-2102
8		1503-1558
	2027-2128 E, MM	
11		0316-0337
	0400-0434 ? E	
12	1826-1846 E	
12/13	2015-0245 E	
13	1028-1445 ? E, M	1337-1433
	1610-1710 ? E, M	1555-1722
		1932-1948
14	0115-0345 ? E	
15	1540-1645 ? E, M	1613-1642
16		1634-1651
17/18	1746-0330 E, M	1941-0349
18/19	1810-2400* E, M	1655-0420
19	EM, MM	0700-0859
22/23	2155-0145 E	
23	1806-1831 E	
23/24	1955-0105 E	
25	1324-1652 E	
25/26	1941-0012 E, M	2000-2039
26		1032-1040
27	1454-1633 ? E, M	1453-1821
	EM, MM	0800-0816

TABLE 4.2 (con't)

<u>Date</u>	<u>College</u>		<u>Macquarie</u>
Feb. 1, 1962	2104-2225	E	1836-2115
2	0243-0307	E	0255-0306
2/3	2212-2357	E	2253-0005
4	0945-1112	E	0941-1223
5		EM	0227-0316
		EM	1921-2224
7	0226-0239	? E	
9/10			2101-0300
10/11	1900-0220	E	2133-0353
11	1301-2308	E, M	1319-1756
12	0014-0345	E	0108-0350
13	0428-0545	E	
	1220-1305	M	
14	0100-0304	E	0027-0328
			0602-0732
15			0437-0543
	1525-1620	? E	1522-1627
16	0134-0236	? E	
17	0113-0233	M	
			0310-0322
19		EM	1608-1701
	1742-1750	M, EM	
20			0024-0209
	0250-0445	E	0353-0508
	1609-2308	E, M	1534-2229
24/25	2302-0015	? E	
26	1240-1531	E, MM	1253-1531

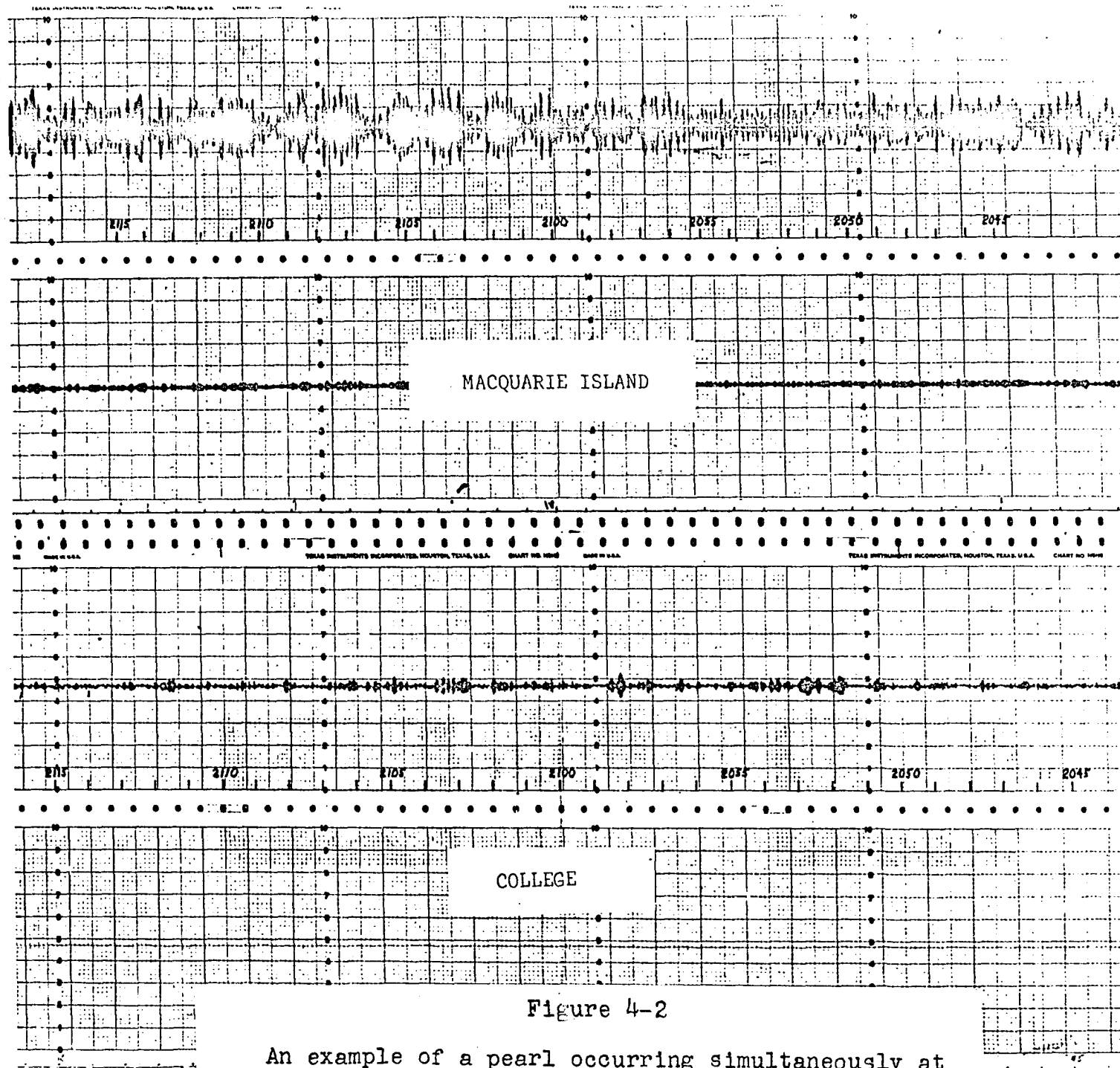
*No College data available for January 19, 1962.

pearls doubtful. Normally these would not have been listed, but some of them occurred at the same time as definitely identified events at Macquarie. Several others of similar appearance were then listed, on the basis they were also pearls of small amplitude. Four of the events, December 23, December 26, January 7, and February 15, have terminal times which agree within ten minutes, and four more agree within thirty minutes. The agreement is much better than would be expected by chance, if the events were not related. Out of the 17 Macquarie events which cannot be matched with College, 7 came during times for which no earth current records were available, and for 4 of these no College data at all was available. Thus, perhaps about 70 per cent of the pearls observed at Macquarie can be seen at College with sensitive, fast-run equipment.

Conversely, one could say that 27 out of 45, or 60 per cent, College events were observed at Macquarie. The difference in percentages, depending on the direction of comparison, is probably insignificant, as this much difference could be accounted for by the difference in the sensitivity and quality of the records.

Though a good correlation exists between the events themselves, it appears to be difficult to produce a one-to-one correspondence with the individual beats. A comparison of fifteen minutes of a pearl event is seen in Fig. 4.2. The beats are seen to be independent of one another. When looking at the entire event, it is also seen that the times of greatest amplitude do not coincide. By this, is meant the portion of the event when the beats reach their greatest amplitude.

The failure of Macquarie and College to be exact conjugates could explain the difference in the times of greatest amplitude. As the



An example of a pearl occurring simultaneously at Macquarie and College, Jan. 1, 1962, 2050-2105 UT

envelope shape on amplitude-time records is probably a beating effect caused by the simultaneous presence of several frequencies, slight changes in the frequency structure could produce large changes in the envelope. Thus differences in the envelopes between conjugate points may not be of significance. The nature of the frequency structure is of greater importance, but, unfortunately, frequency-time records for these stations were not available. Evidence that pearls at Macquarie and College have similar frequency characteristics is given in the next section.

4.3 Comparison of Period at Conjugate Points

In contrast to the disagreements of the previous sections there is one detail that does compare, and that is the period of the carrier wave. Figure 4.4 compares the period for the duration of the event of February 21, 1962. The period was calculated at approximately five minute intervals by measuring over ten cycles. Gaps in the graph indicate nonexistence of pearls. In the early part of the event, both College and Macquarie had a period of about 1 sec. Then the pearls disappeared and when they returned, both stations had a period of 1.3 sec. But after a short time the pearls disappeared again at College. This time they returned much later at a period of 1.6 sec., which did not agree with Macquarie. Note that Macquarie had pearls continuously for six hours, during which the period remained constant, barring minor fluctuations. It looks as if the first two parts of the College event were the same event that Macquarie was seeing, but that later the two stations were looking at different events. Figure 4.3 compares the event of February 11, 1962. Here the period increases from 1.5 sec. to 1.9 sec. and then decreases

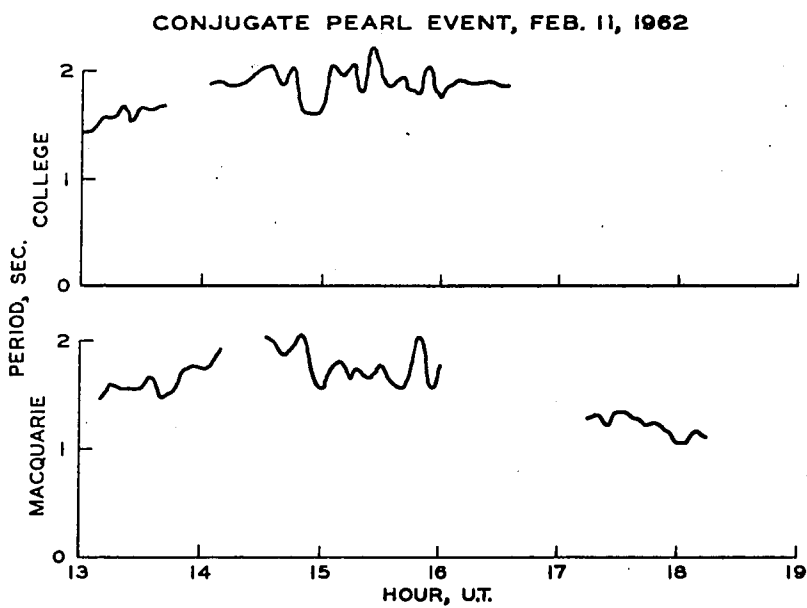


Figure 4-3

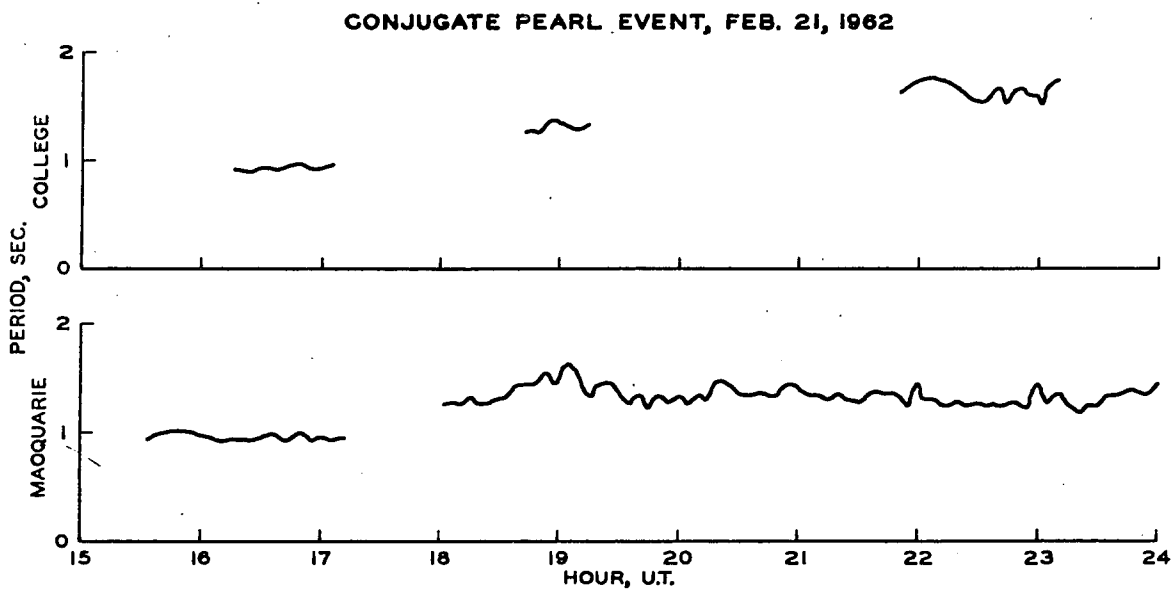


Figure 4-4

Comparison of period at conjugate points

slowly at Macquarie. The agreement in frequency changes between the two stations is good, even to the point of including some minor fluctuations, though the latter may be coincidental. This provides strong evidence that the same pearl can be observed simultaneously at conjugate areas.

CHAPTER V
THE POLARIZATION OF PEARLS

5.1 General

From a theoretical standpoint, the polarization of an observed wave is one of its most important properties. From this can be gleaned information about possible modes of propagation and models to explain their generation. Thus, it was important to obtain some three-component measurements of pearls. Such data was taken between August 23 and 28, 1962 at a paper speed of 3 in/min. This speed provided good resolution, but also produced 1200 feet of records per day, making for a storage and handling problem. During the same period Wallace Campbell collected three-component data at Fort Yukon. Two particularly good pearl events were recorded, one from 0256 to 0431 UT on August 16, and the other from 1952 to 2210 on August 26.

5.2 Method of Analysis

To begin with, short sections of record containing good beats were selected for a detailed analysis of polarization. First a base line for each component was determined by averaging the ordinates of the peaks on both sides over the beat. Base line drift over short intervals is negligible. Then the deviations from the base line were scaled at 0.01 inch intervals, which is equivalent to 0.2 second in time, and adjusted for differences in scale factors between components. Possible errors in alignment between the recording pen and the side pen, marking time, can be accounted for by looking at the alignment at the end of the chart. This is important, as small timing errors between components in a 0.5 cps wave can change the type of polarization observed. Polar plots for the

magnetic disturbance vector, as projected into each of three orthogonal planes (H-D, H-Z, and D-Z), were then constructed.

In addition, polar plots in just the H-D (horizontal) plane were made over a longer duration, in order to see how the polarization changes over an entire beat. In order to maintain clarity in the diagrams, only four seconds are plotted to a pair of axes. The plots are in serial order, each beginning on the last point of the preceding one. The interval between points is again 0.2 second.

5.3 Discussion of Results

Examples of the three basic types of plane polarization, counter-clockwise, clockwise (hereafter referred to as CCW and CW), and linear, are shown respectively in Figs. 5.1, 5.2, and 5.3. Note that in each case, the plane of polarization is almost perpendicular to the magnetic field line. This can best be seen by the plot in H-Z (meridional) plane. This feature was common to all the three-component polar diagrams made. The H-D plot of Fig. 5.1 gives a left-hand ellipse whose principal axis is precessing in the same direction. A tendency toward precession was observed on somewhat less than half the plots. This may be caused by changing ionospheric parameters introducing a Faraday rotation, but it is not obvious that this observed precession is significant or important. For the record it should be added that the direction of precession was usually the same as that of the polarization.

Figures 5.4, 5.5, and 5.6 show how the polarization of the horizontal vector varies over three beats selected from the event of August 16, 1962. The first beat (Fig. 5.4) starts out at 0256:14 linearly polarized in the NW-SE direction. (All directions are referred to magnetic north.) At

COLLEGE, AUG. 16, 1962. 0330 U.T.

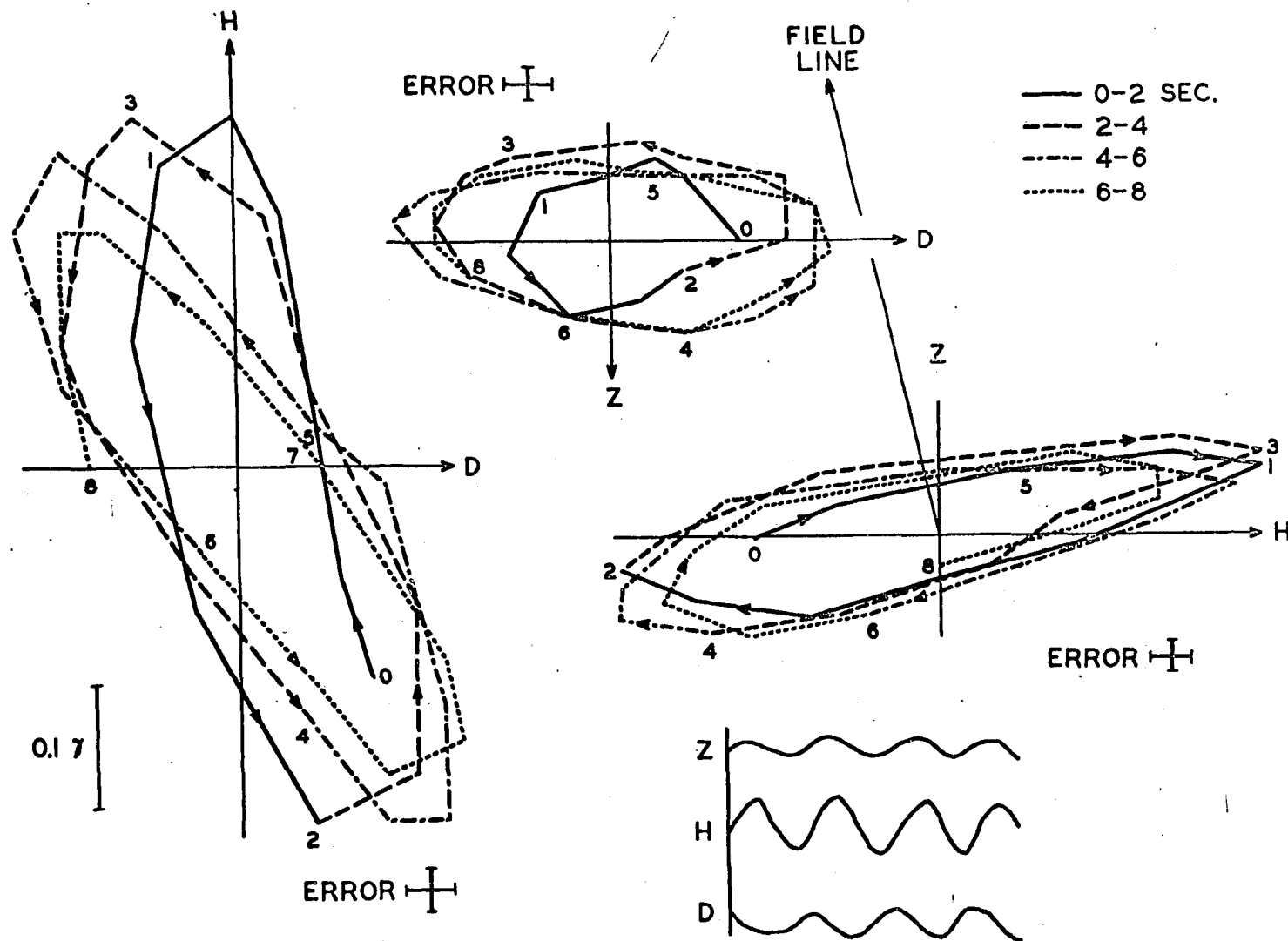


Figure 5-1

An example of left-hand polarization. Plots are made for the magnetic perturbation vector.

COLLEGE, AUG. 26, 1962. 2032 U.T.

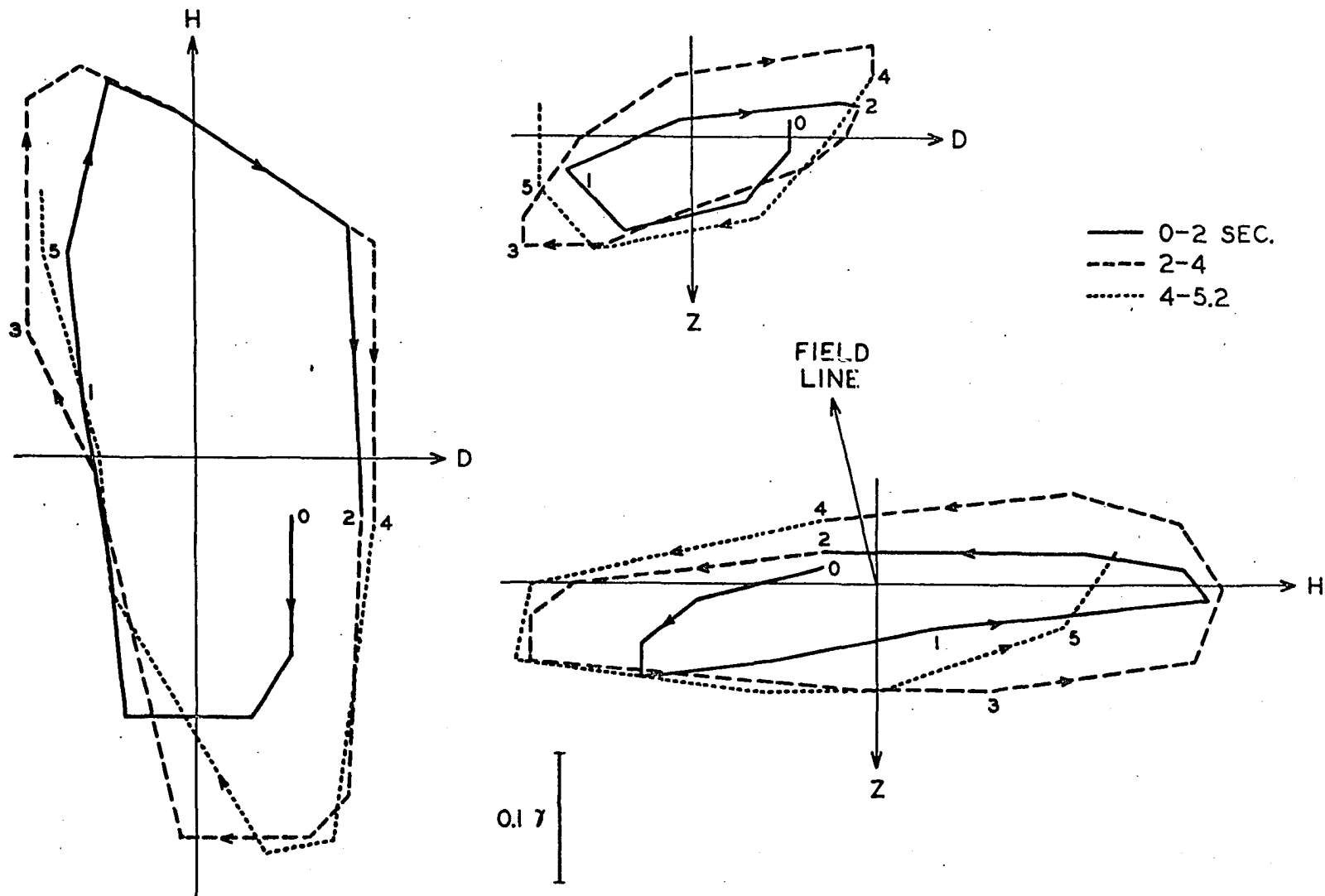


Figure 5-2

An example of right-hand polarization

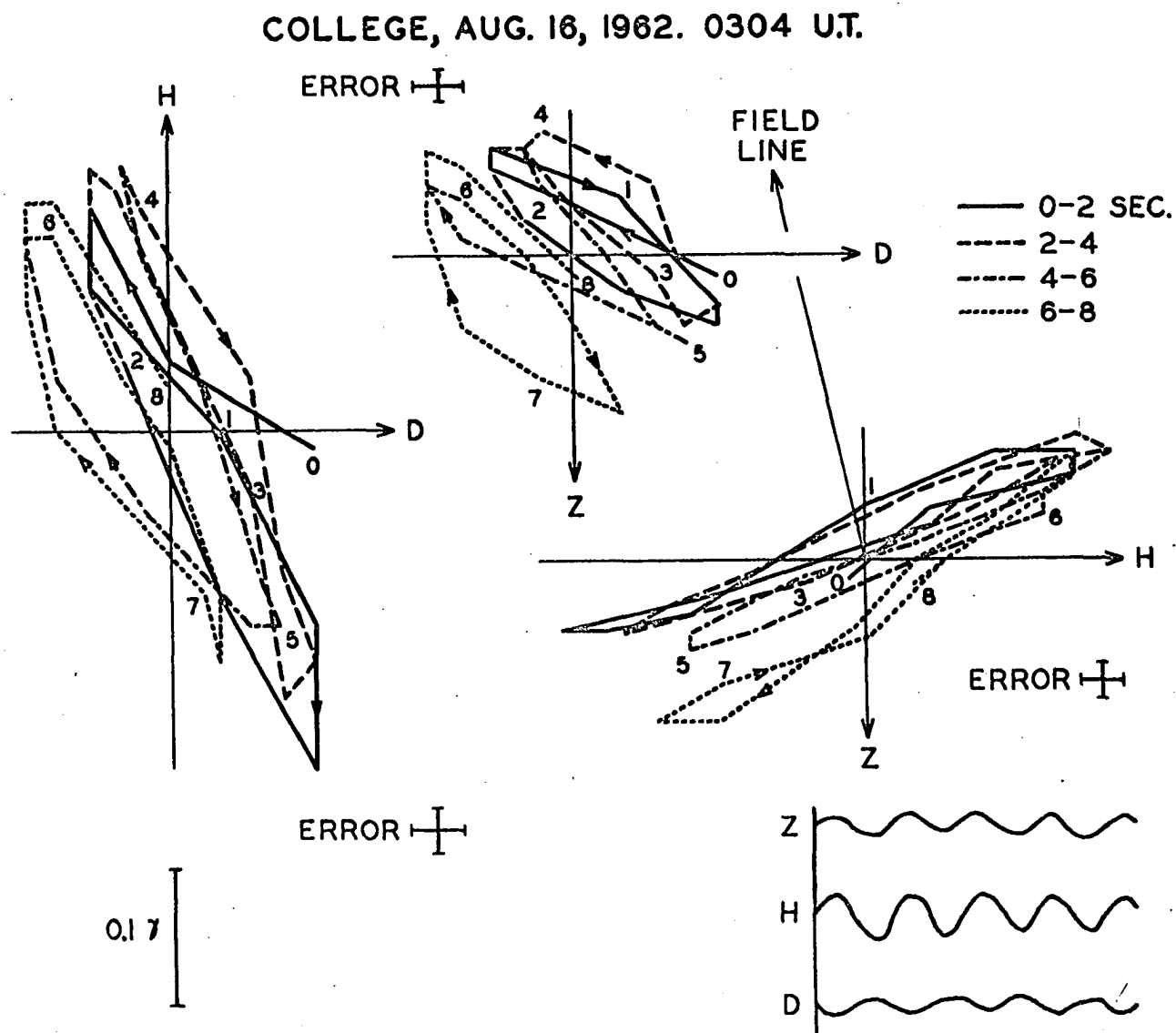


Figure 5-3
 An example of linear polarization

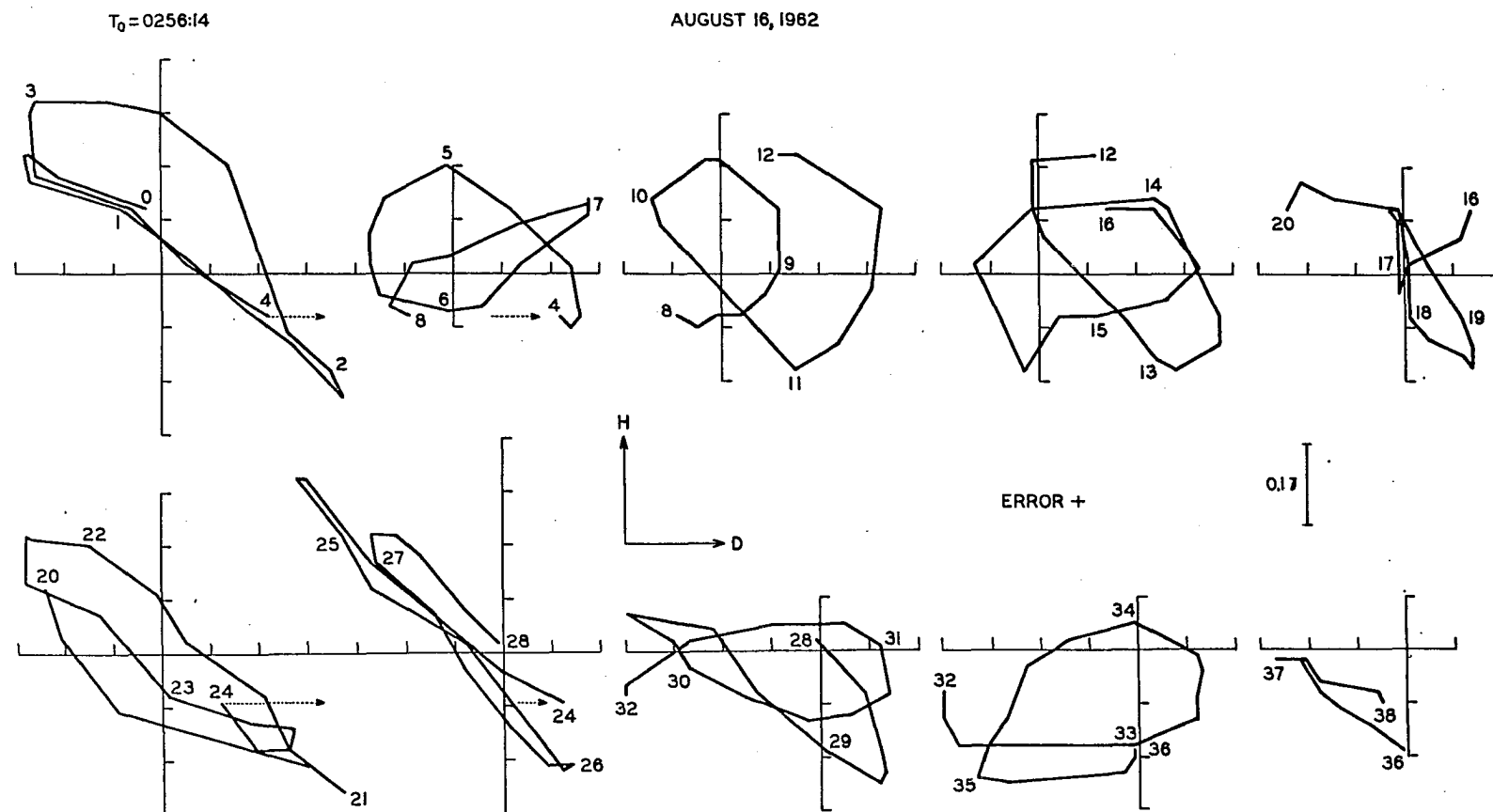


Figure 5-4

Sequential polarization diagrams for the horizontal plane

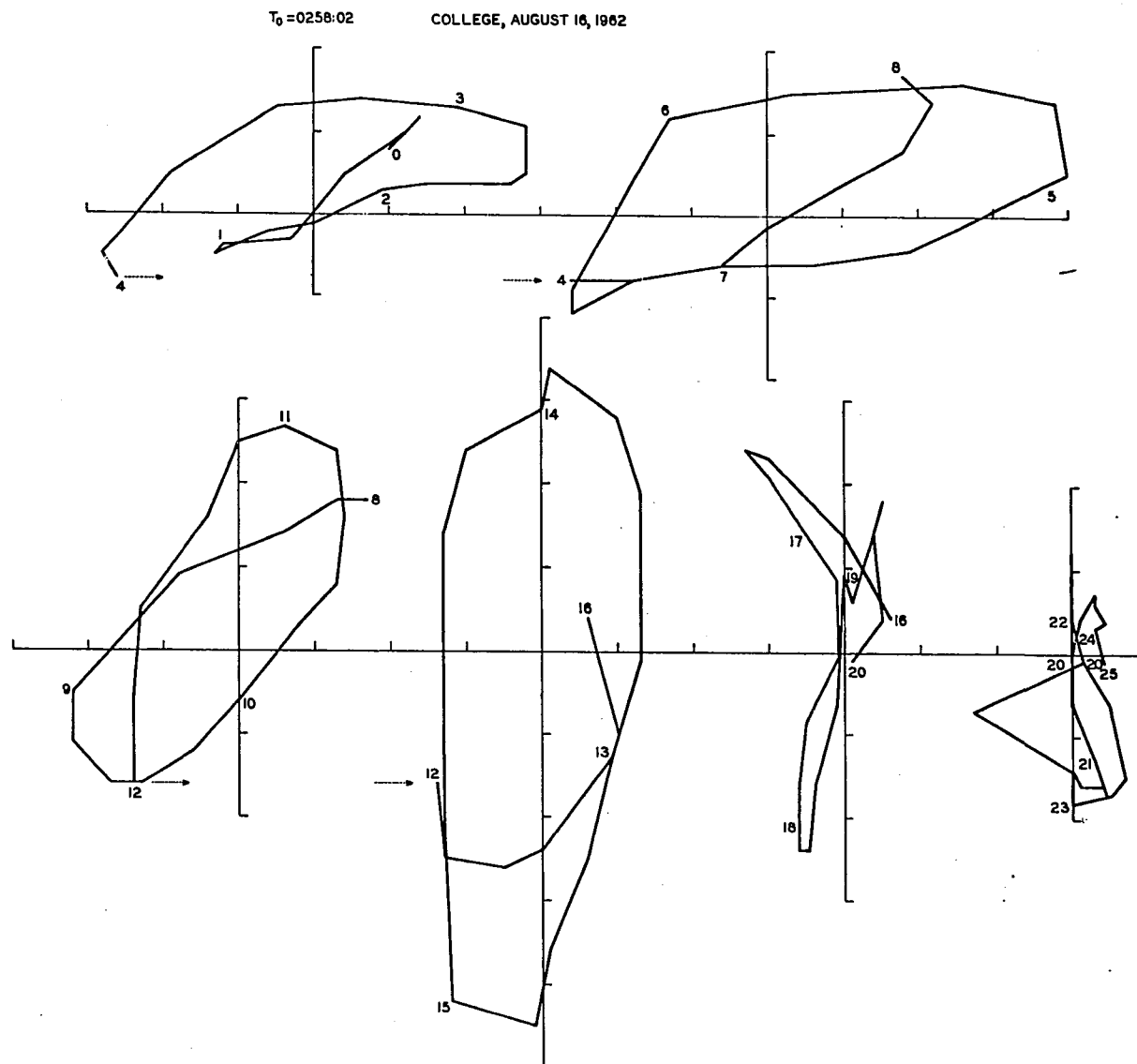


Figure 5-5

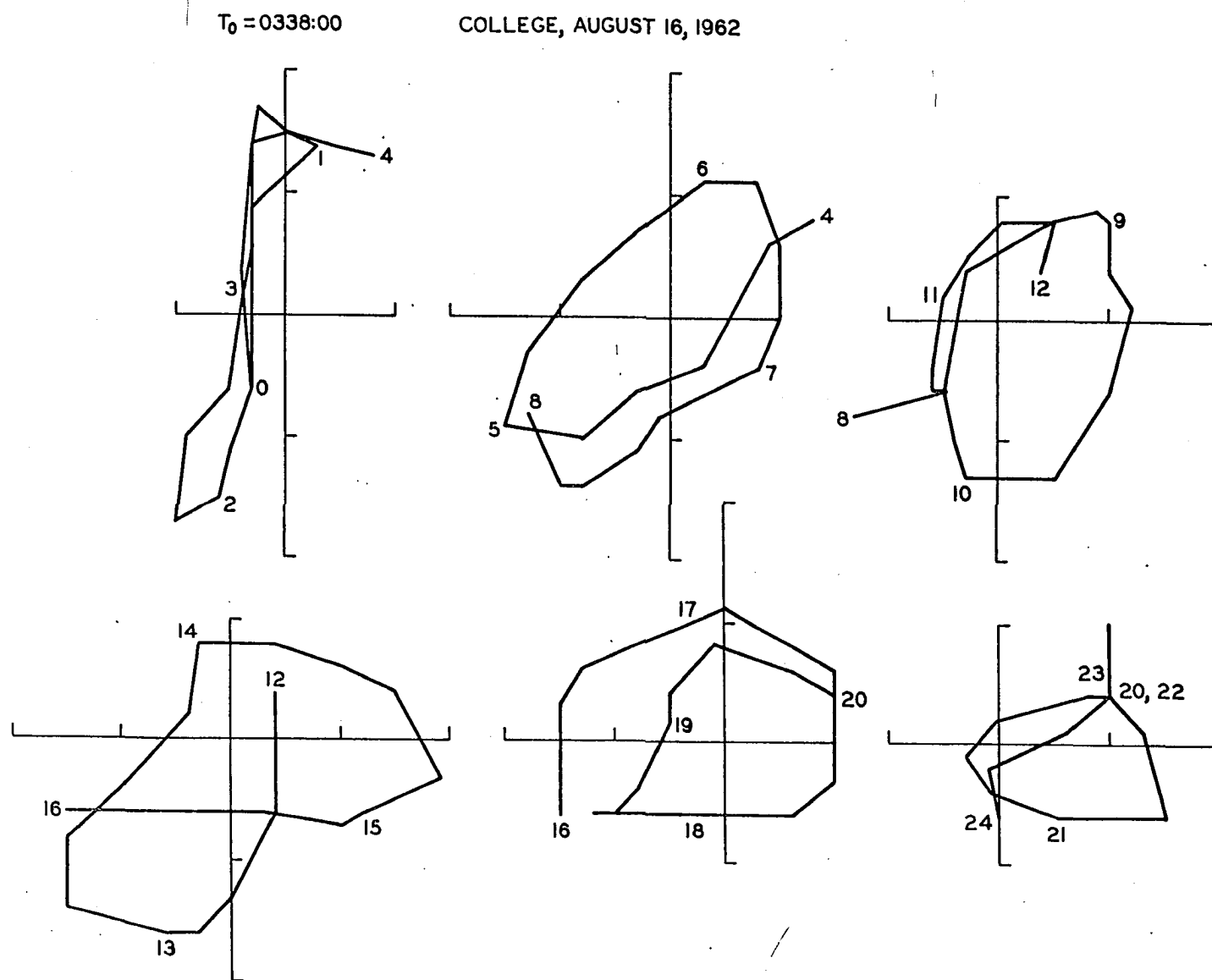


Figure 5-6

0256:16.2 it changes to CCW polarization, which is maintained until 0256:30.6. For the next twelve seconds the perturbation vector stays fairly linear, though in the middle of the interval it broadens into an elongated ellipse and rotates in the left-hand sense. As it emerges from the linear condition it makes a half revolution in the right-hand direction and then suddenly reverses at 0256:43.6. At about 0256:50 the wave reverts to a linear form just before degenerating into an irregular state, which marks the end of the beat. It is interesting to note that these diagrams show a preference toward aligning the major axis of the ellipse in the NW-SE direction.

Figure 5.5 starts just 68 seconds after the termination of the previous series. At the beat's beginning the perturbation vector starts out in a linear state, but quickly changes to CCW after one second. This is maintained for twelve seconds and the wave reverts back to linear before degenerating into irregularity. But here, in contrast to the previous example, the major axis is clearly rotating in the left-hand sense, from an initial E-W orientation to a N-S orientation twenty seconds later. Referring back to the H-D plot of Fig. 5.1, one can see that the major axis in that example has rotated about 45° to the left in eight seconds, going from N-S to NW-SE.

A beat possessing right-hand polarization is diagramed in Fig. 5.6. Initially the wave is linear, but reverses three seconds after the start of the plot and stays that way for the rest of the beat. At first there appears a tendency to precess to the right. But after 0338:08 the polarization is almost circular making it impossible to determine a major axis. Toward the end of the beat the circle grows smaller, as if it were winding up on itself.

Table 5.1 provides a list of the beats analyzed by polar diagrams with a tabulation of their properties. To summarize the results in order of importance:

- 1) The perturbation vector is nearly confined to the plane perpendicular to the field line.
- 2) Linear, right- and left-handed elliptical polarization are all observed.
- 3) Linear polarization is often observed at the beginning and end of a beat.
- 4) Left-handed polarization is more common than right-handed.
- 5) The direction of polarization can change in the middle of a beat.
- 6) About half the waves show precession, usually in the same direction as the polarization.

When seen on a frequency-time display, such as a sonagram, pearls usually have a fine-structure consisting of a regular series of rapidly rising tones. Overlapping of two or more tones could easily explain the complicated envelopes seen on amplitude-time displays. As shown in the next chapter, Alfvén waves propagating along a field line would be expected to have left-handed circular polarization aligned perpendicular to the field line. The relatively small amount of right-handed polarization observed could simply be an effect of two left-handed waves beating together. Beating could also account for the linear and elliptical polarization observed (Pope, 1964a).

TABLE 5.1
Summary of Polar Diagrams

Date	Time (UT)	Type of Polarization	Precession
<u>3 - Component</u>			
Aug. 16, 1962	0300	RH to LH	No
	0304	L	No
	0330	LH	Yes, LH
	0334	LH to L	No
	2001	LH to L	Yes, LH
	2032	RH	No
	2103	L	No
	2121	RH to L	Yes, RH
	26		
<u>Horizontal Plane Only</u>			
16	0256:14	L to LH	Not clearly
	18	LH	
	22	LH	
	26	LH	
	30	L	
	34	L	
	38	L	
	42	RH to LH	
	46	LH	
	50	L	
16	0258:02	L to LH	Yes, LH
	06	LH	
	10	LH	
	14	LH	
	18	L	
	22	L	
16	0338:00	L	Yes, RH, for first 8 sec.
	04	RH	
	08	RH	
	12	RH	
	16	RH	
	20	RH	

RH: right-hand elliptical polarization

LH: left-hand elliptical

L: linear

CHAPTER VI

HYDROMAGNETIC WAVE PROPAGATION IN THE UPPER MAGNETOSPHERE

6.1 Introduction

The subject of hydromagnetic wave propagation in all its complexity has been treated extensively in the literature. I would like to develop those aspects of the subject which are particularly apropos to the actual conditions found in the upper magnetosphere and for waves with frequencies in the vicinity of 1 cps. The generation of these waves is a highly speculative subject and will not be considered other than to state that their origin probably lies in the interaction of the solar wind and the magnetosphere.

The assumption of a uniform plasma is commonly made, so that the solutions will have the form of plane harmonic waves. However, as will be shown later, such an assumption is not really valid at heights below 10,000 km. Here the plasma density changes significantly within one wavelength.

Another assumption commonly made is that of a cold plasma, i.e., all collisions and hence, all pressure terms and momentum exchange between classes of particles are neglected. This is valid as long as the collision frequencies are less than the wave frequency. This assumption can be safely made for the frequency range of interest for heights above 3000 km, but lower than this, ion-electron collisions become important. For the magnetosphere this assumption is less restrictive than that of a uniform plasma.

Also commonly made, is the small amplitude assumption, which allows the equations to be linearized. This one breaks down for large pulsations

as the limits of the magnetosphere are approached. However, micro-pulsations in the 1 cps range seldom exceed a few gamma, and this assumption can be safely justified for heights lower than 50,000 km.

The plasma will be considered to consist only of electrons and ions. Effects of neutral particles may be ignored as long as the wave frequency is greater than the ion-neutral collision frequency. This condition is met by staying above 300 km. Since the atmosphere consists almost entirely of hydrogen above 3000 km, only one type of ion need be considered. Also, it follows that all ions are singly ionized. The plasma will be considered to be neutral, i.e., $n_e = n_i$.

Thus, analysis of small amplitude plane waves in a cold plasma is sufficient to explain hydromagnetic wave propagation in those regions with heights between 10,000 and 50,000 km, but more elaborate treatments will be required elsewhere.

Mks rationalized units will be used in the following derivations.

Useful references in the field are Alfvén and Fälthammar, "Cosmical Electrodynamics", 1963, Ch. 3; Spitzer, "Physics of Fully Ionized Gases", 1962, Ch. 2 and 3; and Stix, "Theory of Plasma Waves", 1962, Ch. 1 and 2. Prince and Bostick (1963) have extensively developed the treatment of the theory including the effects of neutrals. Francis and Karplus (1960) and Karplus, Francis, and Dragt (1962) tackle the problem of hydromagnetic propagation through the anisotropic ionosphere. They use numerical integration techniques, rather than assuming a harmonic wave solution and deriving a dispersion relation.

6.2 Hydromagnetic Propagation in a Uniform Cold Plasma

The purpose of this section will be to derive a dispersion relation, suitable for all directions of propagation, for hydromagnetic waves at

frequencies around 1 cps. The polarization properties of these waves will also be discussed.

Start with Maxwell's equations,

$$\nabla \times \vec{B} = \mu \vec{J} + \mu \epsilon \frac{\partial \vec{E}}{\partial t} \quad (1)$$

$$\nabla \times \vec{E} = - \frac{\partial \vec{B}}{\partial t} \quad (2)$$

and define the conductivity tensor by

$$\vec{J} = {}^2\sigma \cdot \vec{E} \quad (3)$$

Let \vec{B} be composed of a steady component, \vec{B}_0 , which is derivable from a multipole potential expansion, and a time-varying component, \vec{b} , which is small, i.e., $|\vec{b}| \ll |\vec{B}_0|$. Neglect the displacement current. Let \vec{b} , \vec{J} , \vec{E} , vary as $e^{-i\omega t}$, which states that the various plasma parameters do not change significantly during one period. Since $\nabla \times \vec{B}_0 = 0$ and $\frac{\partial \vec{B}_0}{\partial t} = 0$, Maxwell's equations become

$$\nabla \times \vec{b} = \mu \vec{J} \quad (4)$$

$$\nabla \times \vec{E} = i\omega \vec{b} \quad (5)$$

Take the curl of (5), and substitute from (4) and (3) to obtain the wave equation

$$\nabla \times (\nabla \times \vec{E}) = i\omega \mu ({}^2\sigma \cdot \vec{E}) \quad (6)$$

So far nothing has been stated concerning the structure of the plasma, nor the form of the conductivity tensor, other than that it is of second order.

The conductivity tensor for a cold plasma can be obtained by considering the equations of motion for electrons and ions, and the definition of current density.

$$m_e \frac{d\vec{v}_e}{dt} = -i\omega m_e \vec{v}_e = -e (\vec{E} + \vec{v}_e \times \vec{B}_0) \quad (7)$$

$$m_i \frac{d\vec{v}_i}{dt} = -i\omega m_i \vec{v}_i = e (\vec{E} + \vec{v}_i \times \vec{B}_0) \quad (8)$$

$$\vec{J} = n_e e (\vec{v}_i - \vec{v}_e) \quad (9)$$

Let \vec{B}_0 lie along the z-axis, so that (7) becomes in rectangular coordinates

$$-i\omega m_e v_{ex} = -e (E_x + v_{ey} B_0) \quad (10)$$

$$-i\omega m_e v_{ey} = -e (E_y - v_{ex} B_0) \quad (11)$$

$$-i\omega m_e v_{ez} = -e E_z \quad (12)$$

Solving for v_{ex} , v_{ey} , v_{ez} gives

$$v_{ex} = \frac{i\omega m_e E_x + e^2 B_0^2 E_y}{e^2 B_0^2 - \omega^2 m_e^2} \quad (13)$$

$$v_{ey} = \frac{-e^2 B_0^2 E_x + i\omega m_e E_y}{e^2 B_0^2 - \omega^2 m_e^2} \quad (14)$$

$$v_{ez} = -\frac{ie E_z}{\omega m_e} \quad (15)$$

Similarly,

$$v_{ix} = \frac{-i\omega m_i e E_x + e^2 B_o E_y}{e^2 B_o^2 - \omega_{m_i}^2} \quad (16)$$

$$v_{iy} = \frac{-e^2 B_o E_x - i\omega m_i e E_y}{e^2 B_o^2 - \omega_{m_i}^2} \quad (17)$$

$$v_{iz} = \frac{ie E_z}{\omega m_i} \quad (18)$$

Make the following approximations

$$\omega \ll \omega_{ce}, \omega_{ci} \ll \omega_{ce}, \omega^2 \ll \omega_{ce} \omega_{ci}$$

where $\omega_{ce} = \frac{eB_o}{m_e}$ and $\omega_{ci} = \frac{eB_o}{m_i}$ are the gyrofrequencies. The second inequality is equivalent to $m_e \ll m_i$. Then from (9)

$$J_x \approx -\frac{in_e m_i e^2 \omega E_x}{e^2 B_o^2 - m_i^2 \omega^2} + \frac{n_e m_i^2 e \omega^2 E_y}{B_o (e^2 B_o^2 - m_i^2 \omega^2)} \quad (19)$$

$$J_y \approx -\frac{n_e m_i^2 e \omega^2 E_x}{B_o (e^2 B_o^2 - m_i^2 \omega^2)} - \frac{in_e m_i e^2 \omega E_y}{e^2 B_o^2 - m_i^2 \omega^2} \quad (20)$$

$$J_z \approx \frac{in_e e^2 E_z}{m_e \omega} \quad (21)$$

Thus, it can be seen that the conductivity is given by

$$2\sigma = \begin{pmatrix} \sigma_1 & \sigma_2 & 0 \\ -\sigma_2 & \sigma_1 & 0 \\ 0 & 0 & \sigma_o \end{pmatrix} \quad (22)$$

where

$$\sigma_0 \approx \frac{n_e e^2}{m_e \omega} \quad (23)$$

$$\sigma_1 \approx - \frac{n_e m_i e^2 \omega}{e^2 B_0^2 - m_i^2 \omega^2} \quad (24)$$

$$\sigma_2 \approx \frac{n_e m_i^2 e \omega^2}{B_0 (e^2 B_0^2 - m_i^2 \omega^2)} \quad (25)$$

σ_1 is often called the Pederson conductivity, while σ_2 is the Hall conductivity.

To obtain the dispersion relation for a plane wave, allow \vec{E} to vary spatially as $e^{i\vec{k} \cdot \vec{r}}$. Thus $\nabla \times$ becomes $i\vec{k} \times$ and the wave equation (6) becomes

$$-\vec{k} \times (\vec{k} \times \vec{E}) = i\omega\mu (\vec{\sigma} \cdot \vec{E}) \quad (26)$$

Without loss of generality, let \vec{k} lie in the z-x plane at an angle θ with respect to \vec{B}_0 , so that

$$\begin{aligned} k_x &= k \sin \theta \\ k_y &= 0 \\ k_z &= k \cos \theta \end{aligned} \quad (27)$$

Writing (26) out in rectangular coordinates using (22) and (27) gives

$$\begin{aligned} k^2 E_x \cos^2 \theta - k^2 E_z \sin \theta \cos \theta &= i\omega\mu(\sigma_1 E_x + \sigma_2 E_y) \\ k^2 E_y \cos^2 \theta + k^2 E_z \sin^2 \theta &= i\omega\mu(-\sigma_2 E_x + \sigma_1 E_y) \\ -k^2 E_x \sin \theta \cos \theta + k^2 E_z \sin^2 \theta &= i\omega\mu\sigma_0 E_z \end{aligned} \quad (28)$$

In order for (28) to have non-trivial solutions, the following determinant must be zero.

$$\begin{vmatrix} k^2 \cos^2 \theta - i\omega\mu\sigma_1 & -\omega\mu\sigma_2 & -k^2 \sin \theta \cos \theta \\ i\omega\mu\sigma_2 & k^2 - i\omega\mu\sigma_1 & 0 \\ -k^2 \sin \theta \cos \theta & 0 & k^2 \sin^2 \theta - i\omega\mu\sigma_0 \end{vmatrix} = 0 \quad (29)$$

This yields a quadratic in k^2

$$\begin{aligned} & (\sigma_0 \cos^2 \theta + \sigma_1 \sin^2 \theta)k^4 - i\omega\mu[\sigma_0\sigma_1(1 + \cos^2 \theta) \\ & + (\sigma_1^2 + \sigma_2^2) \sin^2 \theta]k^2 - \omega^2\mu^2\sigma_0(\sigma_1^2 + \sigma_2^2) = 0 \end{aligned} \quad (30)$$

which produces the following dispersion relation

$$\frac{k^2}{\omega^2} = \frac{i\mu \left[\frac{\sigma_0\sigma_1(1 + \cos^2 \theta)}{\sigma_1^2 + \sigma_2^2} + \sin^2 \theta \right] \pm \mu \sqrt{\frac{4\sigma_0^2\sigma_2^2 \cos^2 \theta}{(\sigma_1^2 + \sigma_2^2)^2} - \left(\frac{\sigma_0\sigma_1}{\sigma_1^2 + \sigma_2^2} - 1 \right)^2 \sin^4 \theta}}{2 \frac{(\sigma_0 \cos^2 \theta + \sigma_1 \sin^2 \theta)\omega}{\sigma_1^2 + \sigma_2^2}} \quad (31)$$

From (23), (24), and (25), we have

$$\frac{\sigma_0}{\sigma_1^2 + \sigma_2^2} = - \frac{iB_o^2(e^2 B_o^2 - m_i^2 \omega^2)}{n_e m_e m_i^2 \omega^3} = - \frac{iB_o^2(\omega_{ci}^2 - \omega^2)}{n_e m_e \omega^3} \quad (32)$$

$$\frac{\sigma_1}{\sigma_1^2 + \sigma_2^2} = \frac{iB_o^2}{n_e m_i \omega} \quad (33)$$

$$\frac{\sigma_2}{\sigma_1^2 + \sigma_2^2} = -\frac{B_o}{n_e e} \quad (34)$$

Eliminating the conductivities, (31) becomes

$$\frac{k^2}{\omega^2} = \frac{i\mu \left[-\frac{e^2 B_o^2 (1 + \cos^2 \theta)}{m_e m_i \omega^2} + \sin^2 \theta \right] + \mu \sqrt{-\frac{4e^2 B_o^2 \cos^2 \theta}{m_e \omega^2} - \left(-\frac{e^2 B_o^2}{m_i m_e \omega^2} - 1 \right)^2 \sin^4 \theta}}{2 \left[-\frac{iB_o^2 (\omega_{ci}^2 - \omega^2) \cos^2 \theta}{n_e m_e \omega^3} + \frac{iB_o^2 \sin^2 \theta}{n_e m_i \omega} \right] \omega} \quad (35)$$

Divide numerator and denominator by $i\mu$, introduce the plasma frequency,

$$\omega_p^2 = \frac{n_e e^2}{\epsilon m_e}, \text{ and the Alfvén velocity, } V_A = \frac{B_o}{\sqrt{\mu n_e m_i}}, \text{ and use } c = \frac{1}{\sqrt{\mu \epsilon}} \text{ to}$$

obtain

$$\frac{k^2}{\omega^2} = \frac{1 + \cos^2 \theta - \frac{\omega_c^2 \sin^2 \theta}{\omega_p^2 V_A^2} + \sqrt{\frac{4\omega_c^2 \cos^2 \theta}{\omega_{ci}^2} + \left(1 + \frac{\omega_c^2}{\omega_p^2 V_A^2} \right)^2 \sin^4 \theta}}{2V_A^2 \left[\left(1 - \frac{\omega^2}{\omega_{ci}^2} \right) \cos^2 \theta - \frac{\omega_c^2 \sin^2 \theta}{\omega_p^2 V_A^2} \right]} \quad (36)$$

Though $\frac{\omega_c^2}{\omega_p^2 V_A^2} \ll 1$ in the problem under consideration, these terms are

retained to allow propagation across the field to be considered. If θ is not near $\frac{\pi}{2}$, these terms may safely be neglected. This is a general dispersion relation which will treat hydromagnetic wave propagation in

those regions of the magnetosphere with heights between 10,000 and 50,000 km, for frequencies around 1 cps. The approximations used will be justified in the next section. The approximation $\omega \ll \omega_{ci}$ was not made, as this does not hold above 20,000 km.

To obtain the classical Alfvén modes, we now make the approximation $\omega \ll \omega_{ci}$. Then (36) becomes, provided θ is not near $\frac{\pi}{2}$.

$$\frac{k^2}{\omega^2} = \frac{1 + \cos^2 \theta \pm \sin^2 \theta}{2V_A^2 \cos^2 \theta} \quad (37)$$

$$= \begin{cases} \frac{1}{V_A^2 \cos^2 \theta} & \text{Alfvén or slow wave} \\ \frac{1}{V_A^2} & \text{modified Alfvén or fast wave} \end{cases}$$

As the approximation, $\omega \ll \omega_{ci}$ is not a particularly good one, it will be necessary, in general, to use the more complete dispersion relation (36).

For longitudinal propagation, $\theta = 0$, and (36) yields

$$\frac{\omega^2}{k^2} = V_A^2 \left(1 \mp \frac{\omega}{\omega_{ci}} \right) \quad (38)$$

where the upper sign corresponds to the Alfvén mode and the lower to the modified Alfvén mode. It is evident that the Alfvén mode will cease to propagate when $\omega \geq \omega_{ci}$. The group velocity will be given by

$$v_g = \frac{d\omega}{dk} = \frac{V_A \left(1 \mp \frac{\omega}{\omega_{ci}} \right)^{3/2}}{1 \mp \frac{\omega}{2\omega_{ci}}} \approx V_A \left(1 \mp \frac{\omega}{\omega_{ci}} \right) \quad (38a)$$

Both the phase and group velocities of the Alfvén mode decrease with increasing frequency, while the modified wave does the opposite.

For transverse propagation, set $\theta = \frac{\pi}{2}$ in (36), and obtain

$$\frac{\omega}{k} = \begin{cases} \frac{i\omega c}{\omega_p} & \text{Alfvén} \\ v_A & \text{modified Alfvén} \end{cases} \quad (39)$$

An interesting result is that the Alfvén mode degenerates into an evanescent plasma oscillation for this direction of propagation. The resonance angle for which this mode ceases to propagate is given by

$$\tan^2 \theta_r = \frac{\omega_p^2 v_A^2}{\omega_c^2} \left(1 - \frac{\omega^2}{\omega_{ci}^2} \right) \quad (40)$$

No resonance exists at this angle, or any other angle, for the modified Alfvén mode, since the numerator in (36) goes to zero at this angle when the minus sign is chosen. In order to support this last statement it is necessary to show that $\lim_{\theta \rightarrow \theta_r} \frac{k^2}{\omega^2}$ remains finite and non-zero. Applying L'Hopital's rule

$$\lim_{\theta \rightarrow \theta_r} \frac{k^2}{\omega^2} = \frac{1 + \frac{\omega_c^2}{\omega_p^2} + \frac{-\frac{2\omega^2}{\omega_{ci}^2} + \left(1 + \frac{\omega_c^2}{\omega_p^2} \frac{\omega^2}{v_A^2}\right) \sin^2 \theta_r}{\sqrt{\frac{4\omega^2 \cos^2 \theta_r}{\omega_{ci}^2} + \left(1 + \frac{\omega_c^2}{\omega_p^2} \frac{\omega^2}{v_A^2}\right) \sin^4 \theta_r}}}{2v_A^2 \left(1 - \frac{\omega^2}{\omega_{ci}^2} + \frac{\omega_c^2}{\omega_p^2} \frac{\omega^2}{v_A^2}\right)} \quad (41)$$

Since $\omega_p^2 v_A^2 \ll \omega^2 c^2$, and $\theta_r \approx \frac{\pi}{2}$, the above limit reduces to approximately $\frac{1}{v_A^2}$.

The polarization of these waves when $\theta = 0$ can be obtained from the y-component of (28).

$$i\omega\mu\sigma_2 E_x + (k^2 - i\omega\mu\sigma_1)E_y = 0 \quad (42)$$

Substituting for the conductivities from (24) and (25), we have for the electric polarization in the x-y plane

$$\frac{iE_x}{E_y} = \frac{eB_0}{m_i \omega} - \frac{(e^2 B_0^2 - m_i^2 \omega^2) B_0 k^2}{\mu_e m_i^2 e \omega^3} = \frac{\omega_{ci}}{\omega} - \frac{(\omega_{ci}^2 - \omega^2) v_A^2 k^2}{\omega_{ci} \omega^3} \quad (43)$$

To determine the polarization for longitudinal propagation, substitute (38) into (43) and obtain

$$\frac{iE_x}{E_y} = \frac{\omega_{ci}}{\omega} - \frac{\omega_{ci}^2 - \omega^2}{\omega(\omega_{ci} \pm \omega)} = \frac{\omega_{ci}}{\omega} - \frac{\omega_{ci} \pm \omega}{\omega} = \mp 1 \quad (44)$$

Again the upper sign refers to the Alfvén mode, and we can see that it is left-handed circularly polarized. The modified Alfvén wave is then a right-handed circular wave.

In general these waves will be elliptically polarized. This can be seen by calculating

$$\frac{i(E_x \cos \theta - E_z \sin \theta)}{E_y}$$

which will give the electric polarization in the plane normal to the propagation direction. From the z-component of (28) obtain

$$-k^2 E_x \sin \theta \cos \theta + (k^2 \sin^2 \theta - i\omega\mu\sigma_o) E_z = 0 \quad (45)$$

Combining this with (42), (23), (24), and (25) we have

$$\frac{i(E_x \cos \theta - E_z \sin \theta)}{E_y} = \frac{\omega_{ci} \omega_p^2 \cos \theta \left[1 - \left(1 - \frac{\omega^2}{\omega_{ci}^2} \right) \frac{v_A^2 k^2}{\omega^2} \right]}{\omega^3 c^2 \left(\frac{k^2 \sin^2 \theta}{\omega^2} + \frac{\omega_p^2}{\omega^2 c^2} \right)} \quad (46)$$

Introducing the general dispersion relation (36) and using $\omega_c^2 \ll \omega_p^2 v_A^2$, wherever it can be made without losing the ability to treat transverse propagation, the right side of (46) becomes

$$\frac{\omega_{ci} \omega_p^2 v_A^2 \cos \theta \left(1 - \frac{\omega^2}{\omega_{ci}^2} \right) \left[\sin^2 \theta \pm \sqrt{\frac{4\omega^2 \cos^2 \theta}{\omega_{ci}^2} + \left(1 + \frac{\omega_c^2}{\omega_p^2 v_A^2} \right)^2 \sin^4 \theta} \right]}{\omega^3 c^2 \left\{ \left[\sin^2 \theta \pm \sqrt{\frac{4\omega^2 \cos^2 \theta}{\omega_{ci}^2} + \left(1 + \frac{\omega_c^2}{\omega_p^2 v_A^2} \right)^2 \sin^4 \theta} \right] \sin^2 \theta + \frac{2v_A^2 \omega_p^2}{\omega^2 c^2} \left(1 - \frac{\omega^2}{\omega_{ci}^2} \right) \cos^2 \theta \right\}} \quad (47)$$

If one stays away from $\theta = \frac{\pi}{2}$, this rather complicated expression reduces to

$$\frac{i(E_x \cos \theta - E_z \sin \theta)}{E_y} = - \frac{\omega_{ci}}{2\omega \cos \theta} \left(\sin^2 \theta \pm \sqrt{\frac{4\omega^2 \cos^2 \theta}{\omega_{ci}^2} + \sin^4 \theta} \right) \quad (48)$$

Both (47) and (48) reduce to (44) when $\theta = 0$. When $\omega \ll \omega_{ci}$, (48) shows that as long as θ is not near $\theta = 0$ the Alfvén mode is linearly polarized in the x-z plane, while the modified Alfvén or fast mode is linearly polarized in the y-direction.

For transverse propagation it can be seen from (47) that both modes are linearly polarized in the y-direction, though it should be remembered that the Alfvén mode does not propagate transversely.

Since one often works with magnetic records it would be desirable to express the polarization in terms of the components of the magnetic perturbation vector instead of the electric vector. The transformation can easily be made by means of

$$\vec{k} \times \vec{E} = \omega \vec{b}$$

From this it follows that

$$E_x \cos \theta - E_z \sin \theta = \frac{\omega b_y}{k}$$

and

$$E_y = - \frac{\omega(b_y \cos \theta - b_z \sin \theta)}{k}$$

Thus the electric vector in the x-z plane is associated with the magnetic y-component, and the electric y-component is associated with the magnetic x-z component with the vector aimed in the negative x direction. With these changes all the preceding statements on polarization apply to the magnetic perturbation vector. Though \vec{E} has a component parallel to \vec{k} , \vec{b} does not.

6.3 The Effect of Ion-electron Collisions

It is possible that under 20,000 km the ion-electron collision frequency, ν_{ie} , may approach the wave frequency, ω . Thus, it is desirable to develop a technique for handling ion-electron collisions, when their frequency is comparable to the wave frequency, but still considering $\nu_{ie} \ll \frac{m_i \omega}{m_e}$ and $\nu_{ie} \ll \omega_{ce}$.

The effects of collisions will appear as momentum exchange terms in the equations of motion, (7) and (8). If we assume that $m_i \gg m_e$, the rate of momentum exchange between electrons and ions is given by $m_e \nu_{ie} (\vec{v}_e - \vec{v}_i)$ and the equations of motion become

$$-i\omega m_e \vec{v}_e = -e(\vec{E} + \vec{v}_e \times \vec{B}_0) - m_e \nu_{ie} (\vec{v}_e - \vec{v}_i) \quad (49)$$

$$-i\omega m_i \vec{v}_i = e(\vec{E} + \vec{v}_i \times \vec{B}_0) + m_e \nu_{ie} (\vec{v}_e - \vec{v}_i) \quad (50)$$

or approximately

$$m_e (\nu_{ie} - i\omega) \vec{v}_e = -e(\vec{E} + \vec{v}_e \times \vec{B}_0) + m_e \nu_{ie} \vec{v}_i \quad (51)$$

$$-im_i \omega \vec{v}_i = e(\vec{E} + \vec{v}_i \times \vec{B}_0) + m_e \nu_{ie} \vec{v}_e \quad (52)$$

Since $n_i = n_e$, $\nu_{ie} = \nu_{ei}$. The z-components of the above equations are

$$m_e (\nu_{ie} - i\omega) v_{ez} - m_e \nu_{ie} v_{iz} = -eE_z \quad (53)$$

$$-m_i \nu_{ie} v_{ez} - im_i \omega v_{iz} = eE_z \quad (54)$$

Solving for the v_z 's

$$v_{ez} = - \frac{ieE_z}{m_e(\omega + iv_{ie})} \quad (55)$$

$$v_{iz} = \frac{ieE_z}{m_i(\omega + iv_{ie})} \quad (56)$$

Then

$$J_z = n_e e(v_{iz} - v_{ez}) = \frac{in_e e^2 E_z}{\omega + iv_{ie}} \left(\frac{1}{m_i} + \frac{1}{m_e} \right) \approx \frac{in_e e^2 E_z}{m_e(\omega + iv_{ie})} \quad (57)$$

Thus

$$\sigma_o = \frac{in_e e^2}{m_e(\omega + iv_{ie})} \quad (58)$$

Similarly, the x- and y-components of (51) and (52) can be solved for v_{ex} , v_{ey} , v_{ix} , and v_{iy} . From these J_x and J_y , and hence σ_1 and σ_2 , can be found. However, if the above approximations are used, it will be found that σ_1 and σ_2 are not changed from (24) and (25). Hence, the main effect of introducing ion-electron collisions is to replace m_e by $\frac{m_e(\omega + iv_{ie})}{\omega}$.

The basic dispersion relation (36) now becomes

$$\begin{aligned} 1 + \cos^2 \theta - \frac{\omega(\omega + iv_{ie})c^2 \sin^2 \theta}{\omega_p^2 V_A^2} \\ \pm \sqrt{\frac{4\omega^2 \cos^2 \theta}{\omega_{ci}^2} + \left[1 + \frac{\omega(\omega + iv_{ie})c^2}{\omega_p^2 V_A^2} \right]^2 \sin^4 \theta} \\ \frac{k^2}{\omega^2} = \frac{2V_A^2 \left[\left(1 - \frac{\omega^2}{\omega_{ci}^2} \right) \cos^2 \theta - \frac{\omega(\omega + iv_{ie})c^2 \sin^2 \theta}{\omega_p^2 V_A^2} \right]} \end{aligned} \quad (59)$$

The actual effect of the ion-electron collisions on the dispersion relation is very small. Provided θ is not near $\frac{\pi}{2}$, we can use the

approximation $\left| \frac{\omega(\omega + iv_{ie})c^2}{\omega_p^2 v_A^2} \right| \ll 1$, and obtain the same dispersion

relation as approximating $\frac{\omega^2 c^2}{\omega_p^2 v_A^2} \ll 1$ in (36) would give. In the case

of transverse propagation the modified Alfvén wave is unaffected, but the Alfvén wave is given by

$$\frac{k^2}{\omega^2} = - \frac{\omega_p^2}{\omega(\omega + iv_{ie})c^2}$$

$$\text{Then } \frac{k}{\omega} \approx \frac{i\omega_p}{c\omega} \left(1 - \frac{iv_{ie}}{2\omega} \right) = \frac{\omega_p v_{ie}}{2c\omega^2} + \frac{i\omega_p}{c\omega}$$

The Alfvén wave will now propagate transversely, though it will be highly damped.

Thus, the only place where ion-electron collisions play a significant role is in the transverse propagation of the Alfvén mode.

The dispersion relation (59) bears some resemblance to the Appleton-Hartree formula, especially as to the role played by collisions. However, the approximations used in deriving the respective equations are different, as the Appleton-Hartree relation is for radio frequencies, and equation (59) was derived for ultra-low frequencies.

6.4 Justification of Assumptions

It will now be worthwhile to tabulate the various plasma parameters and justify the assumptions used in the preceding sections. Four models of the magnetosphere will be considered, corresponding to day and night

and maximum and minimum of the sunspot cycle. The basic data has been taken from Prince and Bostick, EE Res. Lab., Univ. Texas, Report No. 133, Appendix II, 1964.

In order to derive a dispersion relation for the Alfvén modes, it was necessary to assume that \vec{b} , \vec{E} , \vec{J} , and \vec{v} vary spatially as $e^{i\vec{k}\cdot\vec{r}}$, which implies that the plasma is uniform. A reasonable criterion for uniformity is that $|\vec{k}|$ must not change by more than ten per cent within one wavelength,

$$\frac{1}{|\vec{k}|} \frac{d|\vec{k}|}{ds} \leq \frac{0.1}{\lambda} \quad \text{or} \quad \left| \frac{dV}{ds} \right| \leq 0.1 f$$

where V is the phase velocity, s the path length along the direction of propagation, and f the wave frequency.

The first case to be considered is that of a wave propagating radially in the equatorial plane at the Alfvén velocity. Here the requirement is stated simply as

$$\left| \frac{dV_{Ae}}{dr} \right| \leq 0.1 f$$

where V_{Ae} is the equatorial Alfvén velocity and r the geocentric height. Fig. 6.1 shows the magnetosphere divided into uniform and non-uniform regions. As the frequency becomes higher more of the magnetosphere can be considered uniform. For frequencies greater than 45 cps, all of the magnetosphere above 500 km is uniform. If the wave period is greater than 100 sec, none of the magnetosphere can be considered uniform. Off the equatorial plane the Alfvén velocity will be increased by the factor $\sqrt{1 + 3 \sin^2 \lambda}$, where λ is the geomagnetic latitude, and the severity of

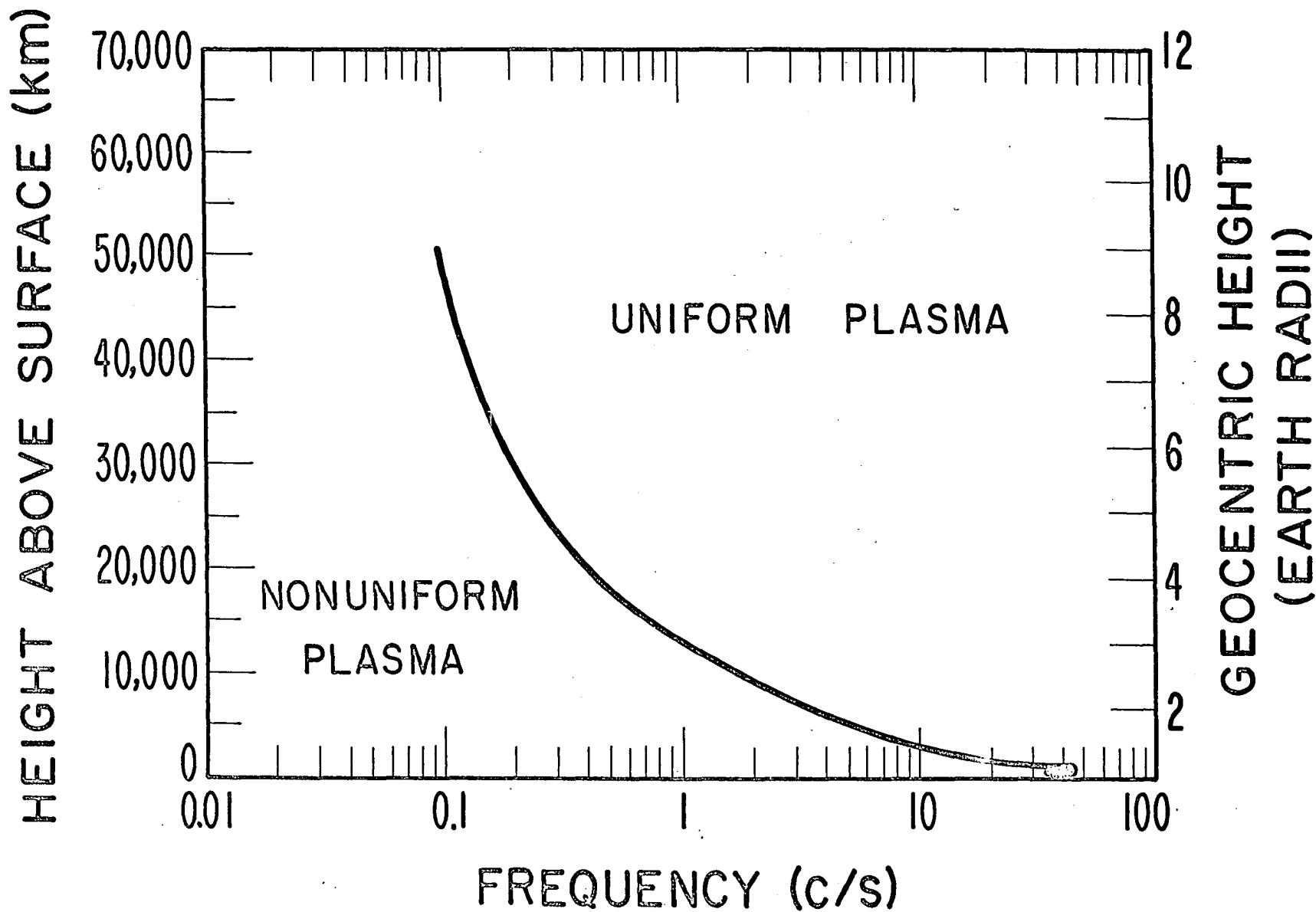


Figure 6-1

the restriction will be increased. The restriction will be relaxed if the propagation direction is different from that of the gradient of the Alfvén velocity.

A more realistic type of propagation is that of an Alfvén wave traveling along a field line. If the field is assumed to be a dipole field, the equation of a field line is

$$r = r_e \cos^2 \lambda$$

Then, with s along the field line

$$\frac{ds}{dr} = \sqrt{1 + r^2 \frac{d\lambda}{dr}^2} = \frac{\sqrt{1 + 3 \sin^2 \lambda}}{2 \sin \lambda}$$

and

$$\begin{aligned} \frac{dV_A}{ds} &= \frac{dr}{ds} \frac{dV_A}{dr} = \frac{dr}{ds} \sqrt{1 + 3 \sin^2 \lambda} \frac{dV_{Ae}}{dr} + \frac{3V_{Ae} \sin \lambda \cos \lambda}{\sqrt{1 + 3 \sin^2 \lambda}} \frac{d\lambda}{dr} \\ &= 2 \sin \lambda \frac{dV_{Ae}}{dr} - \frac{3V_{Ae} \sin \lambda \cos^2 \lambda}{r(1 + 3 \sin^2 \lambda)} \leq 0.1 f \end{aligned}$$

The boundary of this restriction is shown on a polar plot (Fig. 6.2) for several frequencies. Near the equator the boundary is closer to the earth as the field lines there are almost perpendicular to the velocity gradient. But toward the poles the field lines are close to being parallel to the velocity gradient and the gradient itself is greater, which pushes the boundary away from the earth. The plot is to be interpreted as representing the inner boundary of the uniform plasma for a wave with the specified frequency. The values used in making Fig. 6.1 and 6.2 are given in Table 6.1. They are an average of day, night, sunspot maximum and minimum conditions, and are merely typical values.

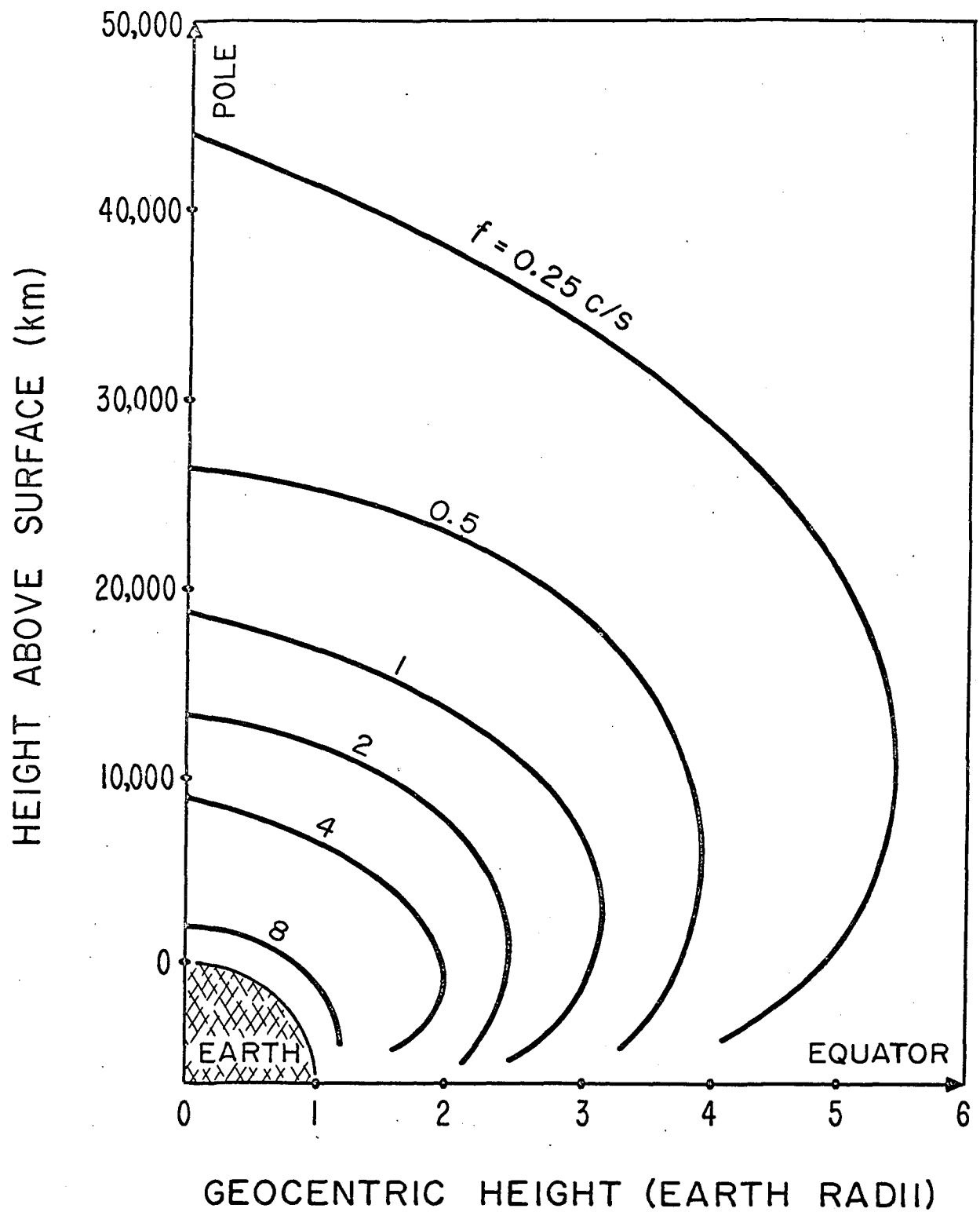


Figure 6-2

TABLE 6.1

Typical Values for the
Gradient of the Equatorial Alfvén Velocity

Height (km)	Geocentric height (km)	V_{Ae} (km/sec)	$\frac{dV_{Ae}}{dr}$ (sec ⁻¹)	$\frac{V_{Ae}}{r}$ (sec ⁻¹)
1000	7370	2020	+3.80	0.274
1500	7870	3570	+2.00	0.454
2000	8370	4020	+0.437	0.480
3000	9370	4200	-0.156	0.448
4000	10,370	3720	-0.469	0.359
5000	11,370	3270	-0.418	0.288
7000	13,370	2490	-0.330	0.186
10,000	16,370	1620	-0.178	0.0990
15,000	21,370	1060	-0.0822	0.0496
20,000	26,370	799	-0.0357	0.0303
30,000	36,370	526	-0.0217	0.0145
40,000	46,370	366	-0.0127	0.00789

Though the Alfvén velocity at a given point may vary by a factor of ten, the change in the graphs will be relatively small. At any rate, it is clear that the assumption of a uniform plasma for waves with frequencies around 1 cps is not really valid over much of the magnetosphere. It is necessary to make this assumption in order to derive a dispersion relation and the polarization properties for Alfvén waves, but it should not be surprising that these waves show observed properties which cannot be explained by or are inconsistent with the simple theory derived in the foregoing sections. In particular, reflection and refraction of energy would be expected if the plasma parameters have large gradients.

The assumption of a collisionless plasma depends mostly upon the ion-electron and the electron-electron collision frequencies, which in turn depends on the electronic temperature, a quantity which is largely speculative. Nicolet (1953) gives the ion-electron collision frequency as

$$\nu_{ie} = \left(59.1 + 4.18 \log \frac{T_e^3}{n_e} \right) \frac{n_e \times 10^{-6}}{T_e^{1.5}}$$

when $\frac{\epsilon k T_e}{e^2 n_e^{1/3}} \gg 1$. The great problem here is deciding what T_e should be.

If we assume that it is the same as the ionic temperature, and that this is 1500° K at sunspot maximum and 1000° K at minimum, we obtain the results displayed in Table 6.2. But there are reasons to believe that the actual electronic temperatures are much higher than what are assumed here.

Chapman (1960) believes that the solar corona plays an important role in determining the temperature of the upper atmosphere. Best estimates of the coronal temperature at the distance of the earth from the sun are between 50,000° and 100,000° K. There must be conduction of

heat downward and a smooth transition from coronal to ionospheric temperatures would be expected. It is not unreasonable to expect temperatures in excess of $10,000^{\circ}$ K above 10,000 km. This would reduce the values in Table 6.2 by a factor of at least 20 and certainly make the collision frequency negligible above about 4000 km.

According to Liemohn and Scarf (1962) evidence from cut-off frequencies observed in whistler data indicate temperatures on the order of $100,000^{\circ}$ K in the outer magnetosphere. Their calculations are based on the assumption that the cutoff is controlled by thermal broadening of the cyclotron resonance.

Scarf (1962) also uses cutoffs observed in micropulsation data to support the existence of high temperatures. He argues that the thermal motion of the ions will have a Larmor radius associated with it, which will determine the smallest wavelength which can propagate. Since few micropulsations are observed with frequencies higher than 3 cps, temperatures of $10,000^{\circ}$ to $100,000^{\circ}$ K would be expected.

These conclusions support Chapman's hypothesis that heat is being conducted downward from an extended solar corona to the ionosphere. More commonly the upper magnetosphere or exosphere is assumed to be isothermal. Above 500 km dissociation and recombination is assumed to be negligible, and diffusion is the most important process at work. Evidence from various sources indicate the temperature at the 500 km level to lie between 1000° - 2000° K (U.S. Standard Atmosphere, 1962; Prince and Bostick, 1964). Hence, under the foregoing assumptions these temperatures would be expected to pervade the exosphere. The crux of the argument lies in deciding the importance of conduction from a hot solar corona.

TABLE 6.2

Ion-Electron Collision Frequencies Based
on the Low Temperature Model

Height (km)	Geocentric height (earth radii)	Day Max (sec ⁻¹)	Day Min (sec ⁻¹)	Night Max (sec ⁻¹)	Night Min (sec ⁻¹)
1000	1.16	75.2	27.6	20.6	6.96
1500	1.24	22.0	11.4	8.96	3.84
2000	1.31	12.4	7.47	6.19	2.93
3000	1.47	7.27	4.38	4.15	2.10
4000	1.63	5.02	3.07	3.22	1.63
5000	1.78	3.86	2.35	2.60	1.32
7000	2.10	2.50	1.52	1.77	0.932
10,000	2.57	1.44	0.876	1.02	0.621
15,000	3.36	0.683	0.413	0.483	0.291
20,000	4.15	0.353	0.215	0.249	0.153
30,000	5.71	0.125	0.0759	0.0884	0.0536
40,000	7.28	0.0601	0.0365	0.0427	0.0264
50,000	8.85	0.0349	0.0212	0.0246	0.0150

Even if the ion-electron collision frequency approaches the wave frequency, the results of the last section indicate that the theory is not greatly affected by its inclusion.

Some comment should be made about electron-electron collisions or, in other words, the electron gas pressure. In the first chapter of his book, Stix discusses briefly some of the effects. To use one of his results, pressure terms will not be important if

$$\frac{n_e^2 v_A^2}{\kappa T_e \omega_p^2} \ll 1,$$

where κ is Boltzmann's constant. This condition is easily met.

Table 6.3 tabulates the various parameters appearing in equations (36) and (47), for the equatorial plane. B_0 , ω_{ci} , ω_{ce} , $\sqrt{\omega_{ce}\omega_{ci}}$, and v_A should be increased by the factor $\sqrt{1 + 3 \sin^2 \lambda}$ for locations with latitude λ . B_0 was calculated for a dipole field, $B_0 = \frac{8.1 \times 10^{15}}{r^3}$. The ion gyrofrequency from $\omega_{ci} = \frac{eB_0}{m_1 M} = 9.66 \times 10^7 \frac{B_0}{M}$, where M is the mean molecular weight and m_1 the mass of a unit molecular weight. Above 2000 km, M is always 1.

If ω is on the order of a few rad/sec, it is clear that $\omega \ll \omega_{ce}$ and $\omega \ll \sqrt{\omega_{ce}\omega_{ci}}$ is always satisfied. The latter inequality also

guarantees that $\frac{\omega_{ce}^2}{\omega_p^2 v_A^2} \ll 1$, since $\omega_{ce}\omega_{ci} = \frac{v_A^2 \omega_p^2}{c^2}$.

In section 6.3, we used the approximations $\frac{m_e v_{ie}}{m_i} \ll \omega$, and $v_{ie} \ll \omega_{ce}$. The largest value of v_{ie} appearing in Table 6.2 is 75.2, which means that $\frac{m_e v_{ie}}{m_i} \leq 0.04$ rad/sec for heights above 1000 km. This

TABLE 6.3
Some Magnetospheric Parameters

Height (km)	B_0 (weber/m ²)	ω_{ci} (rad/sec)		ω_{ce} (rad/sec)	$\sqrt{\omega_{ce} \omega_{ci}}$ (rad/sec)		V_A (m/sec)				Day Max	ω_p (rad/sec)		Night Max	Night Min
		Max	Min		Max	Min	Day Max	Day Min	Night Max	Night Min		Day Max	Day Min		
1000	2.02×10^{-5}	124	848	3.55×10^6	2.10×10^4	5.49×10^4	3.89×10^5	2.28×10^6	7.64×10^5	4.66×10^6	2.86×10^7	7.15×10^6	8.24×10^6	3.51×10^6	
1500	1.66	150	1600	2.92	2.10	6.85	7.32	4.50	1.16×10^6	7.88	1.52	4.53	5.35	2.59	
2000	1.38	475	1330	2.43	3.40	5.70	1.60×10^6	4.66	2.29	7.54	6.34×10^6	3.64	4.42	2.25	
3000	9.84×10^6	951	951	1.73	4.06	4.06	2.52	4.37	3.36	6.57	4.83	2.76	3.60	1.89	
4000	7.23	698	698	1.27	2.96	2.96	2.24	3.85	2.81	5.98	3.98	2.30	3.16	1.66	
5000	5.47	528	528	9.62×10^5	2.26	2.26	1.94	3.36	2.37	5.40	3.47	2.00	2.83	1.49	
7000	3.36	325	325	5.92	1.39	1.39	1.49	2.58	1.78	4.10	2.82	1.60	2.32	1.24	
1,000	1.84	178	178	3.24	7.59×10^3	7.59×10^3	1.08	1.87	1.29	2.24	2.09	1.20	1.75	1.01	
1,000	8.27×10^{-7}	79.9	79.9	1.46	3.41	3.41	7.15×10^5	1.24	8.54×10^5	1.44	1.42	8.18×10^5	1.19	6.84×10^5	
1,000	4.40	42.5	42.5	7.74×10^4	1.82	1.82	5.34	9.24×10^5	6.38	1.10	1.01	5.84	8.45×10^5	4.90	
1,000	1.69	16.3	16.3	2.97	6.96×10^2	6.96×10^2	3.51	6.08	4.17	7.26×10^5	5.92×10^5	3.42	4.95	2.86	
1,000	8.12×10^8	7.84	7.84	1.43	3.35	3.35	2.45	4.25	2.92	5.02	4.07	2.35	3.41	1.98	
1,000	4.53	4.38	4.38	7.97×10^3	1.87	1.87	1.81	3.15	2.16	3.74	3.08	1.78	2.58	1.48	

is much smaller than the wave frequencies of interest. Comparison of Tables 6.2 and 6.3 supports the second inequality.

To justify $\frac{\epsilon \kappa T_e}{e^2 n_e^{1/3}} \gg 1$ in the derivation of the ion-electron

collision frequency, note that the smallest possible value of T_e is 1000° K , and the largest value of n_e above 1000 km is $8.2 \times 10^{10} \text{ m}^{-3}$.

Thus $\frac{\epsilon \kappa T_e}{e^2 n_e^{1/3}} > 10^3$ and the condition is met.

The last assumption made was $\frac{n_e e^2 v_A^2}{T_e \omega_p^2} \ll 1$, which allowed electronic

pressure terms to be neglected. Using the largest possible Alfvén

velocity and the smallest temperature, we obtain $\frac{n_e e^2 v_A^2}{T_e \omega_p^2} < 4 \times 10^{-8}$.

In the beginning of Section 6.2, the displacement current was

neglected. This is equivalent to stating that $\frac{v_A^2}{c^2} \ll 1$, which is

certainly true. To show this, note that we want $\left| \frac{\epsilon \omega E}{J} \right| \ll 1$. From (26)

$|k^2 E| = |\omega \mu J|$. Thus

$$\left| \frac{\mu \epsilon \omega^2}{k^2} \right| \ll 1 \quad \text{or} \quad \frac{v_A^2}{c^2} \ll 1.$$

6.5 Evidence that Pearls are Alfvén Waves

It appears from the College data that the plane of polarization of pearls is essentially perpendicular to the field lines, though there is some evidence that this is not true for middle latitude stations (Pope, 1964). Since the plane of polarization must be perpendicular to the propagation direction, pearls are probably hydromagnetic waves

traveling along the field lines, at least in auroral regions.

Simultaneous occurrence at conjugate points also provides supporting evidence that pearls travel along field lines.

Many investigators (Tepley, 1964; Yanagihara, 1963) have found the time of maximum amplitude to be 180° out of phase between hemispheres, and coherent over the same hemisphere. Tepley sometimes observed a double structure on equatorial records, implying that signals from both hemispheres were received at the equator. It may be that Alfvén waves are bounced back and forth along field lines at auroral latitudes, and then the signal is propagated to lower latitudes as an electromagnetic wave. This would explain hemispheric coherence and might account for the lack of a unique polarization plane observed at low and middle latitudes.

Another consequence of the polarization observed at College is that it rules out the possibility that pearls may be produced directly by trapped particles (Wentworth and Tepley, 1962). Spiraling particles would produce a perturbation magnetic field aligned against the main field, i.e., they would have a diamagnetic effect. This would give rise to linearly polarized waves propagating across the field lines which is not observed.

The lack of correlation between pearls and events associated with particle precipitation, such as aurora, ionospheric disturbances, riometer absorption, magnetic activity, balloon recorded X-rays, etc., also argues against particle hypotheses. Though there are exceptions to the preceding, especially in regard to riometer activity, in general it is true. There is some evidence that pearls tend to follow magnetic storms. But this could be related to the sun via solar wind fluctuations and hydromagnetic waves as well as by particle influx.

It has been suggested that Alfvén waves will experience significant attenuation in their passage through the ionosphere and that variations in ionospheric attenuation can account for differences in the diurnal variation of micropulsations at various stations (Wentworth, 1964). If this were true, one would expect to see some correlation between ionospheric and magnetic activity. But as was shown in chapter three, this was not observed. As attenuation should become stronger as the frequency increases, clipping of the higher frequencies during the day would be expected. Though this should produce drastic changes in the frequency structure at sunrise and sunset, no such effect has been observed.

Finally, no unique effects have been noticed in conjugate point studies when one end is in darkness and the other in daylight (Campbell, private communication). For these reasons it appears that ionospheric attenuation of pearls is unimportant.

When pearls are analyzed by a sonagram as a frequency-time display, they are characterized by a fine structure consisting of a series of rising frequencies (Tepley and Wentworth, 1962). Often the structure exhibits a fan shape, i.e., successive elements show a declining rate of frequency increase. According to equation (38a), higher frequencies should travel slower and hence arrive later. If a wave bounces several times between hemispheres, each successive pass would have its frequency rise more slowly. This model is used by Jacobs and Watanabe (1964) to explain the observed fan structure. But unfortunately sometimes falling frequencies are observed, and even when the structure shows rising tones, the fan structure is only present some of the time.

If pearls are considered to be Alfvén waves bouncing between hemispheres and constrained to travel along field lines, it is clear that field lines lower than 65° cannot be playing a role. The travel times would be much too short to match against existing data. Tepley (1964), Heacock (1962, 1963), and Campbell and Stiltner (1965) all indicate that the interhemispheric travel times are on the order of one or two minutes, which is reasonable for the higher latitude field lines. Since at high latitudes, small changes in latitude mean large changes in travel time, a given event may have a repetition time quite different from another event observed at the same station without violating the concept of bouncing waves.

Further evidence that waves are not traveling along low-latitude field lines is the existence of rising frequency tones on sonagrams taken at low-latitude stations. These field lines never get very far from the earth and the ratio $\frac{\omega}{\omega_{ci}}$ will always remain small compared to unity. Under these conditions equation (38a) predicts virtually no dispersion and the tones should appear almost vertical on the sonagrams. The latitude dependence of the form of the fine structure warrants further study.

For these reasons, it is suggested that relatively pure Alfvén waves are detected by ground-based equipment in the auroral zone, but that at lower latitudes one sees the effects of coupling to secondary waves. However, the situation is much more complicated than can be explained by simple theory. The non-uniformity of the plasma in the ionosphere and lower magnetosphere will cause the reflection of energy and coupling to other modes. WKB solutions of equation (6) might provide further insight into the nature of these effects.

6.6 Generative Models

It should be stated at the outset that this is an area in which there is much speculation and little agreement. The definitive model for the generation of pearls that can explain satisfactorily all the observed properties has not yet been produced. The three general classes of models are: 1) those which make use of hydromagnetic waves generated at the magnetopause; 2) those involving trapped particles; and 3) those using interactions between hydromagnetic waves and particles.

Typical of the first group is the model elaborated by Jacobs and Watanabe (1962). The interaction of the solar wind with the magnetopause is postulated to generate noisy fluctuations which propagate as Alfvén waves along the geomagnetic field lines down to the ionosphere at high latitudes. As the original fluctuations are noisy, some sort of filtering mechanism must operate so that only regular pulsations are transmitted to the surface. Jacobs and Watanabe believe that standing waves are established between the top of the ionosphere and the height at which the maximum Alfvén velocity occurs, approximately 1500 to 2000 km. (Others have suggested that the entire field line exhibits resonances, which are observed as regular pulsations. Except for field lines at very low latitudes, the fundamental resonance is much too long in period to account for pearls and there is no reason to expect to see only the higher harmonics.) The effective width of the transmitted frequency determines the envelope or the beating of pearls. Secondary waves are generated which then propagate to lower latitudes via the duct between the ionosphere and the height of maximum Alfvén velocity.

This model can explain the characteristic frequency, the beating and the polarization of pearls, but it fails to explain the opposite

phases observed between conjugate points and the series of rising tones seen on sonagrams. In a second paper Jacobs and Watanabe (1963) changed their model to one of bouncing particles in order to remove these deficiencies.

In the revised model bouncing protons, instead of stochastic fluctuations, generate standing Alfvén waves in the aforementioned duct. To account for the observed fine structure, protons are believed to be bouncing at several latitudes simultaneously. Since the Alfvén velocity and the angle of field line inclination is greater at higher latitudes, emissions stimulated at high latitudes will have a higher frequency than those generated at middle latitudes. At the same time protons bouncing at the higher latitudes will have a longer bounce period, and therefore after each successive bounce, the higher frequencies will be further retarded with respect to the lower frequencies, producing the fan-shaped fine structure.

One difficulty with Jacobs and Watanabe's revised theory is that the resonant frequency is greatly dependent on ionospheric conditions which often differ drastically between conjugate points. Simultaneous frequency analyses taken at conjugate points are usually similar.

Wentworth and Tepley (1962) postulated another type of bouncing particle model, this one using electrons whose bounce period is equal to the wave period. The diamagnetic effect of the spiraling electrons would give rise to a hydromagnetic wave which is detected on the ground. Two fundamental difficulties with this theory is that it predicts beats to occur simultaneously in both hemisphere and the magnetic polarization to be aligned along the field lines. The reason for the latter is that

the electrons would produce a perturbation magnetic field aligned against the main field. Since $\vec{k} \cdot \vec{b} = 0$, this could only produce modified Alfvén waves propagating across the field lines. This is in contrast to the polarization reported in chapter five. Wentworth later rejected the bouncing electron model in favor of Jacobs and Watanabe's proton model, primarily because the wrong phase shift between hemispheres was predicted. A summary of all the particle models is given by Tepley (1964). As pearls can last for several hours, all these models share the formidable problem of explaining the stability of the postulated particle bunches.

The last model to be discussed is one that involves the interaction of a beam of charged particles with a hydromagnetic wave. One type of interaction is Landau damping, in which the particles have a velocity parallel to the magnetic field approximately equal to the Alfvén velocity. If a majority of the particles have a velocity less than the Alfvén velocity, the particles will be accelerated and the wave will be damped. In the reverse situation energy will be transferred from the particles to the wave causing the wave to grow in amplitude.

Cornwall (1965) has postulated a model in which cyclotron instabilities play the major role. In contrast to Landau damping the particles, probably protons, have velocities much greater than the Alfvén velocity. If $\omega \ll \omega_{ci}$, this instability will generate waves with a frequency of

$$\omega \approx \frac{V_A \omega_{ci}}{V}$$

where V is the average particle velocity along the field. A beam of 500 kev protons at $L = 3.5$ could generate waves at pearl frequencies.

Cornwall discusses the possible existence of suitable protons in his paper. After generation the Alfvén wave packets will bounce between hemispheres with the repetition time as observed on the sonagrams equal to one round trip. With each passage of the beam through the wave packet, reinforcement of the wave would be expected. Cornwall does not attempt to explain the rising tones in the fine-structure. This could not be considered to be a dispersion effect, as it was postulated that $\omega \ll \omega_{ci}$ in order for the cyclotron instability to be important. Under these conditions no dispersion would take place.

In order to satisfy $\omega \ll \omega_{ci}$ for pearl frequencies, it will be necessary to stay below 20,000 km which corresponds to $L = 4$ in the equatorial plane. Thus unless the instability is occurring near the mirror points of the protons, high latitude field lines are not participating. As it is also necessary to maintain $V_A \ll V$, the instability cannot be occurring near the mirror points where $V = 0$. The observed polarization of pearls indicates that it is the high latitude field lines which are important in the propagation of these waves. Since $V_A \approx 10^6$ m/sec at a height of 20,000 km, it will be necessary for the protons to have energy of at least 500 kev. The conditions placed on the gyrofrequency and energy of the protons are rather restrictive.

The purpose of this last section has been to review some of the pearl models which have been postulated in recent years. Their important features have been discussed in relation to the observational evidence and some of the problems with each model have been emphasized. It was not the purpose of the author to favor one model or to arrive at any definite conclusions. All of the models have significant discrepancies with the observational data, but perhaps more satisfactory models will evolve from those presented here.

REFERENCES

- Alfvén, H. and C-G. Falthammar, "Cosmical Electrodynamics", 2nd Ed., Oxford, 1963.
- Anderson, K. A., C. D. Anger, R. R. Brown and D. S. Evans, "Simultaneous Electron Precipitation in the Northern and Southern Auroral Zones", J. Geophys. Res., 67, p. 4076-4077, 1962.
- Anger, C. D., J. R. Barcus, R. R. Brown and D. S. Evans, "Auroral Zone X-Ray Pulsations in the 1- to 15-Second Period Range", J. Geophys. Res., 68, p. 1023-1030, 1963.
- Ansari, Z. A., "The Spatial and Temporal Variations in High Latitude Cosmic Noise Absorption and Their Relation to Luminous Aurora", Geophys. Inst. Rpt. 138, Univ. Alaska, 1963.
- Basler, R. P., "Radio Wave Absorption in the Auroral Ionosphere", J. Geophys. Res., 68, p. 4665-4681, 1963.
- van Bemmelen, W., "On Pulsations", Appendix to Observations Made at the Royal Magnetical and Meteorological Observatory at Batavia, 29, 1906, pub. 1908.
- Benioff, H., "Observations of Geomagnetic Fluctuations in the Period Range 0.3 to 120 Seconds", J. Geophys. Res., 65, p. 1413-1422, 1960.
- Berthold, W. K., A. K. Harris and H. J. Hope, "Correlated Micropulsations at Magnetic Sudden Commencements", J. Geophys. Res., 65, p. 613-618, 1960.
- Brown, R. R. and W. H. Campbell, "An Auroral-Zone Electron Precipitation Event and Its Relationship to a Magnetic Bay", J. Geophys. Res., 67, p. 1357-1366, 1962.
- Brown, R. R., K. A. Anderson, C. D. Anger and D. S. Evans, "Simultaneous Electron Precipitation in the Northern and Southern Auroral Zones", J. Geophys. Res., 68, p. 2677-2684, 1963.
- Campbell, W. H., "Studies of Magnetic Field Micropulsations with Periods of 5 to 30 Seconds", J. Geophys. Res., 64, p. 1819-1826, 1959.
- Campbell, W. H. and H. Leinbach, "Ionospheric Absorption at Times of Auroral and Magnetic Pulsations", J. Geophys. Res., 66, p. 25-34, 1961.
- Campbell, W. H. and M. H. Rees, "A Study of Auroral Coruscations", J. Geophys. Res., 66, p. 41-55, 1961.

- Campbell, W. H. and S. Matsushita, "Auroral-Zone Geomagnetic Micropulsations with Periods of 5 to 30 Seconds", J. Geophys. Res., 67, p. 555-573, 1962.
- Campbell, W. H. and E. Stiltner, "Characteristics of Geomagnetic Micropulsations in the 1 cps Range", Radio Science, to be pub. about August 1965.
- Chapman, S., "The Thermosphere - The Earth's Outermost Atmosphere", Ch. 1, Physics of the Upper Atmosphere, ed. J. A. Ratcliffe, Academic Press, 1960.
- Cornwall, J. M., "Cyclotron Instabilities and Electromagnetic Emission in the Ultra Low Frequency and Very Low Frequency Ranges", J. Geophys. Res., 70, p. 61-69, 1965.
- Davidson, M. J., "Average Diurnal Characteristics of Geomagnetic Power Spectrums in the Period Range 4.5 to 1000 Seconds", J. Geophys. Res., 69, p. 5116-5119, 1964.
- Duncan, R. A., "Some Studies of Geomagnetic Micropulsations", J. Geophys. Res., 66, p. 2087-2094, 1961.
- Ebert, H., "Concerning Pulsations of Short Period in the Strength of the Earth's Magnetic Field", Terr. Mag. & Atm. Elec., 12, p. 1-14, 1907.
- Eschenhagen, M., "On Minute Rapid, Periodic Changes of the Earth's Magnetism", Terr. Mag., 2, p. 105-114, 1897.
- Francis, W. E. and R. Karplus, "Hydromagnetic Waves in the Ionosphere", J. Geophys. Res., 65, p. 3593-3600, 1960.
- Green, A. W., Jr., B. H. List and F. P. Zengel, "The Theory, Measurement and Applications of Very Low Frequency Magnetotelluric Variations", Proc. IRE, 50, p. 2347-2363, 1962.
- Grenet, G., Y. Kato, J. Ossaka and M. Okuda, "Pulsations in Terrestrial Magnetic Field at the Time of Bay Disturbance", Sci. Rpt., Tohoku Univ., 5th ser., 6, p. 1-10, 1954.
- Harang, L., "Oscillations and Vibrations in Magnetic Records at High-Latitude Stations", Terr. Mag. & Atm. Elec., 41, p. 329-336, 1936.
- Heacock, R. R. and V. P. Hessler, "Pearl-Type Telluric Current Micropulsations at College", J. Geophys. Res., 67, p. 3985-3995, 1962.
- Heacock, R. R., "Auroral-Zone Telluric-Current Micropulsations, $T < 20$ Seconds", J. Geophys. Res., 68, p. 1871-1884, 1963.

- Heirtzler, J. R., "Simultaneous Geomagnetic Measurements on an Ice Island Surface and 1000 Feet Below", Tech. Rpt. #2, CU-2-63, Lamont Geological Observatory, 1963.
- Holmberg, E. R. R., "Rapid Periodic Fluctuations of the Geomagnetic Field", Monthly Notices Roy. Astron. Soc., Geophys. Suppl., 6, p. 467-481, 1953.
- Hutton, V. R., "Equatorial Micropulsations", J. Phys. Soc., Japan, 17, Suppl. AII, p. 20, 1962.
- IAGA Bulletin #16, "Transactions of the Toronto Meeting, Sept. 3-14, 1957", Rpt. Committee #10, p. 318-347, 1960.
- Jacobs, J. A. and K. Sinno, "Occurrence Frequency of Geomagnetic Micropulsations, Pc", J. Geophys. Res., 65, p. 107-113, 1960a.
- Jacobs, J. A. and K. Sinno, "World-Wide Characteristics of Geomagnetic Micropulsations", Geophys. J. RAS, 3, p. 333-353, 1960b.
- Jacobs, J. A. and T. Watanabe, "Propagation of Hydromagnetic Waves in the Lower Exosphere and the Origin of Short Period Geomagnetic Pulsations", J. Atm. & Terr. Elec., 24, p. 413-434, 1962.
- Jacobs, J. A. and T. Watanabe, "Trapped Charged Particles as the Origin of Short Period Geomagnetic Pulsations", Planetary Space Sci., 11, p. 869-878, 1963.
- Jacobs, J. A. and T. Watanabe, "Micropulsation Whistlers", J. Atmos. & Terr. Phys., 26, p. 825-829, 1964.
- Karplus, R., W. E. Francis and A. J. Dragt, "The Attenuation of Hydromagnetic Waves in the Ionosphere", Planetary Space Sci., 9, p. 771-785, 1962.
- Kato, Y. and T. Watanabe, "A Possible Explanation of the Cause of Giant Pulsations", Sci. Rpt., Tohoku Univ., 5th ser., 6, p. 95-104, 1955.
- Kato, Y. and S.-I. Akasofu, "Outer Atmospheric Oscillation and Geomagnetic Micropulsation", Sci. Rpt., Tohoku Univ., 5th ser., 7, p. 103-124, 1956.
- Kato, Y., J. Ossaka, T. Watanabe, M. Okuda and T. Tamao, "Investigation on the Magnetic Disturbance by the Induction Magnetograph, Part V, On the Rapid Pulsation, psc", Sci. Rpt., Tohoku Univ., 5th ser., 7, p. 136-146, 1956.
- Kato, Y. and T. Watanabe, "Further Study on the Cause of Giant Pulsations", Sci. Rpt., Tohoku Univ., 5th ser., 8, p. 1-10, 1956.

- Kato, Y. and T. Watanabe, "Studies on Geomagnetic Pulsation, Pc", Sci. Rpt., Tohoku Univ., 5th ser., 8, p. 111-132, 1957a.
- Kato, Y. and T. Watanabe, "A Survey of Observational Knowledge of the Geomagnetic Pulsation", Sci. Rpt., Tohoku Univ., 5th ser., 8, p. 157-186, 1957b.
- Kato, Y., "Geomagnetic Micropulsations", Australian J. Phys., 15, p. 70-85, 1962.
- Kato, Y. and T. Saito, "Morphological Study of Geomagnetic Pulsations", J. Phys. Soc., Japan, 17, Suppl. AII, p. 34, 1962.
- Kato, Y. and T. Saito, "Secular and Non-Seasonal Annual Variations of the Exospheric Densities and Those of the Period of pc 4 and pc 5", ULF Symposium, Boulder, Colorado, 1964.
- Liemohn, H. B. and F. L. Scarf, "Exospheric Electron Temperatures from Nose Whistler Attenuation", J. Geophys. Res., 67, p. 1785-1789, 1962.
- Lincoln, J. V., "Geomagnetic and Solar Data", J. Geophys. Res., 67, p. 1665-1669, 1962.
- Lokken, J. E., "Some Preliminary Remarks on the Power Spectrum and Coherence of Daytime Pc Activity", Rpt. 61-7, Pacific Naval Lab., p. 6-10, 1961.
- Matsushita, S., "On the Notation for Geomagnetic Micropulsations", J. Geophys. Res., 68, p. 4369-4372, 1963.
- Nicolet, M., "The Collision Frequency of Electrons in the Ionosphere", J. Atmos. & Terr. Elec., 3, p. 200-211, 1953.
- Oguti, T., "Inter-Relations among the Upper Atmosphere Disturbance Phenomena in the Auroral Zone", Japan Antarctic Res. Expedition Scientific Rpt., Aeronomy, p. 13-19, 1963.
- Ohl, A. I., "Pulsations during Sudden Commencements of Magnetic Storms and Long Period Pulsations in High Latitudes", J. Phys. Soc., Japan, 17, Suppl. AII, p. 24, 1962.
- Podder, A., "Micromagnetic Oscillations as Observed at the Magnetical Section of the Observatory of Irkutsk (Zouy), 1925", Terr. Mag. & Atm. Elec., 31, p. 103-112, 1926.
- Pope, J. H., "An Explanation for the Apparent Polarization of Some Geomagnetic Micropulsations (Pearls)", J. Geophys. Res., 69, p. 399-405, 1964a.

- Pope, J. H., "Preliminary Results of Polarization Studies of Certain Type Pc 1 Micropulsations Recorded at Boulder", paper presented at ULF Conference, Boulder, Colorado, 1964b.
- Prince, C. E., Jr. and F. X. Bostick, Jr., "General Dispersion Relations for a Partially-Ionized Gas", EE Res. Lab., Univ. Texas Rpt. #129, 1963.
- Prince, C. E., Jr. and F. X. Bostick, Jr., "Ionospheric Transmission of Transversely Propagated Plane Waves at Micropulsation Frequencies and Theoretical Power Spectrums", J. Geophys. Res., 69, p. 3213-3234, 1964.
- Rolf, B., "Giant Micropulsations at Abisko", Terr. Mag. and Atm. Elec., 36, p. 9-14, 1931.
- Saito, T., "Statistical Studies on Three Types of Geomagnetic Continuous Pulsations, Part I. Type I pc (5-40 sec)", Sci. Rpt., Tohoku Univ., 5th ser., 14, p. 81-106, 1962.
- Santirocco, R. A. and D. G. Parker, "The Polarization and Power Spectrums of Pc Micropulsations in Bermuda", J. Geophys. Res., 68, p. 5545-5558, 1963.
- Scarf, F. L., "Micropulsations and Hydromagnetic Waves in the Exosphere", J. Geophys. Res., 67, p. 1751-1761, 1962.
- Shand, J. A., C. S. Wright and H. J. Duffus, "A Study of the Distribution of Geomagnetic Micropulsations", Pacific Naval Lab. Rpt. #15, 1959.
- Smith, H. W., L. D. Provazek and F. X. Bostick, Jr., "Directional Properties and Phase Relations of the Magnetotelluric Fields at Austin, Texas", J. Geophys. Res., 66, p. 879-888, 1961.
- Spitzer, L., Jr., "Physics of Fully Ionized Gases", 2nd Ed., Interscience, 1962.
- Stix, T. H., "The Theory of Plasma Waves", McGraw-Hill, 1962.
- Sucksdorff, E., "Occurrences of Rapid Micropulsations at Sodankyla During 1932 to 1935", Terr. Mag. and Atm. Elec., 41, p. 337-344, 1936.
- Sucksdorff, E., "Giant Pulsations Recorded at Sodankyla During 1914-1938", Terr. Mag. and Atm. Elec., 44, p. 157-170, 1939.
- Sugiura, M., "Evidence of Low-Frequency Hydromagnetic Waves in the Exosphere", J. Geophys. Res., 66, p. 4087-4095, 1961.
- Tepley, L. R. and R. C. Wentworth, "Hydromagnetic Emissions, X-Ray Bursts, and Electron Bunches. 1. Experimental Results", J. Geophys. Res., 67, p. 3317-3333, 1962.
- Tepley, L. R., "Low-Latitude Observations of Fine-Structured Hydromagnetic Emissions", J. Geophys. Res., 69, p. 2273-2290, 1964.

- Troitskaya, V. A., "Short Period (Oscillatory) Disturbances in the Terrestrial Magnetic Field; Two Oscillatory Modes of the Terrestrial Magnetic Field and Their Diurnal GMT Cycle", trans. E. R. Hope, Defense Res. Board, Canada, T174R, 1955.
- Troitskaya, V. A., "Pulsation of the Earth's Electromagnetic Field with Periods of 1 to 15 Seconds and Their Connection with Phenomena in the High Atmosphere", J. Geophys. Res., 66, p. 5-18, 1961.
- Troitskaya, V. A., L. A. Alperovich, M. V. Melnikova and G. A. Bulatova, "Fine Structure of Magnetic Storms in Respect of Micropulsations ($T < 20$ Sec)", J. Phys. Soc. Japan, 17, Suppl. AII, p. 63-70, 1962.
- U. S. Standard Atmosphere, 1962, Government Printing Office, Washington.
- Wentworth, R. C., and L. R. Tepley, "Hydromagnetic Emissions, X-Ray Bursts, and Electron Bunches. 2. Theoretical Interpretation", J. Geophys. Res., 67, p. 3335-3343, 1962.
- Wentworth, R. C., "Evidence for Maximum Production of Hydromagnetic Emissions above the Afternoon Hemisphere of the Earth. 1. Extrapolation to the Base of the Exosphere; 2. Analysis of Statistical Studies", J. Geophys. Res., 69, p. 2689-2707, 1964.
- Wescott, E. M., and V. P. Hessler, "The Effect of Topography and Geology on Telluric Currents", J. Geophys. Res., 67, p. 4813-4823, 1962.
- Wescott, E. M. and K. B. Mather, "An Investigation of Solar Induced Phenomena at Magnetic Conjugate Points", Final Rpt., Contract AF 19(628)-2779 and AF 19(604)-6180, Geophys. Inst. Sci. Rpt. 147, Univ. Alaska, 1964.
- Wilson, C. R. and M. Sugiura, "Hydromagnetic Interpretation of Sudden Commencements of Magnetic Storms", J. Geophys. Res., 66, p. 4097-4111, 1961.
- Yanagihara, K., "Some Characters of Geomagnetic Pulsation pt and Accompanied Oscillation spt", J. Geomag. and Geoelec., 10, p. 172-176, 1959.
- Yanagihara, K., "Geomagnetic Micropulsations with Periods from 0.03 to 10 Seconds in the Auroral Zones with Special Reference to Conjugate-Point Studies", J. Geophys. Res., 68, p. 3383-3397, 1963.